

The University Of Sheffield.

THE UNIVERSITY OF SHEFFIELD

On Uncertainty Quantification in Wind Turbine Simulations

by

Paulo Henrique **Gonzaga**

March, 2024

Prof K. Worden, Prof. N. Dervilis

This thesis is submitted to the Department of Mechanical Engineering, University of Sheffield in partial fulfilment of the requirements for the degree of Doctor of Philosophy

THE UNIVERSITY OF SHEFFIELD

Abstract

Offshore wind energy has been on the forefront of the renewable energy sources and is expected to show expansion, demanding efficient design, simulation and production procedures. The rise of power ratings, increase in size of the rotors and deep water are some of the challenges the industry must overcome. The development of reliable simulation predictions is needed with quantified uncertainties and deeper understanding of the randomness that affects the system.

The focus of this project was to develop a framework for uncertainty quantification in wind turbine simulation, focussed in the blade behaviour. Blades are increasing in size and in manufacturing and modelling complexity, which makes optimised numerical models harder to achieve. This situation motivates the assessment of how uncertainties affect prediction capabilities. Simulations inherently involve errors, the understanding and quantification of which help lower conservative safety factors, support risk management and give guidelines to improve models or characterisation of systems.

Blade coupon and full-scale blade tests data were used to characterise and build a structural uncertainties model. Monte Carlo simulations were used to propagate the uncertainty levels in high-fidelity blade structural models.

In a similar manner, aerofoil wind tunnel testing data was used to characterise the behaviour of the blade aerodynamic model. A spatial dependent model is developed to characterise the blade aerodynamic performance uncertainty together with geometric tolerances effect.

These blade stochastic characterisation are then used into Monte Carlo realisations of aeroelastic turbine simulation in order to define the effects in the main load channels during different design load cases. The results from the turbine level propagation, are the basis to establish the risk of blade tower collision and tower nominal load exceedance; which are main design constraints as turbines get bigger with higher blade deflection, showing how the current safety factors can be deemed conservative.

Contents

Abstract i

Acknowledgements v

List of Figures vi

List of Tables viii

1 Introduction 1
- 1.1 On uncertainty quantification . . . 1
- 1.2 Trends in wind energy . . . 2
- 1.3 Wind turbine simulation . . . 5
- 1.4 Project aim and objectives . . . 7
- 1.5 Summary of chapters . . . 7

2 Background Theory 9
- 2.1 Introduction . . . 9
- 2.2 The nature of uncertainties . . . 9
- 2.3 Definitions within uncertainty quantification . . . 11
  - 2.3.1 Propagation and validation . . . 11
  - 2.3.2 Model, numerical and data error . . . 12
  - 2.3.3 Sensitivity analysis . . . 12
  - 2.3.4 Risk analysis . . . 13
  - 2.3.5 Inverse problem or calibration . . . 13
  - 2.3.6 Intrusive vs non-intrusive . . . 13
  - 2.3.7 Monte Carlo . . . 14
  - 2.3.8 Polynomial chaos expansion . . . 15
  - 2.3.9 Bayesian framework . . . 15
- 2.4 Aeroelastic turbine simulation . . . 16
- 2.5 Design of wind turbine blades . . . 17
- 2.6 Blade sources of uncertainties . . . 19
- 2.7 External conditions uncertainties . . . 22

3 Blade testing - from laminate to full-scale testing 24
- 3.1 Introduction . . . 24
- 3.2 Laminate coupon testing . . . 25
- 3.3 Blade weight and centre of gravity . . . 27

3.4 Blade static deflection test . . . 30
3.5 Operational modal analysis . . . 32
3.6 Wind tunnel measurements . . . 35
3.7 Chapter summary . . . 39

4 Blade Structural Uncertainties 40
4.1 Introduction . . . 40
4.2 Material properties as random inputs . . . 41
4.3 Blade structural model . . . 44
4.4 Uncertainty propagation . . . 46
4.4.1 Stiffness and mass distribution . . . 47
4.4.2 Material properties sensitivity analysis . . . 50
4.5 Uncertainty validation . . . 52
4.5.1 Uncertainty propagation: Blade static deflection . . . 53
4.5.2 Statistical Difference and Hypothesis Test . . . 56
4.6 Comparison to IEC61400-5 standard . . . 57
4.7 Chapter summary . . . 59

5 Aerodynamic uncertainties 60
5.1 Introduction . . . 60
5.2 Geometric tolerances . . . 63
5.3 Roughness aerofoil characteristics . . . 66
5.3.1 Wind tunnel measurements . . . 66
5.3.2 Extrapolation from wind tunnel measurements . . . 68
5.4 Stochastic model . . . 69
5.5 Chapter summary . . . 72

6 Turbine Simulation 73
6.1 Introduction . . . 73
6.2 Uncertainties in Aeroelastic Turbine Simulation . . . 74
6.3 DLC 12: Normal Power Production . . . 78
6.3.1 Sensitivity Analysis: DLC 12 . . . 83
6.3.2 Results and discussion: DLC12 . . . 86
6.4 DLC 13: Normal power production in extreme turbulence . . . 87
6.4.1 Sensitivity analysis: DLC 13 . . . 91
6.4.2 Results and discussion: DLC 13 . . . 93
6.5 DLC 61: Parked in 50-year extreme wind . . . 93
6.5.1 Sensitivity analysis: DLC 61 . . . 96
6.5.2 Results and discussion: DLC 61 . . . 97
6.6 Chapter summary . . . 98

7 Conclusion 100
7.1 From coupon testing to full scale testing . . . 102
7.2 Characterising blade aerodynamics uncertainties . . . 103
7.3 Wind turbine loads uncertainties . . . 104
7.4 Further work . . . 105

Bibliography **107**

Acknowledgements

The author would like to thank a number of colleagues and friends for their guidance and support, without whom, he would have not have gotten here.

Professor Keith Worden, for being welcoming and supportive throughout this project, and for always offering his help, advice and valuable feedback, always encouraging me to try different things and most importantly to not give up.

Professor Nikolaos Dervilis, for his feedback and ideas for the research. As well as for his help in always looking things on the bright side.

Dr. Henrik Toft, for his endless patience, feedback and ideas for the research, and never hesitating to offer support. As well as for the humour and advices on all things.

Dr. Lars O. Bernhammer, for sharing his expertise and comprehension in the industrial field, for his support and for helping me understand more about blades.

Dr. Nevena Stevanovic, for offering her insight, advice and support on all things both academics and industrial.

Claus Schroeder, for always offering his support, patience and for doing so with his highest understanding and consideration.

Dr. Julia Chiossi, for always offering her time and advice on life, career or any other subject, and for doing so wholeheartedly.

Andre Tonatto, for always being a present friend, willing to help and support whenever necessary.

Dr. Carlos A. C. Gonzaga, for helping me to navigate the industrial-academic relationship within wind energy, and for being a sympathetic ear.

And many others from Siemens Gamesa Loads & Control Dept. and from the department of mechanical engineering at the University Of Sheffield.

List of Figures

1.1 Wind turbine size evolution [1]. . . . 3
1.2 Wind Turbine Foundation [2]. . . . 4

2.1 Example of uncertainty sources in wind turbine simulation. . . . 10
2.2 Uncertainty propagation [3]. . . . 12
2.3 Uncertainty calibration [3]. . . . 14
2.4 Collar's triangle: interaction between aerodynamic, elastic and inertia forces. . . . 16
2.5 BHawC simulation components. . . . 17
2.6 Typical Cross Section of a Wind Turbine Blade [4]. . . . 18
2.7 Split blade design [5]. . . . 18

3.1 scales in composite materials and structures. Adapted from [6]. . . . 25
3.2 Laminate coupon testing [7]. . . . 26
3.3 Setup for mass and centre of gravity measurements. . . . 28
3.4 Histogram and qq-plot: Blade CG location. . . . 29
3.5 Histogram and qq-plot: Blade mass. . . . 29
3.6 Histogram and QQ-plot: static deflection. . . . 30
3.7 Blade static deflection test. . . . 31
3.8 Operational modal analysis - blade in test. . . . 33
3.9 Measurement grid used. 11 points on the leading edge (blue) and 11 points on the trailing edge (red). Total 22 points. . . . 33
3.10 Oma results, adapted from [8]. . . . 34
3.11 Wind tunnel test data: CL - clean measurements. . . . 36
3.12 Wind tunnel test data: Cd - clean measurements. . . . 37
3.13 Wind tunnel test data: CL - Rough measurements. . . . 37
3.14 Wind tunnel test data: CD - Rough measurements. . . . 38
3.15 Wind tunnel test data. . . . 38

4.1 Scale of wind turbine tests. . . . 41
4.2 Laminate definition, adapted from [9]. . . . 42
4.3 Unidirectional vs Bidirectional fibre orientation. . . . 43
4.4 (A) Reference system for wind-turbine blade, (B) reference for material properties. . . . 45
4.5 (A) Deterministic stiffness distribution, (B) Deterministic mass distribution. . . . 46
4.6 Blade layup. . . . 46
4.7 pdfs and histogram of BIAX properties realisations. . . . 47
4.8 pdfs and histogram of UD properties realisations. . . . 48

4.9 Uncertainty propagation on wind-turbine blade model. 48
4.10 Confidence intervals for blade flapwise/edge stiffness distribution. 49
4.11 Confidence intervals for blade torsional stiffness/mass distribution. 49
4.12 Mean blade stiffness and mass moment. 50
4.13 Blade mass, CG and static deflection sensitivity analysis - main effect. . 51
4.14 Wind Turbine Blade static test: Setup and finite element model. 53
4.15 UQ for static deflection test simulation. 54
4.16 Simulation (MC-LHS) VS Experimental information. 55
4.17 Simulation (MC-LHS) VS Experimental information. 56
4.18 Normalised natural frequencies, IEC tolerances and experimental data. . . 58
4.19 Mass and mass moment, IEC tolerances and experimental data. 59

5.1 Blade aerofoil cross-section, adapted from [10] 61
5.2 Blade twist angle, adapted from [11] 61
5.3 CL and CD for geometric tolerances Monte Carlo simulation. 65
5.4 (A) Aerofoil geometric tolerance and (B) variation in lift coefficient. . . . 66
5.5 Wind tunnel measurements: Clean and tripped (rough) states 67
5.6 Uncertainty in wind tunnel measurements: clean and rough. 67
5.7 Wind tunnel measurements: parametrisation (A) and validation (B) of the model. 68
5.8 Blade regions: interpolation between (C) clean and (R) rough. 70
5.9 Betas pdfs. 70
5.10 CL for blade mixed aerofoil, respectively root, mid and tip. 71

6.1 Turbine aeroelastic model - modules. 75
6.2 BHawC structure - Turbine aeroelastic model. 75
6.3 Power curve - Pitch controlled wind turbine. Adapted from [12] 79
6.4 Normalised wind speed: DLC 12 80
6.5 Samples for DLC12 - LHS 80
6.6 Most likely CoV for cut in wind speed: DLC 12. 81
6.7 Most likely CoV for rated wind speed: DLC 12. 81
6.8 Most likely CoV for cut out wind speed: DLC 12. 82
6.9 Variance decomposition at (A) cut in (B) rated and (C) cut out wind speed. 85
6.10 Normalised wind speed: DLC 13 88
6.11 Most likely CoV for cut in wind speed: DLC 13. 88
6.12 Most likely CoV for rated wind speed: DLC 13. 89
6.13 Most likely CoV for cut out wind speed: DLC 13. 89
6.14 Blade tower collision probability: DLC 12 vs DLC 13. 91
6.15 Variance decomposition at (A) cut in (B) rated and (C) cut out wind speed. 92
6.16 Tower moment: UQ simulations vs nominal. 95
6.17 Normalised Tower moment distribution. 95
6.18 Variance contribution - sensitivity analysis: DLC 61. 97

List of Tables

3.1 Uncertain parameters description . . . 26
3.2 Materials properties experimental CoV. . . . 27
3.3 Normalised blade CG location - experimental. . . . 28
3.4 Normalised blade mass - experimental. . . . 28
3.5 Materials properties experimental CoV. . . . 28
3.6 Normalised static deflection - experimental. . . . 31
3.7 Operational modal analysis results summary. . . . 32

4.1 Uncertain parameters description . . . 44
4.2 Uncertainty levels for blade mean structural parameters. . . . 50
4.3 Variance contribution %- Sensitivity analysis. . . . 51
4.4 Uncertainty levels comparison between simulation and experiment. . . . 54
4.5 Coefficient of variance (%) vs IEC tolerances (%). . . . 58

5.1 Sources of uncertainty included in this chapter. . . . 63
5.2 Parametrised results for geometric uncertainty. . . . 65
5.3 Uncertainty in aerodynamic parameters . . . 67
5.4 Blade regions: Beta pdf definition. . . . 70

6.1 Analysed load outputs. . . . 76
6.2 Uncertainties sources considered for each DLC. . . . 78
6.3 DLC 12 Loads CoV: ULS and FLS . . . 83
6.4 DLC 13 Loads CoV: ULS . . . 90
6.5 ULS Loads mean values: DLC 13 vs DLC 12 . . . 90
6.6 DLC 61: Wind parameters uncertainty characterisation. . . . 94
6.7 Tower loads COV: DLC 61. . . . 96
6.8 Probability of tower load higher than nominal: DLC 61. . . . 96
6.9 Variance contribution - sensitivity analysis: DLC 61. . . . 97

Chapter 1

Introduction

1.1 On uncertainty quantification

The discussion about the origin of uncertainties started long ago and was an important topic also for the great Greek thinkers, Plato's shadow in a cave allegory [13], where humans were only exposed to reality via its shadow in a cave, can be understood as the lack of *certainty* we humans have when looking at reality.

In this work we will not participate in the debate on reality, but assume a Platonic view of it: we are not able to predict (or observe) nature precisely. The issue can be a result of the lack of models or computer power or the impossibility (or impracticability) of measurements, but still one needs to do analysis based on this *incomplete* view of dynamic systems.

In practice this situation arises from several causes: the limited accuracy of measurement instruments, the exceedingly-high cost of performing accurate experiments and/or measurements, the lack of accurate models or the computational need of using simplified ones. In engineering, predictions are the result of a combination of measurements, modelling and simulations. Analyses are regularly performed on the basis of these predictions and the standard assumption made is that reality will not move significantly away from them.

The systematic quantification of the uncertainties in dynamic systems and the characterisation of the uncertainties and their outcomes is crucial for engineering design and analysis, where risks and costs must be reduced as much as possible [14].

The main components of an uncertainty analysis are the *model* and *inputs* whose variations impacts the *outputs* . In engineering, a model is the set of mathematical relationships that represent a physical phenomenon (e.g. the finite element model of a wind turbine blade used to calculate its strain - stress behaviour), and normally takes a set of inputs (e.g. material properties, geometry, etc.) and returns outputs that engineers are interested in (e.g. deflection, stresses). The quality (and accuracy) of these outputs depends not only on the correctness of the model (in terms of fidelity, and physics description), but also on the quality of the inputs.

In the offshore wind energy industry, the quality of models is critical to both the integrity of the turbines and to the financial soundness of the business case. This high quality need has contributed to the increased interest of the research community in defining the uncertainties of output wind-turbine models, which not only allow better decisions to be taken based on the results of these models but also integrates the path for minimising cost of energy.

1.2 Trends in wind energy

The world is in great need of clean, renewable and cheap energy sources. The current climate change predictions are not optimistic (up to 5 ° Celsius of increased average temperatures, more droughts and change in precipitation patterns, among many more effects that can alter the way society lives [15]); there is a constant fear that what is being done is not enough to prevent or to lower human impact on the environment and climate change. Technology and industrial development is one of main contributors to negative impacts on the climate and environment, but it can also be the leading force to a sustainable future.

Wind power is no stranger to the human race; the earliest known wind-powered grain mills and water pumps were used by the Persians in A.D. 500-900 and by the Chinese in A.D. 1200 [16]. Fast forwarding to the present day, there is an established industry of wind-power generation.

The technology development seen by the wind industry is nevertheless unprecedented: sizing of the turbines (Fig.1.1), direct-drive generators [17], and the application of new composite materials are just some of the developments that have allowed offshore wind to arrive at the status it enjoys today.

The evolution from onshore wind power to offshore has already overcome much scepticism: the rough environment, the transmission infrastructure, the efforts in reducing LCOE (Levelised Cost of Energy), made this challenge particularly difficult. From the first 5MW offshore wind park commissioned on the Danish coast in 1991 [18], to the gigantic 1.2GW Hornsea park finished in the UK by 2020 [19], offshore wind energy has come a long way.

Even though much has been accomplished to mature the technology and reduce costs to make offshore wind power more competitive, there is still a major ambition to lower it even further. The interaction between the phenomena involved in generating energy from wind (use of anisotropic materials, aerodynamics/aeroelasticity, wind forecasting, sea waves, wind-farm dynamics, electromagnetism, among others), can still be too complex for current prediction capabilities.

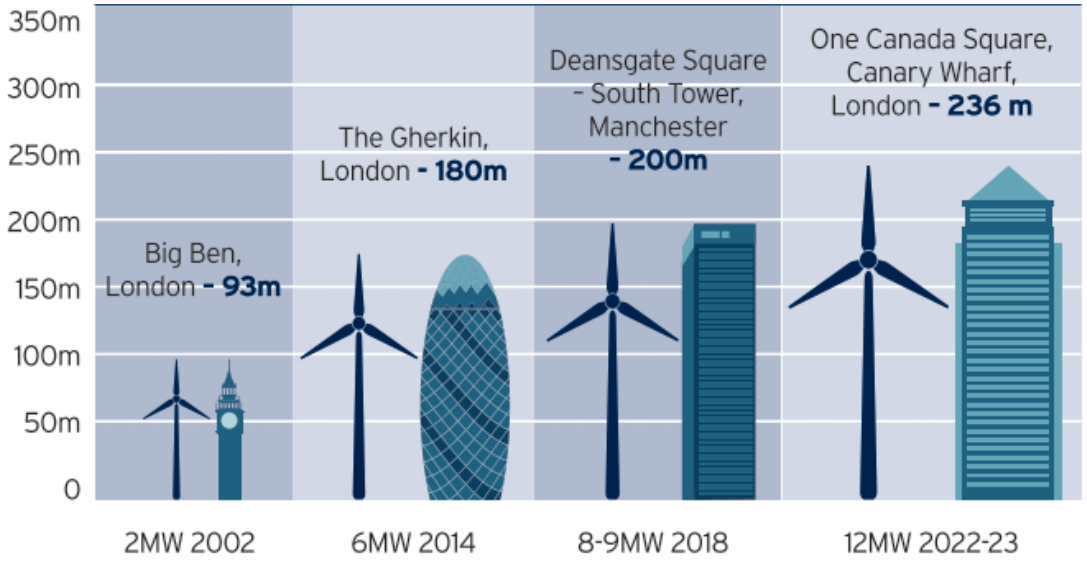


FIGURE 1.1: Wind turbine size evolution [1].

Wind power is expected to keep showing continuous expansion in the future. The European market has made wind one of the priorities for the green transition following the latest developments in the international scenario. Utilisation of wind energy increased in installed capacity by around 20% in recent years. The United Kingdom's industrial strategy department unveiled its plans and expectations for the offshore wind market, announcing huge investments in the next few years, as well as an expected expansion of the market: offshore wind should provide 10% of the UK electricity by 2020 [1]. This trend is followed by other countries, current giga Watt parks are under development in the USA [20] and Taiwan [21] for example.

Another important trend dependent on wind energy, is the concept known as "power to X", which is an umbrella term for technologies that convert renewable electricity into something else, including hydrogen, synthetic methane, fuels, ammonia, heat, etc. These technologies often involves the production of hydrogen by using renewable energy to split water into its elements in an electrolyser, with no greenhouse gas emissions as a by-product [22]. The potential of so-called "green-hydrogen" is diverse, from transportation fuel to energy storage, contributing to the expected demand for wind energy in the near future.

Also fundamental to offshore-wind energy developments is the foundation concept. Up to this date, the traditional bottom-fixed monopile foundation (first to the left in Fig.1.2) has been the major type employed in wind parks, this is because of its cost efficient and fast installation in depths up to 40m. In contrast, future parks are expected to implement floating solutions, Scotland recently announced the ScotWind [23] project with a capacity of 25GW, out of which 15GW are expected to be floating. The necessary technology developments (with relation to turbine control, manufacturing and installation) are certainly expected to bring important contributions to both research and industry.



FIGURE 1.2: Wind Turbine Foundation [2].

For wind to make a bigger contribution to the world energy supply, it is imperative that the cost of wind energy is brought down even further, which means that wind turbines

must be designed to be exactly as strong as necessary, but no stronger [24]. This aim requires that every aspect of the design, installation, operation and maintenance has to be optimised.

Uncertainties are omnipresent in wind-energy applications, both in external conditions (such as soil, wind and waves), and in the models that are used to predict key quantities such as loads, availability/reliability, costs and energy yield [3].

Just recently, Ørsted (the world's largest offshore wind developer) announced that their forecast models overestimate energy production, as they lack sophistication to predict the effect of wake and blockage, but they are still very optimistic on the growth prospects for offshore wind [25].

In the effort to increase the fidelity and understand the limitation of the models, uncertainty quantification analysis is an important tool. It is a crucial advantage to know where the variation of KPIs (key performance indicators) are coming from. In wind turbine design, these contributions can come from phenomena that are not well characterised (e.g. vibration, damping), or from the interaction of different modules or different components.

The blades of a wind turbine are some of the most critical components; they are constructed out of a mix of composite materials, including glass and carbon fibre, resin and balsa wood. The blades are required to withstand a diverse range of loads, maintain their aerodynamic profile and have a useful life of over 20 years.

Uncertainty quantification in wind applications (turbine models, wind forecasting, energy production), is still a young research theme, but the presence of uncertainties in wind turbine outputs, lifetimes, and failure probabilities leads to an increased financial investment risk. Consequently, there is room (and a need), for reducing the costs of offshore wind energy by using a probabilistic approach for the design of wind turbines and wind farms, in which the effect of uncertainties is understood and quantified [3].

1.3 Wind turbine simulation

As wind turbines become larger, lighter and more flexible, simulation tools are extremely important to predict, understand and design these machines, as prototyping and testing becomes more expensive and with higher risks.

The behaviour of a wind turbine is made up of a complex interaction of components and sub-systems. The main elements are the rotor, tower, hub, nacelle, foundation, power train and control system. Understanding the interactive behaviour between the components provides the key to reliable design calculations, optimised machine configurations and lower costs for wind-generated electricity [26].

There are several software, both commercial and proprietary, specifically designed for simulation of wind turbines, and most of them work as a framework coupling computational modules for aerodynamics, hydrodynamics, control system dynamics, electrical systems and structural dynamics, to enable aero-hydro-servo-elastic simulation in the time domain. Some of the most used aeroelastic tools are:

- OpenFast: Created with the goal of being a community model developed and used by research laboratories, academia, and in industry. It is managed by a dedicated team at the National Renewable Energy Lab, and extensively used as a framework for both onshore and offshore wind-turbine design.
- OrcaFlex: It is a generic marine systems design and analysis software, that has a dedicated model for marine environment for offshore floating applications and can be used coupled with other tools (focused on) it is maintained and commercialised by BAE systems.
- HawC2: (Horizontal Axis Wind turbine simulation Code 2^{nd} generation) is an aeroelastic code intended for calculating wind turbine response in the time domain. The core of the code was developed mainly within the years 2003-2007, by the Aeroelastic Design Research Program at DTU Wind Energy, DTU Risø Campus in Denmark.
- BhawC: is the Siemens Gamesa Renewable Energy in-house aeroelastic simulation tool used to study the dynamic response of wind turbines. The model consists of substructures for foundation, tower, nacelle, drivetrain, gearbox, hub, and blades. The structure is modelled primarily with finite beam elements, and the aerodynamics is modelled using blade-element momentum theory. The code is coupled to a controller identical to that on the real turbine.

In this thesis, model uncertainty (which is uncertainty from imperfections and idealisations made in physical model formulations) will not be investigated, neither will the numerical

errors associated with solving the model. The assumption is that both the formulation and the implementation of the software used to simulate the wind turbine (which will be discussed further) are correct. The focus will be on characterising and propagating the input uncertainties through the model, investigating its effect on the turbine loads.

1.4 Project aim and objectives

This thesis seeks to obtain an efficient and systematic approach to work with uncertainties in wind-turbine systems, focussing on the impact of the uncertainties related to the blade and their subsequent effect on wind-turbine predictions. Such a methodology is required to work seamlessly with the turbine and blade models already developed. Contributions are made in developing specific solutions, focusing on three main challenges:

1. Investigating and defining a suitable uncertainty quantification methodology that can be used within an already-established wind-turbine simulation infrastructure (following the IEC61400 standard as closely as possible).
2. Developing a framework to characterise blade uncertainties (structural and aerodynamic) from different scales of testing (all the way from coupon to full-scale blade testing), building a probabilistic model to describe the blade.
3. Propagating the uncertainties and describing the effects of such in different scenarios- focussing in deepening the understanding of blade and turbine behaviour.

1.5 Summary of chapters

The outline of this thesis is as follows:

Chapter 2 — The background theory is presented. An introduction to key components and challenges to uncertainty quantification implementation, sources of uncertainties in wind turbines and types of framework relevant to the research objectives targeted by this thesis are discussed. Specifics of wind turbine simulation, physics and definitions are also included.

Chapter 3 — The experimental data made available by the industrial partner is outlined. The experimental setups as well as the discussion of data treatment and privacy are

included. The knowledge, conclusion and model validation made with these experiments are one of the main novelty in this thesis, allowing the development of an uncertainty framework based on experimental data. Such experiments are seldom available and normally cannot be performed in bulk with precision and repeatability necessary to uncertainty quantification applications outside an continuous high technology industrial product development framework.

Chapter 4 — Focus in the blade structural model and its uncertainty. The novel probabilistic model formulation for the blade material properties together with a sensitivity analysis is included with the validation of such model with relation to the blade static deflection testing.

Chapter 5 — Focus in the blade aerodynamic uncertainties. A probabilistic model formulation for the blade geometric uncertainties and their impact in the drag and lift coefficients is presented. The wind tunnel testing data for clean and rough behaviour are used to build a spatial stochastic model, taking into account all the different sources of uncertainties impacting the blade aerodynamic behaviour.

Chapter 6 — The uncertainties' characterisation developed in previous chapters are propagated through the wind turbine model, different load conditions are explored and the impact of the structural and aerodynamic blade uncertainties are discussed for blade and tower loads.

Chapter 7 — Summarises the research in this report, showing the main conclusions and the path from testing to turbine simulation and uncertainty quantification. The novelty and further work topics are also presented.

Chapter 2

Background Theory

2.1 Introduction

The growing attention in wind-energy applications to the importance of defining the uncertainty effects on systems and simulations is parallel with the need for optimised and reliable systems, which in turn helps lowering of energy costs. There is an unlimited number of uncertainty sources that can have a direct impact on turbine output variability. The sources in wind-turbine simulation can be related to each turbine component. Figure 2.1 shows the main components and the uncertainty sources related to the blade. This list is not comprehensive, but focussed on sources that can be linked to the most relevant blade-related effects, which are the main focus of this study.

This chapter presents a short summary of the main concepts related to uncertainty quantification in wind-turbine systems: uncertainty nature, types of framework, aeroelastic simulation, blade design and uncertainty sources.

2.2 The nature of uncertainties

The main goals behind uncertainty quantification are to better understand and if possible, reduce the effect of uncertainties. The first step is to characterise the uncertainties (i.e. determine their nature), it is usual to categorise them in two different groups: *epistemic* or *aleatory*.

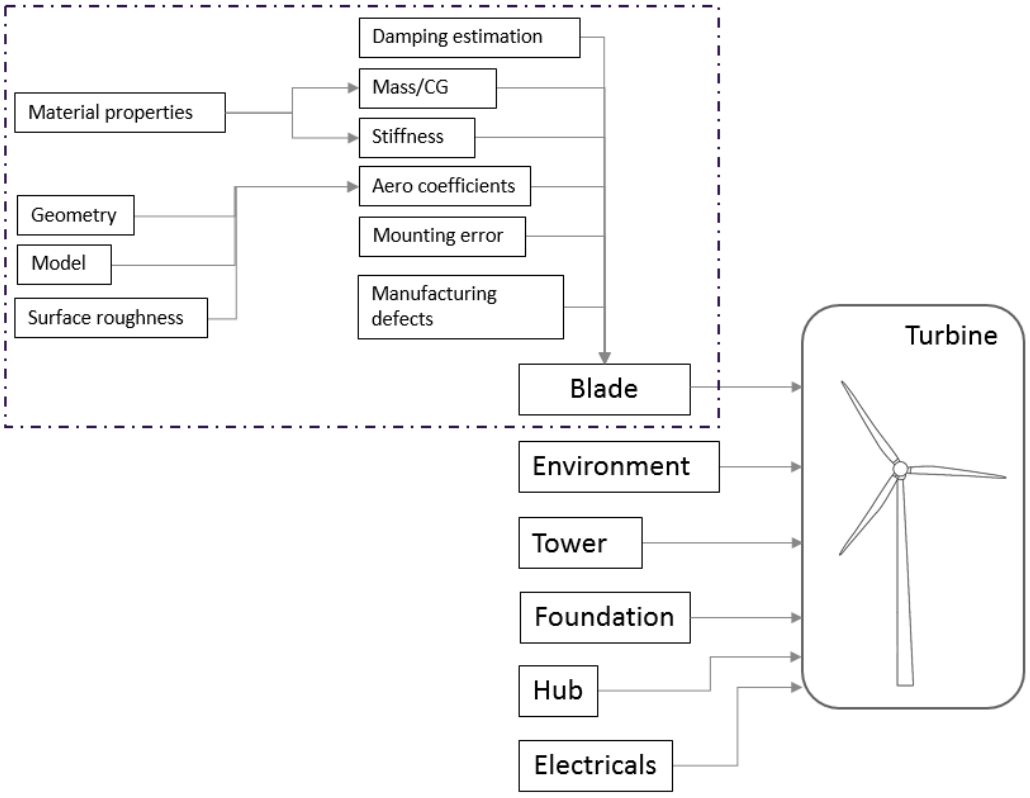


FIGURE 2.1: Example of uncertainty sources in wind turbine simulation.

Epistemic uncertainty is the scientific uncertainty in the model of the process. It is a result of limited data, and more often, limited knowledge. But with more knowledge it can be reduced.

Aleatory uncertainty is because of random variability, which is unpredictable (and irreducible) no matter how much information there is and should be described by probability. In statistics, aleatory uncertainty is present in almost all data that are obtained, because of random variability between the members of a population that one samples from, or due to random measurement errors [27]. The following example is based in [28]:

> "Let X be a basic random variable describing a material property constant, such as the strength of a glass-fibre reinforced composite laminate. Should uncertainty in X be categorized as aleatory or epistemic? The answer depends on the circumstances. If the desired strength is that of the laminate in an existing blade, then the uncertainty should be categorized as epistemic if specimens taken from the blade can be tested, yielding information about the strength. The testing may, of course, involve

> random errors of measurement, particularly if non-destructive methods are used. On the other hand, the uncertainty in the strength of laminates in a future blade should be categorized as aleatory, if there will be no attempts to make more detailed modelling related to, for example, the control of the laminate production. Until the blade has been produced, no amount of testing will reduce the variability inherent in the strength of laminate of the future blade".

It is also important to note that, defining the (aleatory) uncertainty bounds is often the only attainable result of an uncertainty quantification (UQ) framework. Nevertheless, this information is critical to understand the optimisation path towards uncertainty reduction (better characterisation or control of the laminate production in the previous example), i.e. aleatory uncertainties get better characterised with an increase in knowledge, whereas epistemic uncertainties get reduced with an increase in knowledge.

2.3 Definitions within uncertainty quantification

2.3.1 Propagation and validation

Propagation of uncertainties is the process of defining the probabilistic model of a system's output based on its input uncertain characterisation, i.e. to propagate uncertainties "through" a model. The model can be any equation (or set of equations, e.g., a finite element model), describing a process that uses inputs (or parameters) that are uncertain, for example, the function f in equation (2.1), where μ is a set of random inputs, S is the set of other (deterministic) inputs, such as the independent variables space and time and finally, Y the QoI (quantities of interest). The main goal in propagation is defining the effect that variabilities on the inputs μ, cause on the output, Y. In wind-turbine simulations, the QoIs are frequently the turbine and foundation loads, energy production and the levelised cost of energy (LCOE). Figure 2.2 illustrates the propagation for uncertain inputs of a computational model. Another important objective of propagating uncertainties in models (or simulations) is the validation against measurements performed on the real system, which will always be affected by uncertainties (e.g. random uncertainties), this way, in order to have a model fully validated this step

must be performed by considering both the experimental and computational uncertainties.

$$Y = f(\mu, S) \tag{2.1}$$

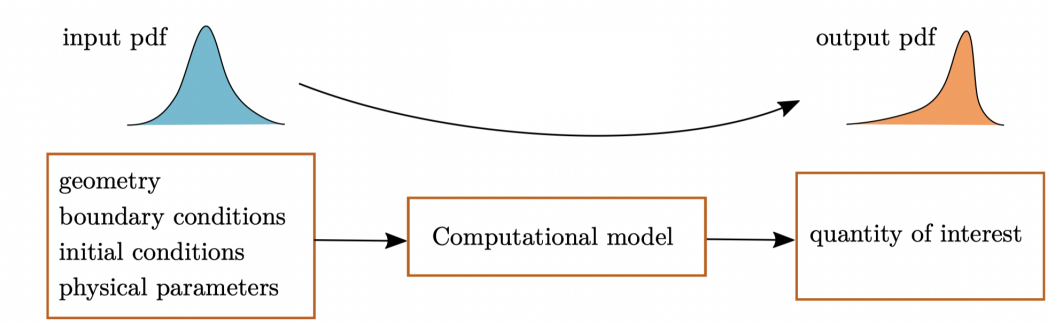


FIGURE 2.2: Uncertainty propagation [3].

2.3.2 Model, numerical and data error

It is important to understand the differences between real-world systems and numerical predictions, and where they come from. Advanced models are continuously developed, those are normally based on constitutive equations, conservation laws, state equations, thermodynamic laws, etc, and they account for essential characteristics of the system being studied. Nevertheless, it is often the case that simplification of the mathematical models is performed to facilitate their solution, leading to the model to not be able to exactly reproduce the real system, which thus characterises a "model error". Once a model is selected, it necessary to solve it numerically, which typically involves discretisation and other approximations, so that the model can be solved computationally. This process will introduce "numerical errors" that can, in theory, be reduced to a required lower level (e.g by using a finer discretisation) [29]. The mathematical model also needs to be complemented with data and parameters that define the geometry, boundary and initial conditions. In many situations these data are not available, which leads to the use of data that partially reflect the nature of the systems, inducing so-called "data errors".

2.3.3 Sensitivity analysis

Sensitivity analysis is the study of relative uncertain or variation of input effects. In a sensitivity analysis, the goal is to define which input quantities have most influence on the QoIs. This provides important information that is crucial to the design, optimization

and decision support. A main distinction is between local and global sensitivity analysis. Local sensitivities are typically defined via partial derivatives: the change of the model output with respect to a change in inputs at a given condition. Global sensitivity analysis, defines what part of the model output can be attributed to the model input, over the entire range of input values [3]. This is an important tool for resource allocation, once, for example, the analysis defines that one input dramatically affects the QoI but a second input does not, resources (time and investment) can be focused to lower the uncertainty of the first input while no extra effort needs to be put for the second input.

2.3.4 Risk analysis

Once the inputs' probabilities are characterised, the risk and/or reliability analysis can be performed by determining the probabilities of the system exceeding critical values or thresholds. An important goal of risk analysis is to mitigate, control and build contingencies measures that avoid, e.g. system downtime, extended maintenance stops or asset damage [30]. With relation to wind turbine systems, risk analysis are performed together with or as a part of Failure, Modes, Effects and Criticality Analysis, often referred as its acronym FMECA. Such methods can rely heavily in statistical analysis, probability modelling and qualitative judgement.

2.3.5 Inverse problem or calibration

The uncertainty propagation and sensitivity techniques handle the study of the input uncertainties on QoIs without using experimental data. However, when such data is available, one can calibrate the models by estimating parameters in order to obtain more accurate predictions under uncertainties. Calibration is often described as an *inverse problem*. Figure 2.3 illustrates the calibration process for uncertain inputs of a computational model when experimental data are available.

2.3.6 Intrusive vs non-intrusive

In the domain of uncertainty quantification (UQ) frameworks, one can categorise the methodologies as either *intrusive* or *non-intrusive*. When the deterministic model is used to map the outputs based on given values of the input parameters, this approach is referred to as non-intrusive. This term means there are no modification to the

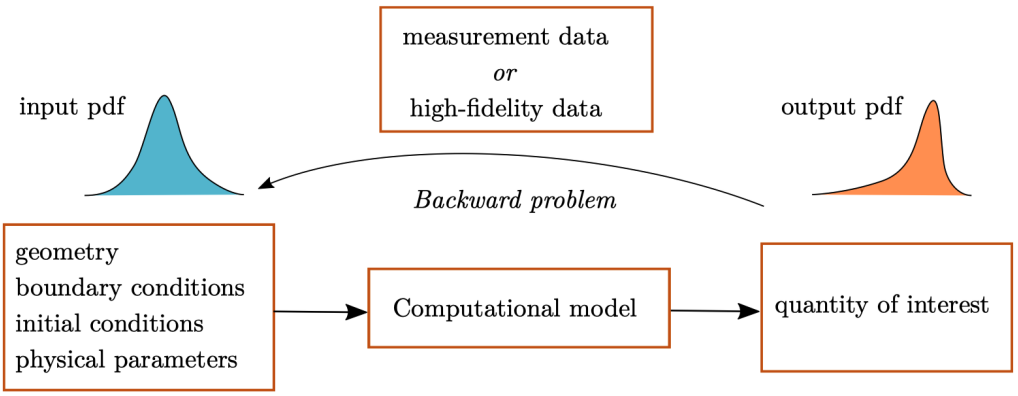


FIGURE 2.3: Uncertainty calibration [3].

deterministic code, and, normally some kind of sampling from a probability distribution is needed. Non-intrusive methods can be applied to any type of nonlinear model. However, if a single model run requires large execution times, these UQ methods may be ineffective, or even computationally intractable.

On the contrary, methodologies referred to as *intrusive* require substantial modification to deterministic models. These frameworks, in general, do not involve sampling, because the problem is transformed so that its responses include stochastic information on the output. Intrusive methods are efficient and relatively easy to apply to linear models. This approach, however, represents only a relatively small class of models. It can be applied to nonlinear models also, but solution of the resulting equations may become very demanding.

2.3.7 Monte Carlo

In the wind industry, including uncertainties in predictions has classically used Monte Carlo methods (MCM) [3]; this is why, even though MCM is the most standard methodology for UQ, both its discussion and application are still extremely relevant. Monte Carlo simulation is, in essence, the generation of random objects or processes by means of a computer in order to infer the statistics of ensembles of the objects. In Monte Carlo techniques, the idea is to run the model many times (or use a sufficiently-long simulation), with the ensemble of random inputs to obtain many quantities of interest using the Law of Large Numbers and other methods of statistical inference [31]. Hence, MCMs require a large number of repeated solutions of the same deterministic problem with different (randomly sampled from a probabilistic distribution) parameters. Although very robust and flexible, MCM is affected by a slow convergence rate, especially for large

and complex systems; however, convergence can always be assured. This fact leads to expensive simulations, both in terms of time consumption and computational costs [32]. Therefore when investigating models that are complicated deterministic systems with a large ensemble of random inputs, Monte Carlo methods might not be the best strategy if time and computer processing time are constraints.

2.3.8 Polynomial chaos expansion

Polynomial chaos expansion (PCE), is a non-sampling based method to determine the evolution of uncertainty in a dynamical system, when there is probabilistic uncertainty in the system parameters [33]. PCE comes from the homogeneous chaos theory of Wiener [34], and associated with a Galerkin projection, it has been shown to be a successful approach to solve uncertainty quantification problems; by representing the stochastic processes and variables in a set of orthogonal bases of random variables. The original polynomial chaos expansion [35] used a mean-square convergent expansion as multidimensional Hermite polynomials of normalised Gaussian variables [36]. Xiu [37], generalised the PCE problems to other types of pdfs (gamma, beta, uniform) and polynomial families (Hermite, Laguerre, Jacobi), allowing a more accurate representation of stochastic systems and parameters. Restrictions of the approach are that the accuracy degrades as the dimension of the problem increases and nonlinearities are hard (sometimes impossible) to represent with PCE.

2.3.9 Bayesian framework

A Bayesian framework (via Bayes theorem - see equation 2.2), combines background (prior) knowledge with observed data to form a posterior distribution. Bayesian methods are critical for quantifying the behaviour of systems; they capture the uncertainty about a system's behaviour using probability distributions, and update this understanding as new information becomes available. Probabilistic predictions that incorporate this uncertainty can then be made to evaluate system performance and make decisions [38]. The Bayesian framework models both aleatory and epistemic uncertainties as probabilistic, i.e., the parameters to be calibrated are treated as random variables. Bayesian calibration or updating relies on experimental data being available; this methodology is often computationally expensive, but very useful to evaluate system performance and

to support decisions.

$$P(A \mid B) = \frac{P(B \mid A)P(A)}{P(B)} \tag{2.2}$$

where A and B are events, $P(A \mid B)$ is the probability of A given B is true, $P(B \mid A)$ is the probability of B given A is true, P(A) and P(B) the independent probabilities of A and B.

2.4 Aeroelastic turbine simulation

Aeroelasticity studies the interaction between the aerodynamic, inertia and elastic forces to which wind turbines are subjected. This interaction is illustrated by "Collar's triangle", shown in Figure 2.4. Aeroelastic simulations of wind turbines are an important tool to support the expansion of wind energy, and provide the industry and the certifying institutions with models capable of performing complete simulations of the behaviour of wind turbines over a wide range of configurations and operational conditions [26]. A minimum set of these conditions is described in standards of wind-turbine simulation in order to guarantee the safety and reliability of the design.

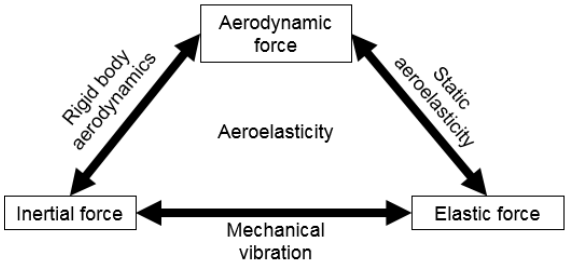


FIGURE 2.4: Collar's triangle: interaction between aerodynamic, elastic and inertia forces.

To model and simulate wind turbines, several aeroelastic tools and methods are available, which include aerodynamic and structural components to determine loads and dynamic responses of structure [39].

The turbine simulations performed in this study used the in-house aeroelastic simulation code BHawC, which has been used in Siemens Gamesa Renewable Energy for almost 20 years (illustrated in Figure 2.5). The code is being continuously validated against measurements from prototype turbines. The structural model in BHawC is built around the co-rotational formulation, providing geometric nonlinearity [40]. The substructures for the tower, shaft and blades are modelled using beam elements which are defined by

continuous cross-section properties tabulated either in a reduced or in a 6-by-6 cross-section format [41].

The blade modules can also be differentiated between structural and aerodynamic. On the first, all the information regarding blade stiffness and mass distribution are defined, on the latter the aerodynamic properties (lift, drag and moment coefficients) are defined for every airfoil section throughout the blade.

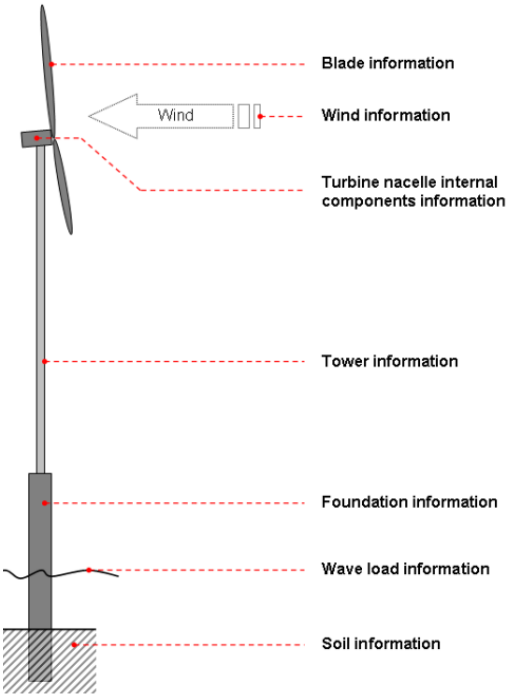


FIGURE 2.5: BHawC simulation components.

2.5 Design of wind turbine blades

A wind-turbine blade structure is defined in terms of its outer geometry and inner structural layout; it can be made from different materials and will be subjected to varying loads from winds and the varying effect of gravity because of the rotation of the rotor.

There will always be a conflict between increased aerodynamic performance given by slender aerofoils versus increased structural performance given by thicker aerofoils; therefore an optimised balance needs to be sought in order to develop high performing blades.

A typical turbine blade design is based on a load-carrying laminate in a rectangular hollow beam (also referred to as spar), with high-strength composite at the bottom and top of the rectangle (also referred as spar cap) (Figure 2.6) that supports the aerodynamic outer geometry [42].

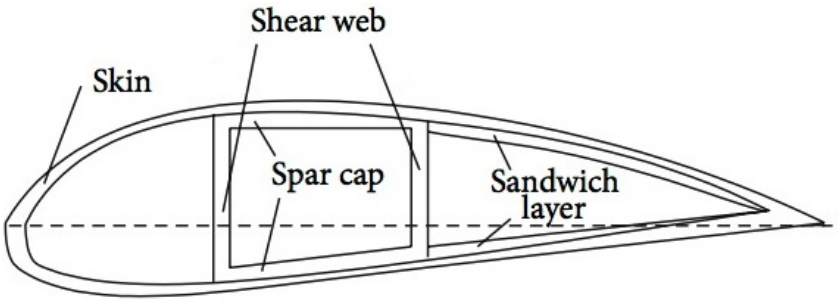


FIGURE 2.6: Typical Cross Section of a Wind Turbine Blade [4].

Currently, manufacturers are seeking greater cost effectiveness by increased turbine size rather than minor increases via improved blade efficiency. Although, blade aerodynamic (and structural) optimisation are still focus of much research and development, there is a shift in focus to understand better the limitations of big blades as larger models become problematic because of construction, transport and assembly issues.

New concepts such as "split blade" (the blade is divided in several pieces to be assembled on site during wind turbine installation, see Fig. 2.7) are often discussed and could dominate the market in a near future ,once (if) the technology is mature enough.

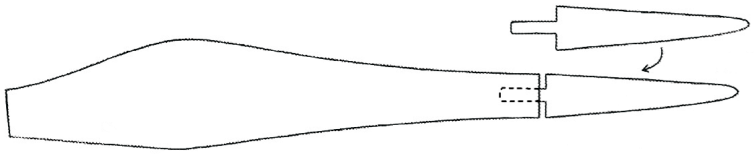


FIGURE 2.7: Split blade design [5].

Therefore, the traditional blade construction/design is likely to maintain its general shape and expected to increase in size until a plateau is reached. The discipline of blade optimization has been continuously investigated, and changes to blade shape may then occur as manufacturers incorporate new aerofoils, tip designs and structural materials [43].

Some of the main efforts in blades are developments with wide leading-edge nose and large camber, changes in the roughness of blade surfaces, damping and equilibrium state (i.e. the blades steady deformation shape under operating loads).

2.6 Blade sources of uncertainties

On this section the blades' source of uncertainties are introduced, these sources can impact directly the blade's behaviour in operation but they also impact the accuracy of engineering models established, i.e., the effect of these uncertainties will bring deviations to the parameters considered in deterministic model predictions. Effects on material properties, manufacturing defects, geometric uncertainties, surface roughness are discussed:

1. Material properties:

   The effect of structural uncertainties and imperfections on the mechanical and thermal properties of composite materials has long been confirmed [44]. Many uncertainties in a wind blade design directly affect the material properties or are more easily modelled this way (as epistemic uncertainties in the material properties), meaning that phenomena that changes or deteriorates materials properties are modelled directly as deterioration of the properties they cause. Random defects can potentially become stress concentration regions which may evolve into sites for damage initiation. The deviation from the idealised material architecture, which is mainly introduced to the system during manufacturing, can be found at various scales of the material and must be accounted for while modelling [45]. Hu [46] extensively discusses composite-material property characterisation, including the physical phenomena that may be responsible for the uncertainties.

2. Material sensitivity to environmental conditions:

   Composite materials can be degraded by environmental attack, such as moisture diffusion, thermal spikes, ultraviolet radiation, and thermal oxidation, among many others. If no model is available, this effect is seen as a pure aleatory uncertainty in the material properties of the composite and/or in the failure mode. The main challenge is to have a model that is detailed (and accurate), enough to describe both the sensitivity and the environmental conditions. Nevertheless, this uncertainty source is expected to show both epistemic and aleatory natures.

Li [47], showed that moisture diffusion can decrease the strength of composites, degrade the fibre/matrix interface and swell and plasticise the resin to lower its glass transition temperature. These effects support the requirement of having adequate characterisation of the environment the blades are required to withstand.

3. Manufacturing defects:

   According to Griffin [48], a number of production-related flaws may occur in larger structures, which can be avoided in smaller structures, and rarely appear in test coupons. Typical of these, are fabric joints, overlaps of adjacent rolls of fabric, and flaws where individual strands terminate during production. Other factors which are more likely in larger blades include: fibre waviness, large-scale porosity, large resin-rich areas, and resin cure variations through the thickness. These factors can have an unpredictable effect on the behaviour of the structure, and directly affect stiffness. Large blades are likely to use the heaviest-possible reinforcing fabrics or prepreg ply thickness to achieve manufacturing efficiency. Increases in fabric weight, and therefore thickness, may affect basic in-plane properties, delaminations, and problems associated with ply drops [49]. Moreover, thick composite laminates have an increased likelihood of hidden flaws and multiple flaws being grouped in the same local area. Most of these defects have aleatory behaviour and are hard to model or predict, but can still have a large effect on the overall response of composite structures.

4. Geometric:

   Ernst [50], asserts that the estimation of failure probabilities caused by ultimate or fatigue loading, as well as the calibration of partial safety factors for wind turbines, has been the focus of numerous studies. However, no detailed information about geometric uncertainties of the rotor blades and how these can be modelled are available. Geometric tolerances have to be determined in the design, and be consistent with assumptions and documented in the drawings/design specifications, because they can have a considerable effect on the rotor performance, besides being a requirement for certification [51]. Wind-turbine blades, are typically moulded in two halves which are bonded together. Because of the manufacturing process and the large dimensions of the rotor blades (see [1]), significant variations of the aerofoil and blade geometry can arise. Furthermore, there are also unknown deformations during operation. These unknowns influence the aerodynamic loads, which also affect the reliability of other wind-turbine components, meaning that

uncertainties in geometry have contributions from both epistemic nature (as there might be steps to produce a more precise geometry during production) and aleatory, because some deformations (or deviations from expected geometry) are caused by random, unpredictable events.

5. Testing/Experimentation:

   The goal of a blade fatigue test is to verify that the as-built blade structure is capable of sustaining the full spectrum of loads it will experience during its lifetime. A typical wind-turbine load spectrum may consist of more than 500 million load cycles, occurring over a wide range of load amplitude ratios. To determine the test load, the design loading is compressed by increasing the load/amplitude and a damage-equivalent load is computed to achieve the same total damage in a fraction of the number of cycles [52]. Traditionally, full-scale tests are performed on a very limited number of samples; only one or two blades of a given design are tested so that no statistical distribution of production blade strength can be obtained [53], which makes difficult the assessment of uncertainties in the test itself. As discussed by Nielsen *et al* [53], for complicated composite structures such as wind turbine blades, this type of accelerated test is often questioned because of the uncertainty related with the S/N curve approach and because the Palmgren-Miners rule is highly questionable for composite materials and structures. Design decisions based on such information are then affected by both inaccurate modelling and aleatory uncertainty.

6. Damping:

   The damping properties of large composite components are influenced by interfaces and local inhomogeneities resulting in uncertainties and nonlinearities of the characterising parameters. Available numerical models are not yet sufficiently accurate to capture the relationship between damping and its effects in a composite structure [54], and often refer to a simplified model of the blade. For instance, the influence of the deflection on the damping behaviour cannot be modelled by using existing material models, even though this influence has been experimentally demonstrated; this can be interpreted as epistemic uncertainty. For that reason, the real dynamics of such structures are consequently described incompletely or with limited accuracy, if the damping is not taken into account, being an important source of epistemic uncertainty affecting the dynamics of wind turbine blades.

7. Aerofoil surface roughness:

   The performance of wind-turbine aerofoils - measured in terms of the aerodynamic coefficients of lift, drag, and moment - is considered a major source of uncertainty in wind-turbine simulation. During operation, the surface of a blade can be contaminated by dust, dirt, insects, erosion, etc. The changes in surface roughness during operation may result in significant uncertainties in power capture and loading [55]. Special attention has been given to investigate the effect of uncertainties on aerodynamic behaviour of blades, traditionally surface roughness is simulated via the application of zigzag-tape (or tripwire) in wind-tunnel experiments, so that a "rough behaviour" can be defined [56]. This way, for any given section along the span of a blade a designer can choose to use clean, rough or moderate roughness aerofoil characteristics [57]. Thick aerofoils (which are normally used close to the root section), respond differently to surface roughness than slender aerofoils (normally used towards the tip of the blade). The expected level of contamination also differs through the blade span; thus, the motivation to understand roughness effects can be related to different things, for example, if the sensitivity towards roughness is reduced for inboard aerofoils, the design can primarily focus on the high structural demands, while for outbound aerofoils could mean a more robust aerodynamic performance. Because the boundary layer towards the tip of the blade is much smaller than at the root (for standard multi-mega Watt turbine blades length there can be a boundary layer thickness difference of 3x between these two regions), therefore the surface roughness impact on the aerodynamic performance of tip of the blade is much higher.

2.7 External conditions uncertainties

Uncertainties in external conditions have an utmost importance in the design of wind turbines. Both (but not only), loads calculations and optimisation of operational parameters rely on a truthful characterisation of such factors. Van den Bos [3], reviews the most influential sources of uncertainties on external conditions, including: wind modelling, sea climate, airflow and wake effects. Other contributions to UQ in external conditions are found in [58], [59], [60], [61], [62], [63], [64] and others.

Generally in these studies, only a few uncertain parameters are taken into account; this is because of the computational cost associated with propagating a large set of

uncertain parameters in a model. The statistical approach has classically been the basis for many wind and wave models. Physics-based models are now increasing in fidelity and popularity because of continuing advances in computational power and methodology. Another growing trend in the wind community is the use of data-driven techniques for the derivation of simplified models. These data are often obtained from high-fidelity models, although experimental data can in principle be used as well; this has received little attention so far [3].

Chapter 3

Blade testing - from laminate to full-scale testing

3.1 Introduction

This chapter introduces the experimental base of this research. The experiments described here were conducted by Siemens Gamesa Renewable Energy in Denmark, or by a specialised technical laboratory under contract with the company. Even though the research described in this report did not design all of the experiments, blade static deflection tests were followed closely in the Siemens Gamesa Aalborg facility. All the other experimental data was made available through a data report and method statement.

Raw data are neither shared nor displayed because of privacy (commercial) restrictions.

Following Figure 3.1, this chapter will present experimental (statistical) results from tests iat three different scales: Laminate, blade profile and full-scale blade tests. These data will be later used to build and/or validate probabilistic models of the blade and blade-related quantities.

In the laminate-testing section, only the first statistical moment of the experimental data was available. For the blade mass, centre of gravity, static deflection and natural frequencies, the data are normalised by their mean value. In sections 3.2 to 3.6, a brief introduction to the experiments is given, together with raw data, which are authorised to be shared.

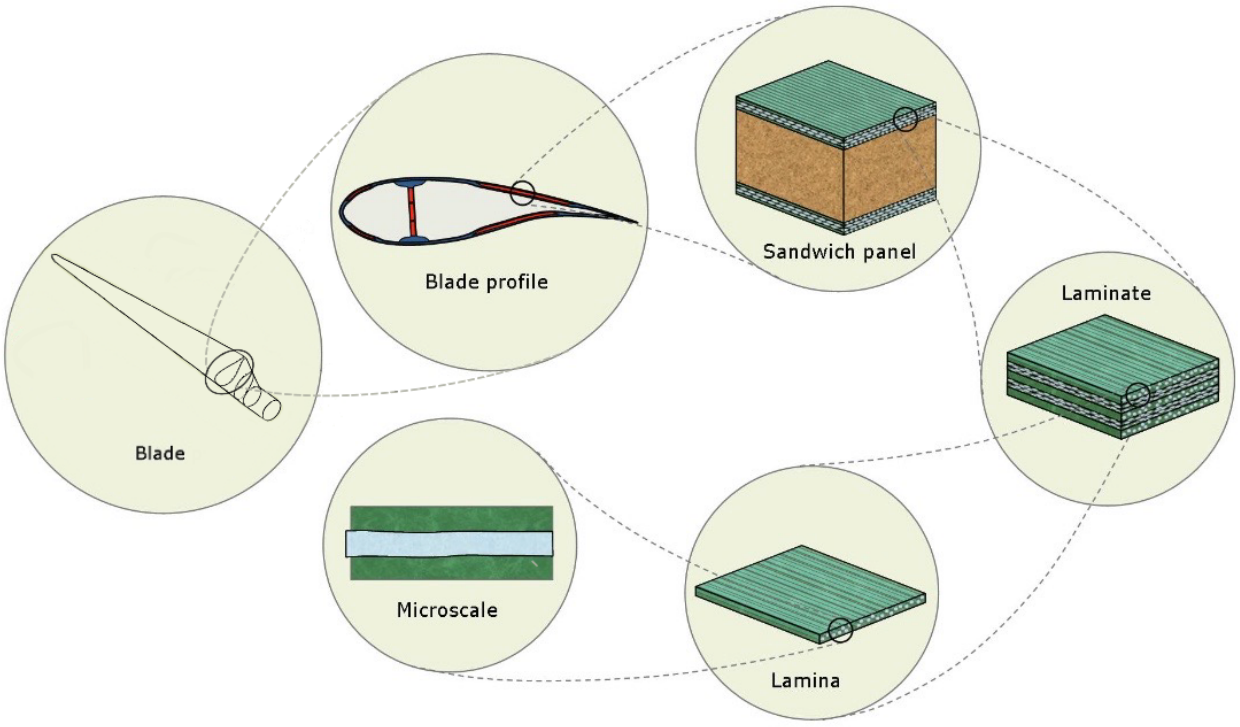


FIGURE 3.1: scales in composite materials and structures. Adapted from [6].

3.2 Laminate coupon testing

In order to define the material properties of the laminate used in the blade (which are the inputs to blade models used in the development), Siemens Gamesa Renewable Energy (SGRE) employs several tensile tests both made in house or accredited laboratories [7] . The specimen of these tests are coupons cut from blade panels. These are manufactured in the same process used during the manufacturing of wind-turbine blades without any heat treatment applied after curing.

The material behaviour of these laminates (see Table 3.1) can be described by six elastic variables, namely the modulus of elasticity along the fibre directions and transversely to it, denoted by E_1, E_2 and E_3, respectively. The in plane shear moduli, G_{12}, as well as the out-of-plane G_{13}, G_{23} are also defined. The thickness and density of the coupons are also recorded and are representative of the variation that can happen in the production of blade laminates and sandwich configurations, illustrated in Figure 3.2. The first sub-figure shows the specimen ready and fitted with the strain gauge sensors before the test, the second sub-figure was taken during the test and the last sub-figure shows the specimen after destructive testing.

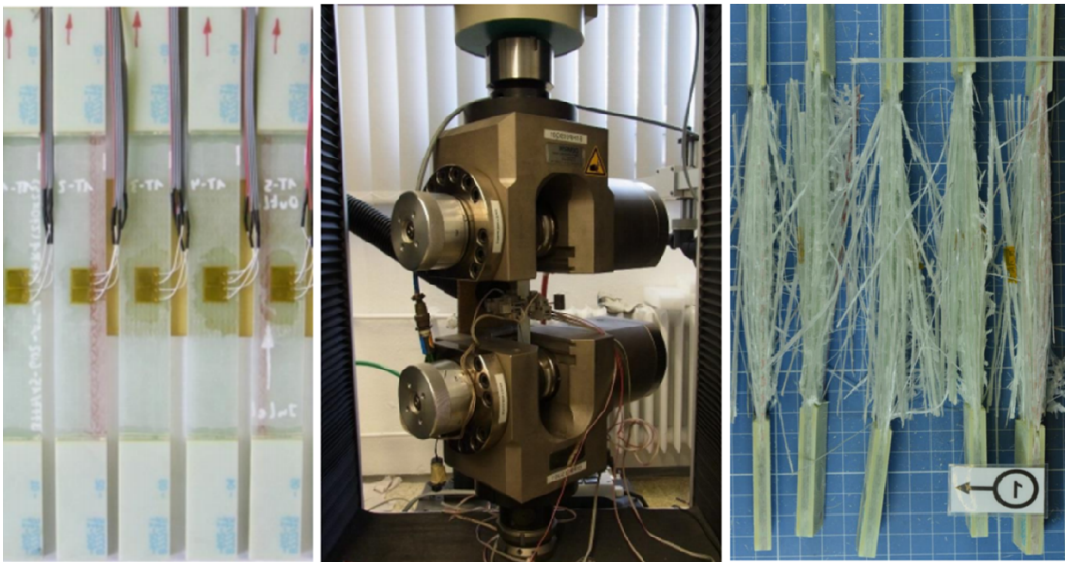


FIGURE 3.2: Laminate coupon testing [7].

TABLE 3.1: Uncertain parameters description

Property	**Description**
E11	Modulus of elasticity in direction 1 [Pa]
E22	Modulus of elasticity in direction 2 [Pa]
E33	Modulus of elasticity in direction 3 [Pa]
G12	In-plane shear modulus of elasticity [Pa]
G13	Out-of-plane shear modulus of elasticity [Pa]
G23	Out-of-plane shear modulus of elasticity [Pa]
ρ	Laminate density [Kg m^3]
t	Laminate thickness [m]

The experimental information available, where the number of tests and coefficient of variation (equation 4.1) for each property, are presented at Table 3.2. The data was normally distributed.

$$CoV = \frac{s}{\bar{x}} \cdot 100\% \tag{3.1}$$

where s is the standard deviation and $\bar{x}$ the mean value (for a sample).

TABLE 3.2: Materials properties experimental CoV.

BIAX - Biaxial laminate					
Property	**CoV %**	**# test**	**Property**	**CoV %**	**# tests**
E_{11}	4	15	G_{12}	3	30
E_{22}	4	15	G_{13}	3	5
E_{33}	4	15	G_{23}	3	5
ρ	0.6	27	t	2	27
UD - Unidirectional laminate					
Property	**CoV %**	**# test**	**Property**	**CoV %**	**# tests**
E_{11}	3	15	G_{12}	3	15
E_{22}	5	15	G_{13}	3	15
E_{33}	5	15	G_{23}	3	15
ρ	0.6	9	t	3	9

3.3 Blade weight and centre of gravity

In order to characterise the blade's mass and centre of gravity (CG), an indoor crane equipped with load cells at every hook lifted two points on each root and tip transport structure as illustrated in Figure 3.3. With the blade remaining still and horizontally suspended, the forces at each suspension point and their radial position were recorded. After weighing the support structures, this value is subtracted from the total recorded load at the measurement devices, to obtain the total blade mass. The mass of the blade bolts is also subtracted from the total mass. The CG is obtained by calculating the moment equilibrium with the measured loads with respect to a pivot point, in this case the blade-root centre. This procedure was performed along the blade span direction. Tables 3.3 and 3.4 present the normalised (by the mean), results of the experiments. In total, 96 blades of the same model were tested within the same conditions. In Figures 3.4 and 3.5, one can see the histogram and quantile-quantile plots where the normal-like behaviour of the distributions can be noted. Covs are presented in Table 3.5. For CG location the min value was 0.9890 and the max 1.016, for blade mass, min value was 0.9845 and max 1.0232, and both data sets can be seen to be approximately normal, with a mean near 1.0 and only minor skewness or kurtosis effects. The tails suggest a few slightly more extreme observations, but overall the distribution fits normality well.

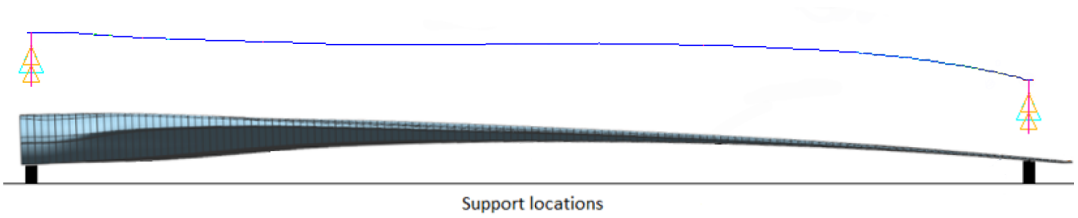


FIGURE 3.3: Setup for mass and centre of gravity measurements.

TABLE 3.3: Normalised blade CG location - experimental.

1.0013	1.0050	0.9934	1.0142	1.0006	0.9986	0.9957	0.9954
0.9954	0.9979	0.9938	0.9890	0.9998	1.0008	1.0016	0.9938
0.9995	0.9999	1.0031	0.9980	1.0012	1.0004	0.9966	0.9980
1.0019	0.9974	0.9949	1.0013	0.9989	1.0061	0.9997	1.0084
1.0104	1.0045	0.9976	0.9972	1.0001	1.0012	0.9987	1.0016
0.9973	0.9996	0.9974	1.0012	1.0032	1.0017	0.9974	1.0026
0.9978	1.0130	1.0023	1.0053	0.9986	0.9980	1.0007	1.0011
0.9988	0.9959	1.0015	0.9951	0.9997	0.9957	1.0006	1.0027
1.0036	1.0034	1.0066	0.9982	0.9914	1.0070	0.9913	0.9994
1.0050	1.0012	0.9979	1.0021	0.9943	0.9977	0.9891	0.9979
1.0025	1.0039	0.9999	0.9972	1.0160	1.0045	1.0017	0.9951
1.0054	1.0018	1.0009	0.9948	0.9951	0.9969	0.9978	

TABLE 3.4: Normalised blade mass - experimental.

0.9896	0.9946	1.0008	1.0058	0.9972	1.0009	0.9852	1.0017
0.9989	1.0066	0.9962	1.0117	0.9930	0.9911	0.9958	0.9921
1.0186	0.9988	1.0006	1.0090	1.0065	0.9925	1.0157	0.9967
0.9946	0.9933	0.9859	1.0030	0.9894	1.0032	1.0036	1.0075
1.0068	0.9876	0.9941	1.0191	0.9919	0.9911	0.9948	1.0057
0.9907	0.9915	0.9990	0.9987	0.9987	0.9999	1.0046	0.9979
1.0128	1.0043	1.0007	0.9927	0.9937	0.9845	1.0106	0.9942
0.9953	1.0158	0.9964	0.9928	1.0187	0.9928	0.9989	1.0040
0.9997	1.0032	1.0045	1.0205	1.0017	1.0016	0.9948	0.9951
0.9912	1.0121	0.9984	0.9975	1.0072	0.9974	0.9973	1.0010
0.9845	0.9955	1.0014	1.0232	1.0220	0.9985	0.9972	0.9905
1.0124	0.9978	1.0014	0.9978	1.0071	0.9927	0.9944	

TABLE 3.5: Materials properties experimental CoV.

Property	**CoV %**	**# test**
Mass	0.92	96
CG	0.55	96

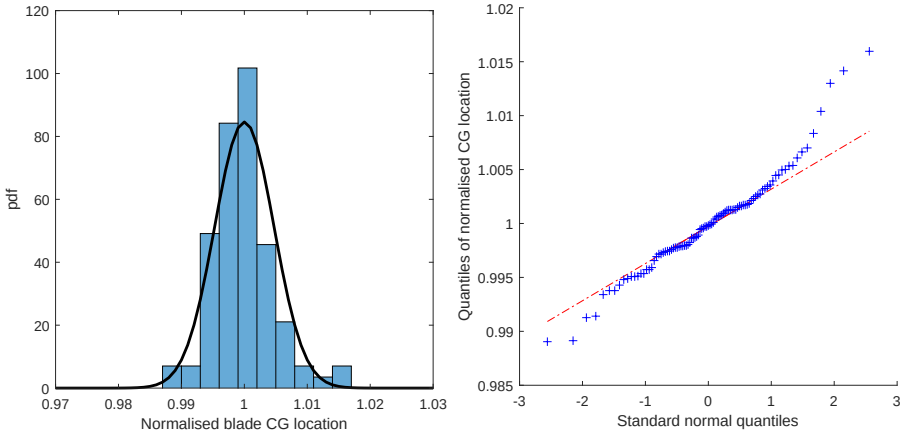


FIGURE 3.4: Histogram and qq-plot: Blade CG location.

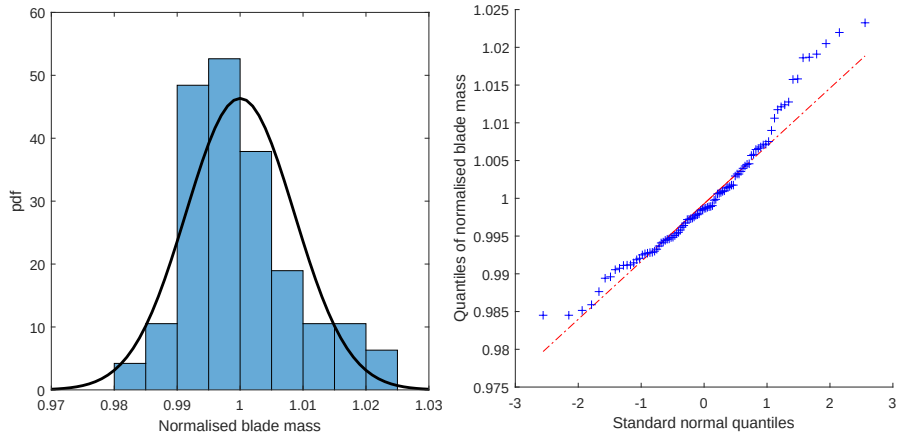


FIGURE 3.5: Histogram and qq-plot: Blade mass.

3.4 Blade static deflection test

The following experiment is carried out to ensure a sufficient blade tip-to-tower clearance. Per IEC [65] standards, a blade-to-blade variation factor is introduced to account for the stiffness variation of production blades, the default value of this factor is 1.1. This value ensures that production blades with stiffness lower than the analytical prediction by up to 10% still meet the tip-to-tower clearance requirement. The blade-to-blade variation factor can be lowered accordingly if the flapwise stiffness of each production blade is proven to be within the lowered variation. The test shown in Fig.3.7 can be described:

- Blade supported in positions 0 and 0.5L (measured horizontal from blade root), pressure side pointing upwards.
- Mold division-line level (parallel to ground). This is 5.625 degrees rotated with respect to the 0-chord line.
- Root end flange tilted 3deg (so that the tip is moved towards the ground).
- One load is applied to the blade in position 0.973L upwards away from the ground:
- Deflection from the loading in position 0.99L is recorded.

The comparison between predicted stiffness (and deflection), with the experimental results is discussed in Chapter 4. Normalised (by the mean), results for 33 identical blades tested under the same conditions, with the same test rig are shown in Table 3.6. Histogram and quantile-quantile plots of this data can be seen in Figure 3.6. The data have a CoV of 2.16%.

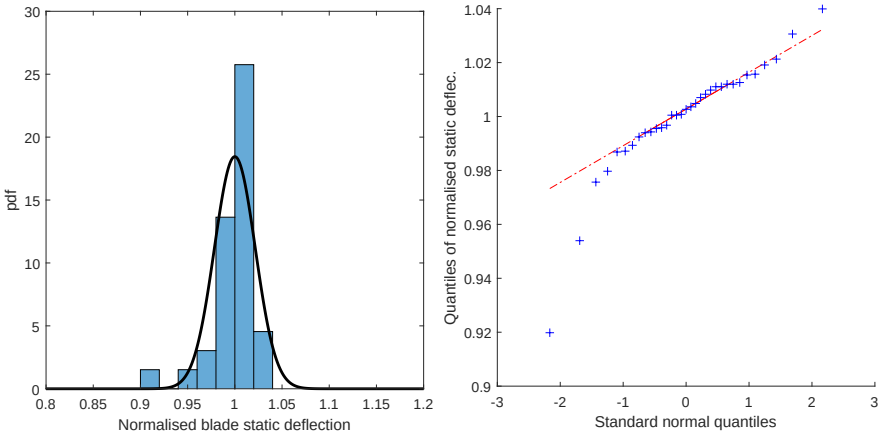


FIGURE 3.6: Histogram and QQ-plot: static deflection.

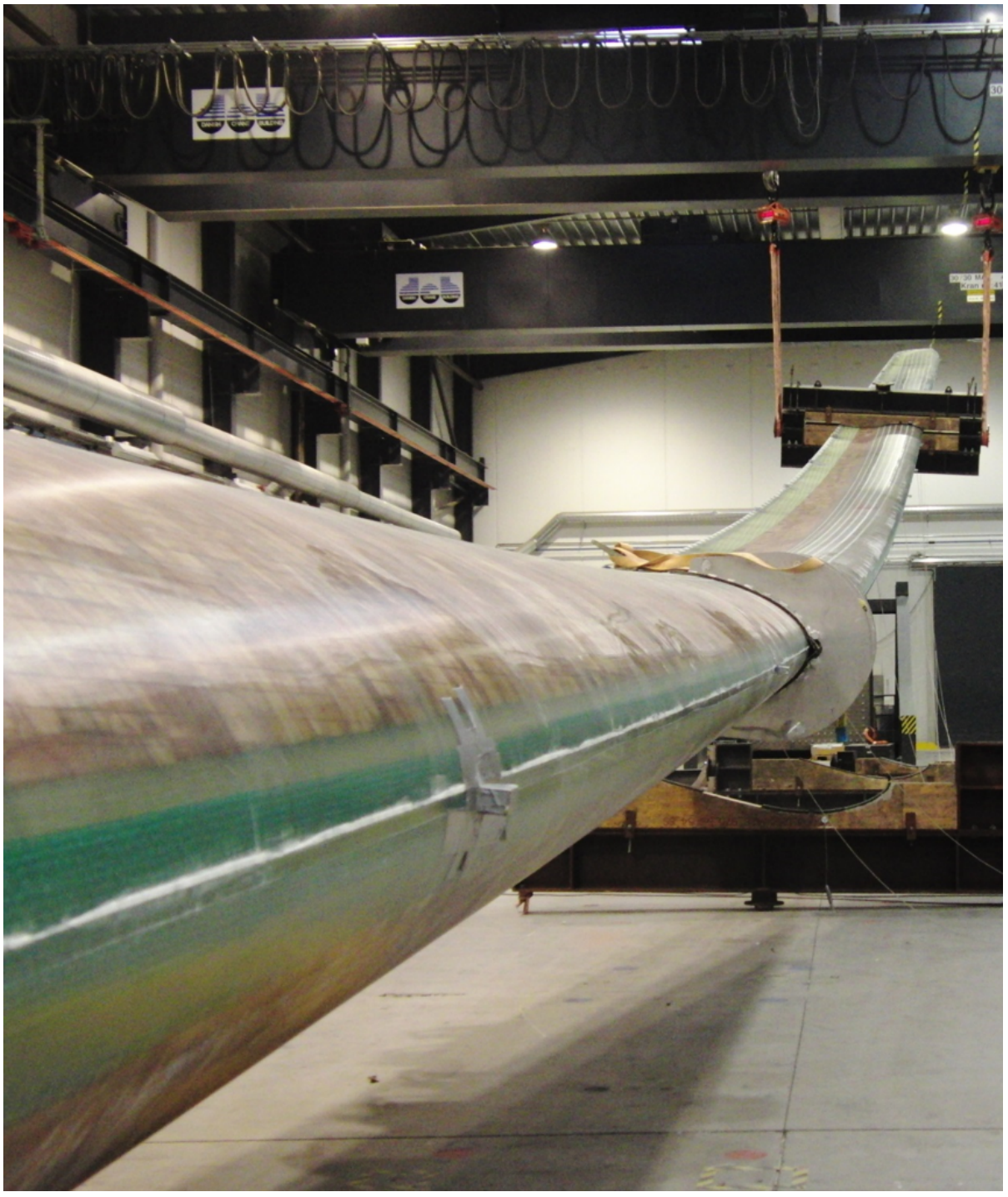


FIGURE 3.7: Blade static deflection test.

TABLE 3.6: Normalised static deflection - experimental.

1.0005	1.0036	1.0120	0.9872	0.9955	1.0110
0.9797	0.9757	0.9924	0.9868	1.0048	0.9539
1.0027	1.0110	1.0005	1.0126	0.9198	0.9968
1.0213	1.0008	0.9958	0.9940	1.0191	0.9943
1.0157	0.9893	1.0306	1.0070	1.0098	1.0154
1.0399	1.0083	1.0120			

3.5 Operational modal analysis

An Operational Modal Analysis (OMA) [66], has been performed on a blade (of the same type as previously discussed in this chapter), a picture of the experiment can be seen in Fig.3.8. A measurement grid consisting of 22 points has been applied on the blade, measuring in all three translational directions. Hence, 66 degrees of freedom have been measured. Within the frequency range used, a total of 15 modes have been found to be well estimated, as can be seen in Figure 3.10. Clamped at-the-root boundary conditions were applied after the blade manufacturing, with leading edge upwards. The blade was excited using an impact hammer with a soft tip at a total of eight excitation points. Sensors distributed along the blade recorded the deformations, and the mode frequencies and shapes were extracted from the measurements. Because of the confidentiality of the blade modal parameters, the natural frequencies are not included in Table 3.7, but these are used in Chapter 4 for model validation. The Modal Phase collinearity (MPC) score is also presented in Table 3.7, these represent the how the mode shape vectors align in phase across different measurement points. For scores near 1 or 100%, it means they have a strong phase consistency and the model identified is clear without interaction from different modes.

TABLE 3.7: Operational modal analysis results summary.

Description	Damping ratio [%]	MPC [%]
1st flapwise	0.25	99.14
1st edgewise	0.23	99.93
2nd flapwise	1.89	99.40
2nd edgewise + 2nd flapwise	0.37	99.97
2nd edgewise + 2nd flapwise (2)	0.35	99.99



FIGURE 3.8: Operational modal analysis - blade in test.

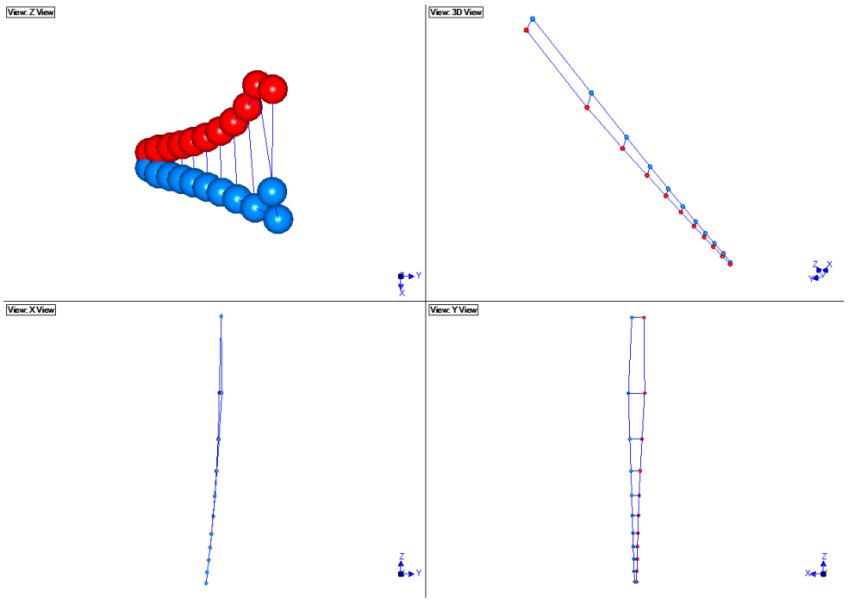


FIGURE 3.9: Measurement grid used. 11 points on the leading edge (blue) and 11 points on the trailing edge (red). Total 22 points.

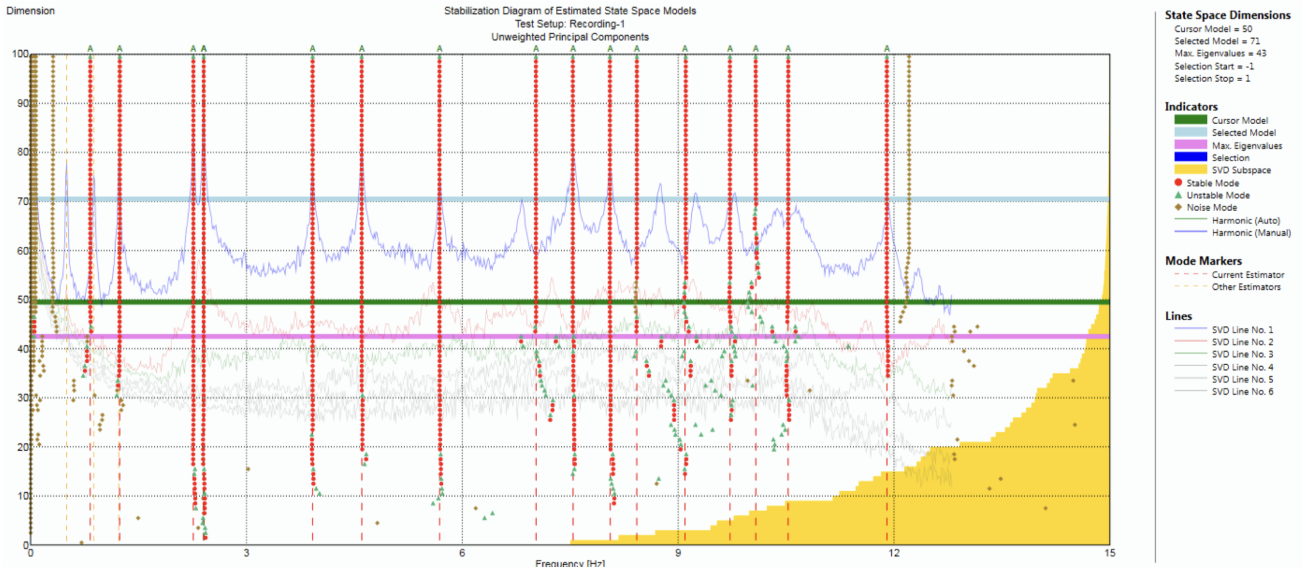


FIGURE 3.10: Oma results, adapted from [8].

3.6 Wind tunnel measurements

This section presents the wind-tunnel measurements on which the model developed in Chapter 5 is based. The raw data, and specific information about each experiment is owned by Siemens Gamesa and its reproduction is not authorised because of commercial restrictions.

The data are a historical collection of tests performed with two different surface roughness conditions. The aerofoil model used has a relative thickness of 18% .

In all tests, the default value of Reynolds number is Re = 4e6. The same aerofoil specimen was used for the 18 different runs on the clean surface roughness condition.

Two independent wind tunnels with a closed test section were used to perform these experiments: One for the clean conditions testing and one for the rough condition testing. Different turbulence intensity levels and different blockage ratios (ratio between frontal area of the object and cross section of the wind tunnel - normally kept between 3 and 5 %) were used. These two factors are the main drivers for the differences seen when testing the same roughness conditions. Such variation in experimental setup is to simulate variations encountered in airflow naturally.

The rough conditions are modelled with the use of ZigZag tape of different thicknesses, varying between 0.2 and 0.6mm in regions between 2-5% of the chord on the suction side, and 5-10% of the chord on the pressure side.

Figures 3.11, 3.12, show the normalised data of the clean aerofoil and Figures. 3.13, 3.14 of the rough aerofoil. Figure 3.15 shows all the experimental points together, where one can observe the effect of roughness (and the scatter between different experiments). These effects will be discussed and described in depth in Chapter 5, but the results show that the clean airfoil achieves higher maximum lift and lower drag at moderate angles of attack, whereas the tripped airfoil experiences earlier stall, reduced peak lift, and a consistent drag penalty due to forced boundary-layer transition.

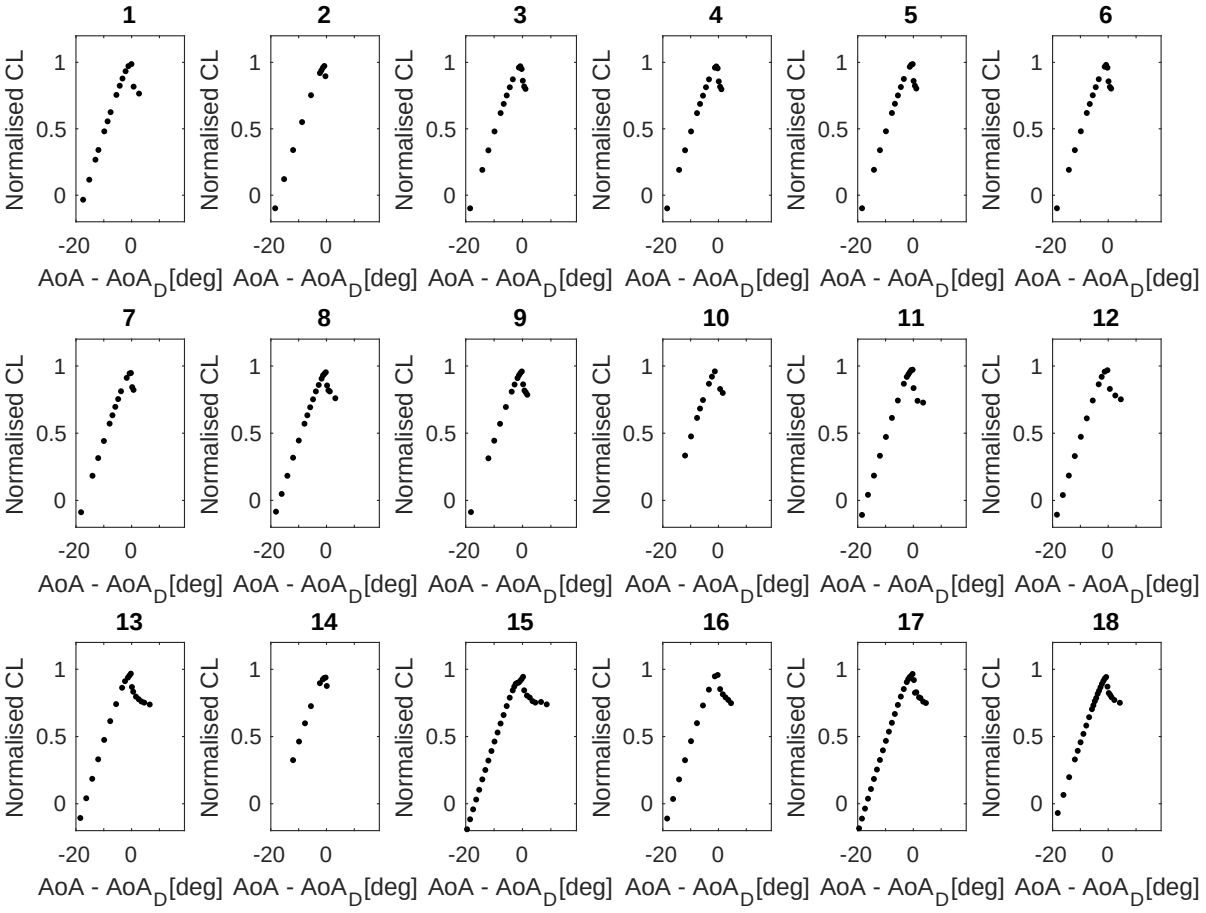


FIGURE 3.11: Wind tunnel test data: CL - clean measurements.

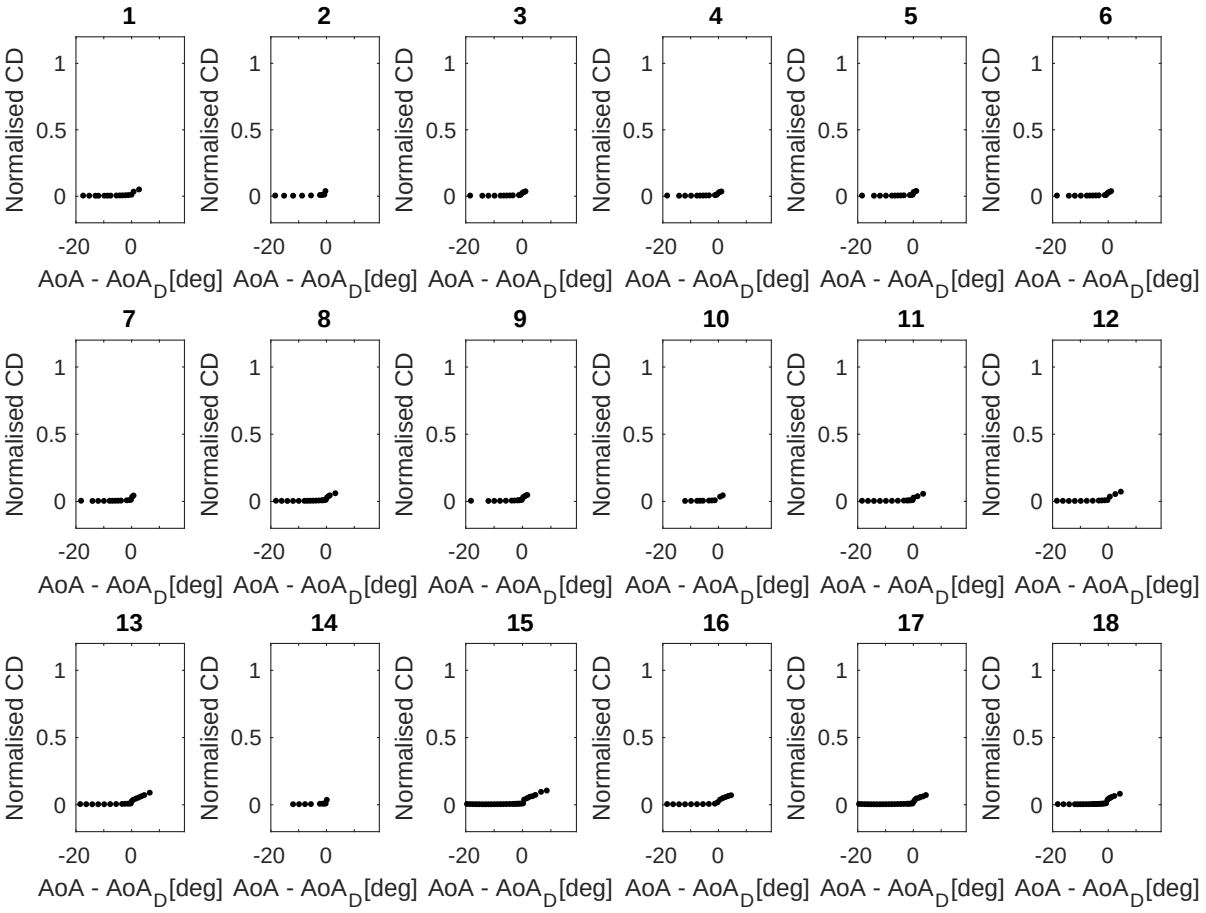


FIGURE 3.12: Wind tunnel test data: Cd - clean measurements.

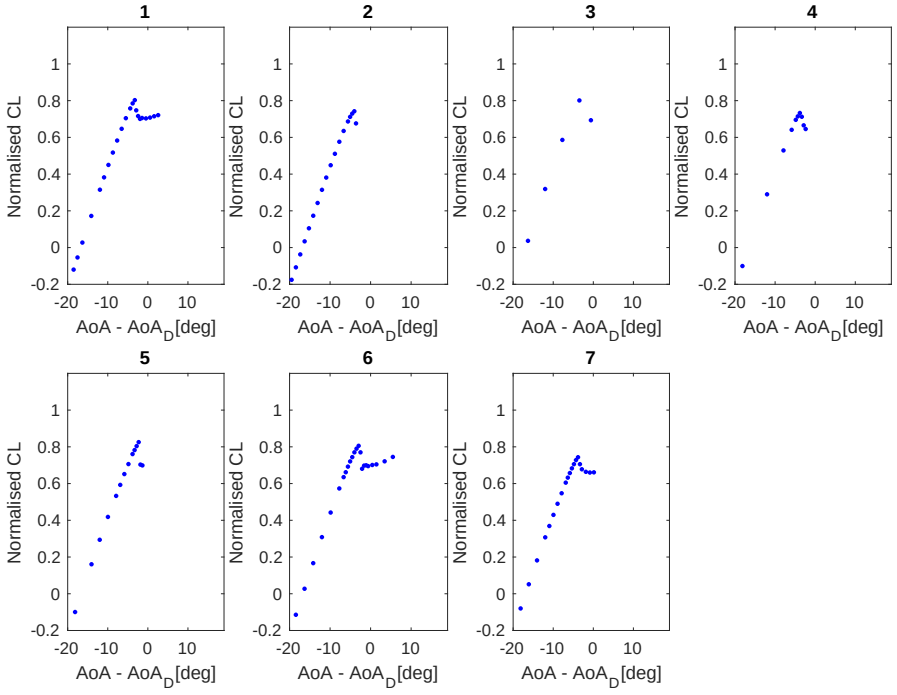


FIGURE 3.13: Wind tunnel test data: CL - Rough measurements.

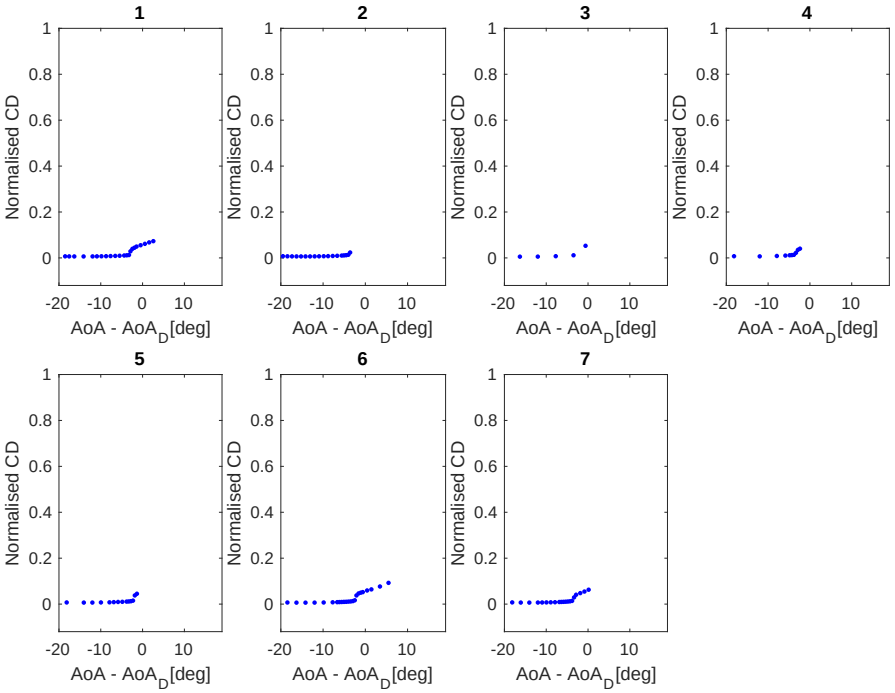


FIGURE 3.14: Wind tunnel test data: CD - Rough measurements.

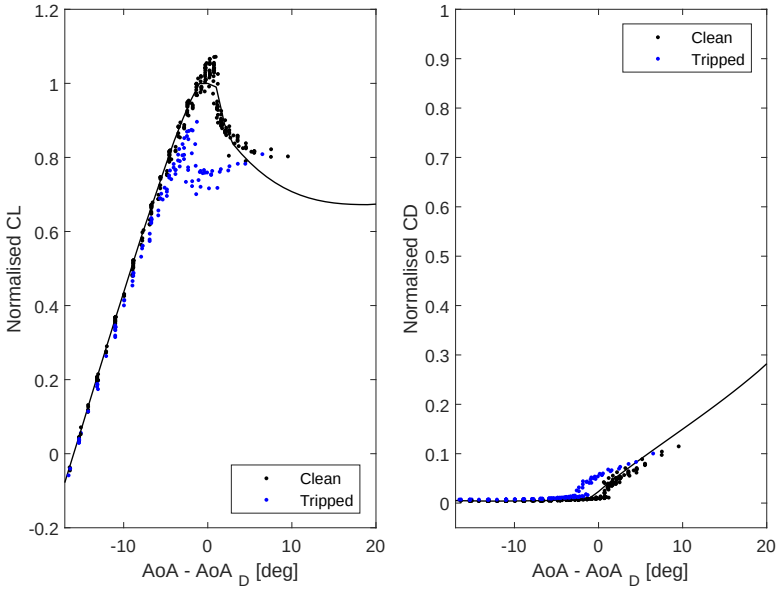


FIGURE 3.15: Wind tunnel test data.

3.7 Chapter summary

This chapter presents the experimental data owned and experiments conducted by Siemens Gamesa Renewable Energy used throughout the following chapters. The design of experiments was also not developed as part of the research described in this report, and all the tests rigs, sensors, samples, blades and procedures are owned by Siemens Gamesa Renewable Energy. Although some details related to its experimental procedures have not been included in this report due commercial restrictions, the data will be extensively analysed and utilised to build and validate probabilistic models related to wind-turbine simulations in the next chapters. Such experimental apparatus, composed of several testing scales (from coupon to full-scale blade test) of the same wind-turbine blade, are seldom available, therefore it is important to acknowledge the industrial partnership on which this research is based and acknowledge its origin and ownership when analysing, building models and comparing to simulations.

Chapter 4

Blade Structural Uncertainties

4.1 Introduction

The blades of a wind turbine are constructed by combining different composite materials - including glass and carbon fibre reinforced polymers with different fibre orientation - and a core material (typically wood or foam). The blades are required to withstand a diverse range of loads, while maintaining their aerodynamic profile, and have a useful life of 20 years or more. These requirements mean that every aspect of their design, installation, operation and maintenance must be optimised.

Structural performance can be directly affected by uncertainties associated with models, making it harder to specify resistance and loadings. The conventional design approach has been to adopt characteristic values and safety factors to compensate for structural variations resulting from the production process.

In order to reduce uncertainties, the wind turbine standards I**EC 61400-1 and IEC 61400-22**, require that tests are performed. These tests can be divided into three different scales: coupon, component and full-scale as shown by Fig.4.1.

At *coupon* scale, the basic material properties, along with their physical and statistical uncertainties are characterised. Probabilistic models of the material properties for blade laminates are described in the following section.

At *component* scale, elements of the blade are tested, e.g., panels with the basic material, aerofoils, connections in the blade or parts of the full-scale blade, etc. This scale can therefore be considered as an intermediate test level.

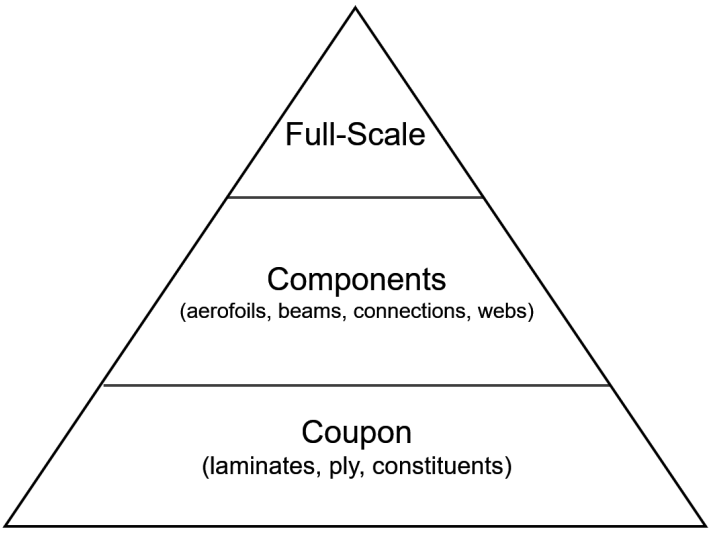


FIGURE 4.1: Scale of wind turbine tests.

At *full-scale* the real blade structure is tested in order to verify the strength and estimate the model uncertainty related to the design models.

Probabilistic analysis permits a more rigorous quantification of the various uncertainties, and ultimately will facilitate a more efficient design. Quantifying the confidence and predictive accuracy of model calculations is a necessary step toward model verification and validation (V&V); this is an enabling methodology for the development of computational models that can be used to make predictions with quantified confidence [67].

This chapter introduces the structural uncertainties of the blade and the application of a UQ framework based on Monte Carlo simulation of a structural model of a wind-turbine blade. The quantities of interest (QoI) are the blade stiffness distribution, mass and centre of gravity (CG) location and static deflection under a specific loading. The material properties of the two main types of blade laminates are characterised as random inputs whose uncertainties are propagated to the QoIs . Statistical hypothesis tests are used to compare/validate the model against the experimental data presented in Chapter 3. A Gaussian process emulator is used to conduct sensitivity analysis on the material properties. Results are compared to the tolerances defined by the IEC standard [68].

4.2 Material properties as random inputs

The properties of a composite are dependent on the material properties for the fibre and matrix materials, along with the manufacturing process. Generally, the material

properties can be modelled at different scales, from the micro-scale considering the adhesion between fibre and matrix, meso-scale where the individual lamina or ply properties are considered or macro-scale where the laminate (sequence of laminae) properties are of interest. Fig. 4.2 shows the three different scales. The material properties referred to in this study are associated with the laminate/macro-scale of the material.

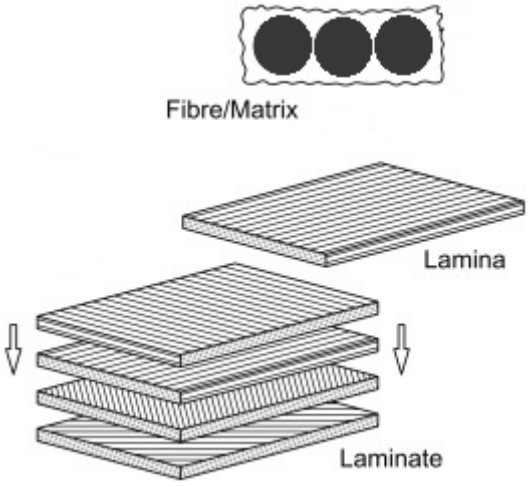


FIGURE 4.2: Laminate definition, adapted from [9].

At the macro-scale ,the material properties are determined based on tests with coupons of the composite laminates. From these tests the material properties for the laminate can be determined, resulting in models for the uncertainties.

The uncertainty in the material properties of the two main types of glass-fibre (illustrated in Fig. 4.3) reinforcements used in the blades will be investigated:

- BIAX (Bidirectional glass-fibre laminate): The fibres in a bidirectional material run in two directions, typically 90 degrees apart. These ply orientations have strength in both directions but not necessarily the same strength.
- UD (Unidirectional glass-fibre laminate): The fibres in a unidirectional material run in one direction and the strength and stiffness is only in the direction of the fibre.

As discussed in Section 2.6, there can be many factors altering the standard behaviour expected from a glass-fibre composite, including random uncertainty during production. In order to include these uncertainties in the blade structural evaluation, its critical

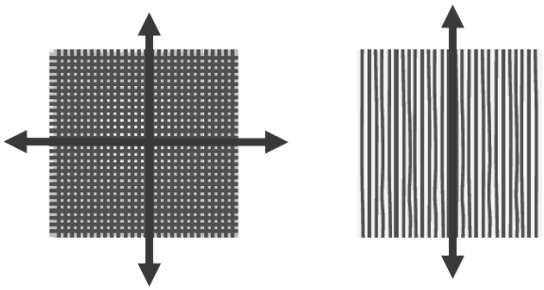


FIGURE 4.3: Unidirectional vs Bidirectional fibre orientation.

to have a valid characterisation of these uncertainties as the material properties are (together with geometry and layup), the main inputs for a blade structural model.

The characterisation of uncertain inputs will have a major effect on the interpretation of the uncertainty behaviour of the system. Bigoni [14], defines three main approaches to the *probability distribution estimation* of inputs:

- Assumption: probability distributions for the parameters are defined relying on experience and wisdom.
- Inference: the probability distributions are reconstructed using measurements of the quantity of interest.
- Measurement: measurements of the parameters are carried out, and probability distributions are fitted to these experiments.

The last approach is always preferred, but seldom available. The costs, effort and time necessary to characterise random parameters by experiments (that have to be repeated, generating enough samples to have a good pdf fit), are usually too high.

The access provided by Siemens Gamesa Renewable Energy (SGRE) to their material test database [7], allowed this study to be conducted with a measurement approach for the characterisation of the uncertainty in laminate material properties.

The material stiffness and strength for the glass-fibre laminates (defined in Table 4.1) are determined from material testing of actual fibre-resin and core materials that are representative of the production blade laminates and sandwich configurations, illustrated in Fig.3.2. Testing for each material property was carried out according to the relevant standards, e.g. [69].

TABLE 4.1: Uncertain parameters description

Property	**Description**
E11	Modulus of elasticity in direction 1 [Pa]
E22	Modulus of elasticity in direction 2 [Pa]
E33	Modulus of elasticity in direction 3 [Pa]
G12	In-plane shear modulus of elasticity [Pa]
G13	Out-of-plane shear modulus of elasticity [Pa]
G23	Out-of-plane shear modulus of elasticity [Pa]
ρ	Laminate density [Kg m^3]
t	Laminate thickness [m]

The experimental information available, where the number of tests and coefficient of variation (Eqn. 4.1) for each property, are presented at Table 3.2.

$$CoV = \frac{s}{\bar{x}} \cdot 100\% \tag{4.1}$$

where s is the standard deviation and $\bar{x}$ the mean value (for a sample).

For each type of fibre, the main material properties related to the main plane direction 1 and 2 and out of plane direction 3,(See Figure 4.4 and Table 4.1), were considered as random input parameters. CoV data from material testing and nominal values were used to fit probability density functions (pdf) to these inputs. The normal distribution was used for all variables, because with a normal distribution, the differential entropy is maximised for a given variance, [70], which means it is the least-assuming distribution one can use when having access to only variance and mean values.

4.3 Blade structural model

The cross-sectional model used in this study is based on the formulations of Krenk and Jeppesen [71]; utilising a line mesh in the calculation of the structural features, the torsion and shear properties of the cross-sections are formulated within a finite-element method (FEM) with the warping function as unknown. The cross section is divided into straight elements with uniform trapezoidal thickness. Every component is simplified and lumped into a thin-walled shell structure with the help of so-called superelements. The Crs (cross-sectional) model also calculates the sectional mass by summing the contribution of each layer of the laminate. The main inputs and outputs of this model can be listed:

- Inputs
  - geometry,
  - material layup,
  - material properties.
- Outputs:
  - blade stiffness distribution in flapwise, edgewise and torsional direction,
  - blade mass distribution,
  - moment of inertia distribution.

The QoIs for this study are the distributions of stiffness in flapwise (EI_X), edgewise (EI_Y) and torsional (GI_Z) directions, as well as blade mass and CG location. All are based on the blade reference frame shown in Fig.4.4A. Elastic moduli are termed in accordance with a material coordinate system seen in Fig.4.4B, where the 1-direction corresponds to the 0° fibre direction, running from blade root to blade tip.

The calculation is repeated for each cross section throughout the blade (Figure 4.4A), along the blade span. Deterministic stiffness and mass distributions can be seen in Fig.4.5A and B, normalised by their maximum value.

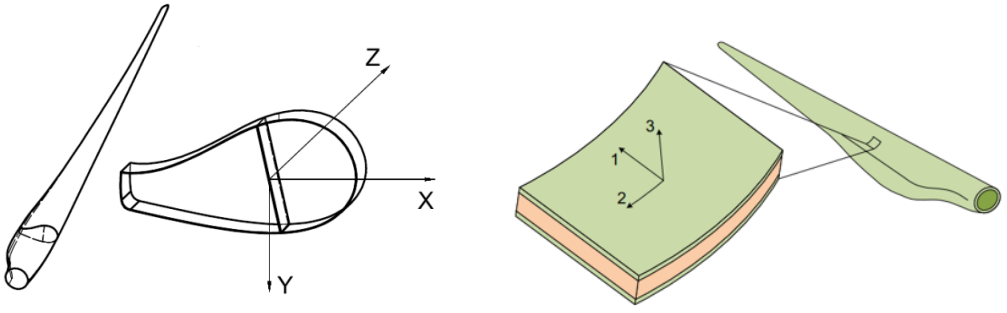


FIGURE 4.4: (A) Reference system for wind-turbine blade, (B) reference for material properties.

The blade layup is important information because, as can be seen in Fig.4.6, there are substantial differences of composition along the blade span; this will show that the type and quantity of laminate used for specific regions of the blade will have different impacts on its responses.

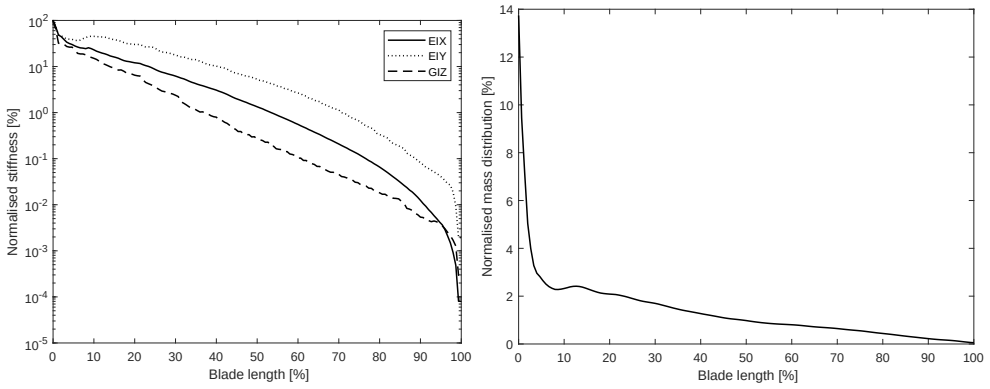


FIGURE 4.5: (A) Deterministic stiffness distribution, (B) Deterministic mass distribution.

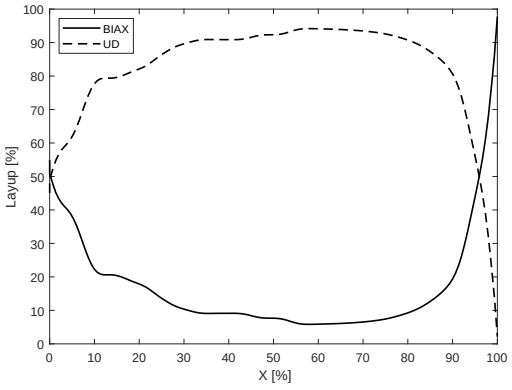


FIGURE 4.6: Blade layup.

4.4 Uncertainty propagation

The Monte Carlo Method (MC), is a widespread methodology for uncertainty propagation because of its straightforward implementation and, most importantly, non-intrusiveness to the deterministic model, as it can be applied with little to no alteration of previously implemented deterministic code. It consists of generating a set of N samples $\mathbf{X}$ from the pdf of $\mathbf{X}$ and using their outputs to estimate statistics. These estimates converge inevitably to the real probabilities as a consequence of the law of large numbers (as long as the number of samples is *large* enough and the random input characterisation is correct, on this research the large enough was found after doubling the number of realisations gave the same results in both first and second statistical moment). It can be summarised:

1. construct pdfs for random inputs;

2. randomly sample from the pdf;

3. evaluate the model for each sample;

4. use the collection of realisations to compute relevant; statistics of the quantity of interest.

Latin Hypercube Sampling (LHS) is widely used in Monte Carlo simulations as a way to improve accuracy and lower computational cost. LHS is a method to generate controlled random samples; the idea is to take the sampling-point distribution close to the probability density function (pdf). It involves dividing the cumulative density function (cdf) into n equal partitions and then sampling a specified number of random data points in each partition. LHS is typically used to save computer processing time when running Monte Carlo simulations. Studies have shown that a well-performed LHS can cut down on processing time by up to 50 percent (versus a standard Monte Carlo with random sampling) [72]. The fitted pdfs and histograms of the laminate property realisations can be seen in Fig.4.7 after applying LHS to generate random inputs for the blade structural model.

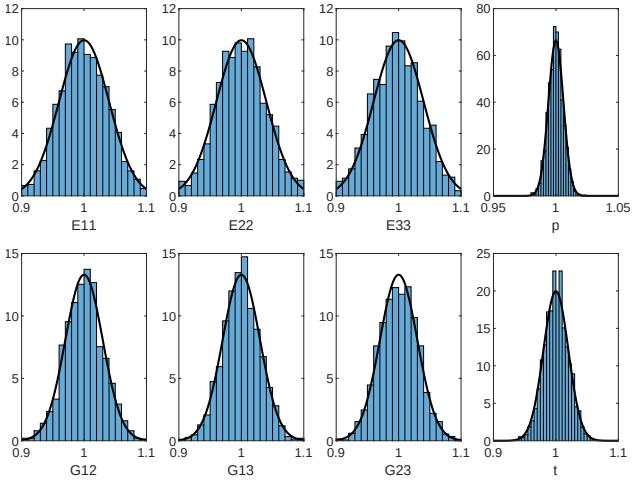


FIGURE 4.7: pdfs and histogram of BIAX properties realisations.

4.4.1 Stiffness and mass distribution

The design and load predictions on blades have had a continuous development with the evolution of high fidelity models. Wind-turbine blades became more flexible and their design more dependent on advanced physical description (more precise modelling) and require better understanding of deviations from the nominal behaviour. The main goal behind propagating uncertainty in the material properties is to determine whether (and if so quantify), there is an effect on the blade stiffness distribution.

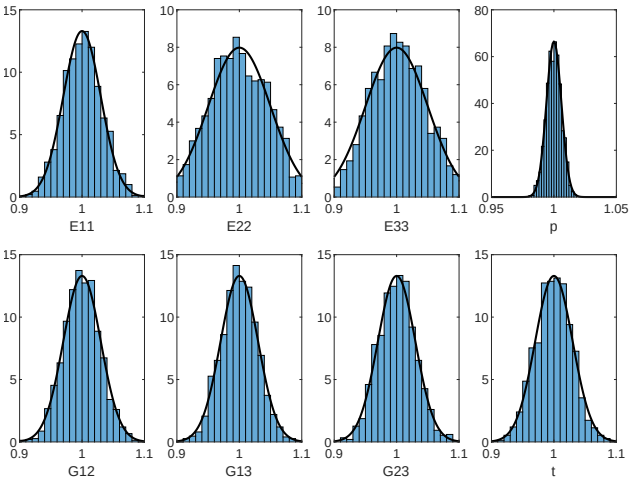


FIGURE 4.8: pdfs and histogram of UD properties realisations.

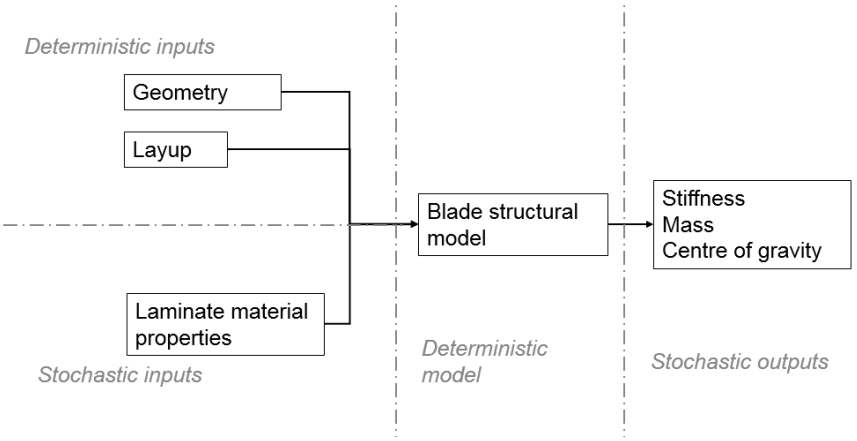


FIGURE 4.9: Uncertainty propagation on wind-turbine blade model.

The uncertainty propagation scheme can be seen in Fig.4.9. This study relies on the following assumptions:

- No correlation between random variables (i.e. all properties were considered to be independent, once there is no data to support this claim, which to be included in the model without could mean a bigger bias).
- No uncertainties in the outer geometry of the blade were considered.
- No uncertainties in the layup of the blade were considered.
- The CG and mass were assumed to be dependent exclusively on the density and thickness of the laminate.

The most relevant stiffness is in the flapwise direction; this is where the biggest blade deflection takes place during turbine operations - it is also the most common stiffness

tested during production. The confidence interval for the flapwise-stiffness distribution can be seen in Fig.4.10, normalised by its maximum value. A few observations can be made:

- Flapwise stiffness is not affected close to the root and to the tip section.
- The biggest CI range thorough the blade is around 10%.
- Flapwise stiffness is most affected by the uncertainties between 20% - 90% of blade length, this is mostly caused by the properties of the UD fibre, which is the fibre most used in this region, as can be seen in Fig.4.5B.

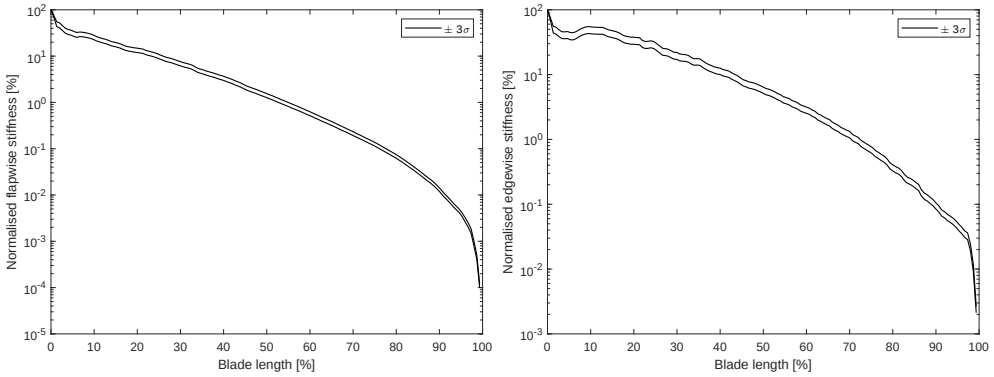


FIGURE 4.10: Confidence intervals for blade flapwise/edge stiffness distribution.

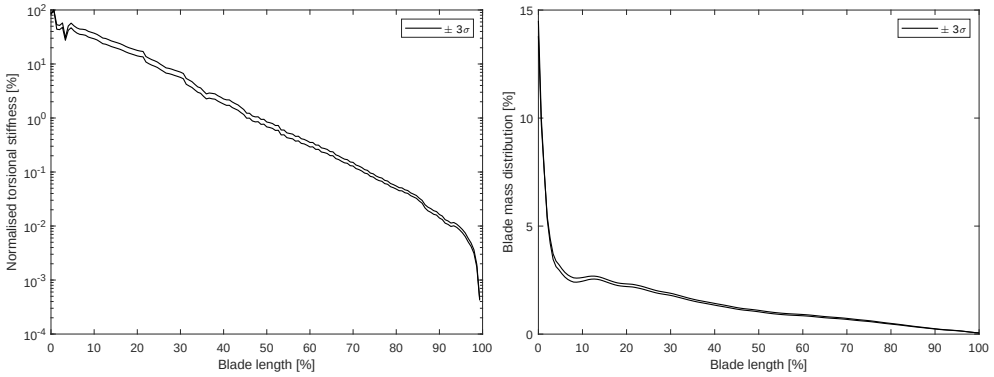


FIGURE 4.11: Confidence intervals for blade torsional stiffness/mass distribution.

It is customary to present the mean stiffness value as a characteristic for the blade. Another common quantity is the mass moment: This is defined as the moment caused by the blade mass around its root section,

$$MassMoment = X_{CG} \cdot M_{blade} \tag{4.2}$$

One can visualise the uncertainty effect on mean stiffness and mass moment by fitting normal distributions to the outputs of the Monte Carlo Latin Hypercube Sampling simulation (MC-LHS). Fitted pdfs for mean blade stiffness and mass moment can be seen in Fig.4.12. Table 4.2 presents the coefficient of variation for each one.

TABLE 4.2: Uncertainty levels for blade mean structural parameters.

Parameter	**Distribution**	**CoV (%)**
Mass moment	Normal	1.2
Mean flapwise stiffness	Normal	2.8
Mean edgewise stiffness	Normal	3.5
Mean torsional stiffness	Normal	2.7

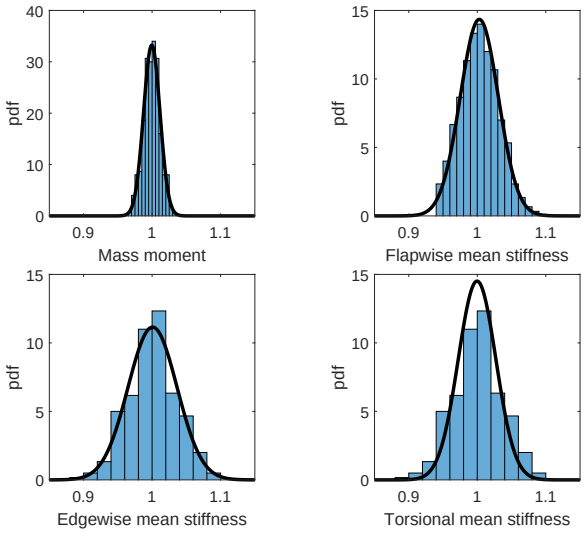


FIGURE 4.12: Mean blade stiffness and mass moment.

4.4.2 Material properties sensitivity analysis

A sensitivity analysis is used to determine what effect each individual input, or pair of inputs, has on the output. The uncertainty of the input parameters is specified using a probability distribution for each input. The software GEM-SA (Gaussian Emulator Machine - Sensitivity Analysis [73]), was used to calculate the main effects and total effects for each parameter here. The emulator can be seen as a model of the model, meaning it correlates inputs to outputs without going through any physical modelling. The physics-based model is treated as an unknown function, with the possible ranges of the input parameters specified by probability distributions. Assuming this model is a smooth function of its inputs, then a response surface can be fitted to the training data using a least-squares regression and the output can be estimated for any set of inputs,

TABLE 4.3: Variance contribution %- Sensitivity analysis.

Property	**CG**	**Mass**	**Property**	**Static Def**
ρ UD	5.04	8.93	E11 UD	98.8
ρ BIAX	0.3	0.8	E11 BIAX	1.2
t UD	92.6	88.3	E22 UD	0.0
t BIAX	2.1	2.0	E22 BIAX	0.0

faster than using the physics based simulation. Details for this procedure are found in [74].

The emulator was trained using an LHS with 100 realisations of the deterministic code. Meaning that 100 different sets of inputs to the blade model were generated and their results (outputs) were fed to the GEM-SA model to fit a equivalent Gaussian Process. This study relies on the following assumptions:

- No correlation between random variables (i.e. all properties were considered to be independent).
- No uncertainties in the geometry of the blade were considered.
- The CG and mass were assumed to be dependent exclusively on the density and thickness of the laminate.
- The static deflection was assumed to be dependent exclusively on the laminate's moduli.

Figures 4.13A and B show pie charts for the contribution of input parameters on the blade mass and CG uncertainty, respectively. As shown, the thickness of the UD is the most influential parameter, both in the blade mass and in the blade CG.

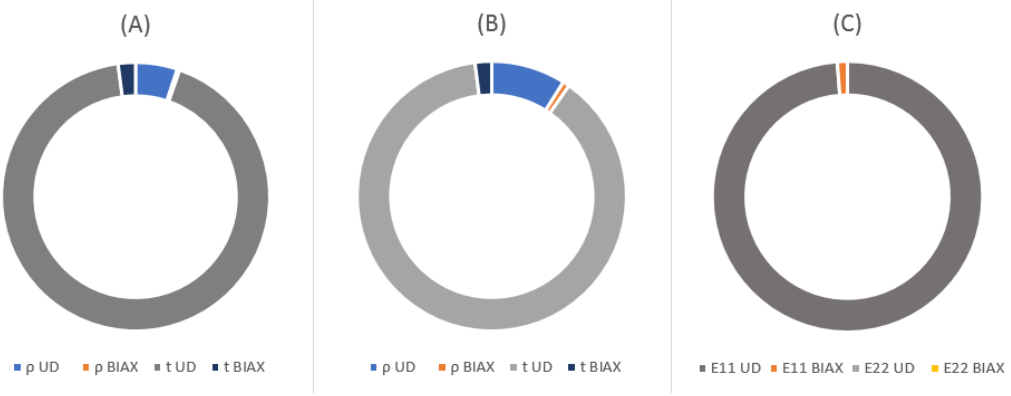


FIGURE 4.13: Blade mass, CG and static deflection sensitivity analysis - main effect.

Figure 4.13C shows the contribution of the material stiffness in the blade static deflection. The E_{11} of the UD dominates the variance of the static deflection test; this is coherent, since the UD is the major laminate type in the spar cap, which is the substructure responsible for the flapwise blade stiffness. It is worth highlighting that the variation of the input parameters is limited (around 3 to 5%, shown in Table 3.2). In Table 4.3, the contributions can be seen for the main properties in each case: CG, mass and static deflection. The other parameters would need bigger variations to have a significant effect in the blade deflection.

4.5 Uncertainty validation

The blades are often considered to be the most critical structural component of the turbine. Therefore, safety standards require full-scale testing for every prototype and after many major design changes. Overall, full-scale tests are seen as a final design verification with the following objectives:

- validate assumptions;
- identify relevant failure modes;
- identify manufacturing details prone to damage initiation.

Requirements for blade testing are part of international standards (e.g. IEC-61400-23 and DNV GL-ST-0376) with which manufacturers are required to comply. The scope for a certification static bending test (section 4.9 on [75]), involves (but is not limited to), testing in:

- positive flapwise direction (from pressure side to suction side);
- negative flapwise direction (from suction side to pressure side);
- positive edgewise direction (from trailing edge to leading edge);
- negative edgewise direction (from leading edge to trailing edge).

The blade static deflection test described in this section is not part of a certification campaign, it is a quality control test whose goal is to check whether the blade can

withstand extreme load cases and give evidence that the blade is neither too stiff nor too flexible. It is a way to evaluate blades per tolerance thresholds, meaning a pass or not pass - if the blade deflects too much for a given load, it then it is sufficient information to not deploy such a blade in an operational turbine. The test setup consists of the blade supported at the root section and at midspan subjected to a negative flapwise load close to the tip. The blade is essentially kept in rigid-body statics because of its own weight pushing it on the supports.

The setup is illustrated by a 3D model in Figure 4.14, together with the finite-element model used to simulate the test. This model is based on the lengthwise stiffness distribution of the blade (which is characterised by the Crs model). Data from static deflection tests of 34 blades of the same type subjected to the same load will be compared with uncertainty propagation results.

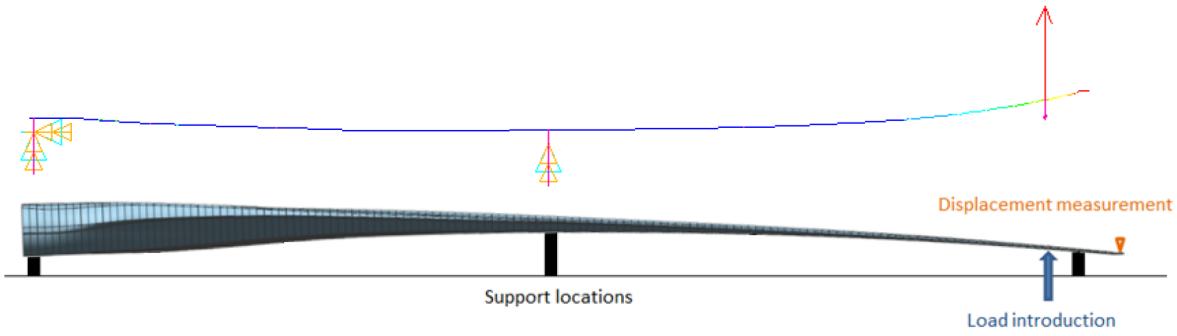


FIGURE 4.14: Wind Turbine Blade static test: Setup and finite element model.

4.5.1 Uncertainty propagation: Blade static deflection

A Monte Carlo with a Latin Hypercube sampling (MC-LHS), scheme shown in Fig.4.15, for the Timoshenko nonlinear beam model (including higher-order terms to account for large deflections) was performed to study the propagation of the material property uncertainty in the blade static deflection test; it can be summarised as:

- Inputs
  - Stiffness distribution: Random variable, realisations come from previous section (Determined by MC-LHS with uncertain material properties).
  - Force: Deterministic variable (fixed amplitude and direction).
- Outputs

– Static deflection: Random variable.

A set of experimental data for the same type of blade studied in Section 4.3 is available for validation. The experimental data consist of 95 tests for CG location and blade mass, and 33 static deflection tests were described in Chapter 3. Both the data and the results from the MC-LHS were normalised in relation to the mean experimental value.

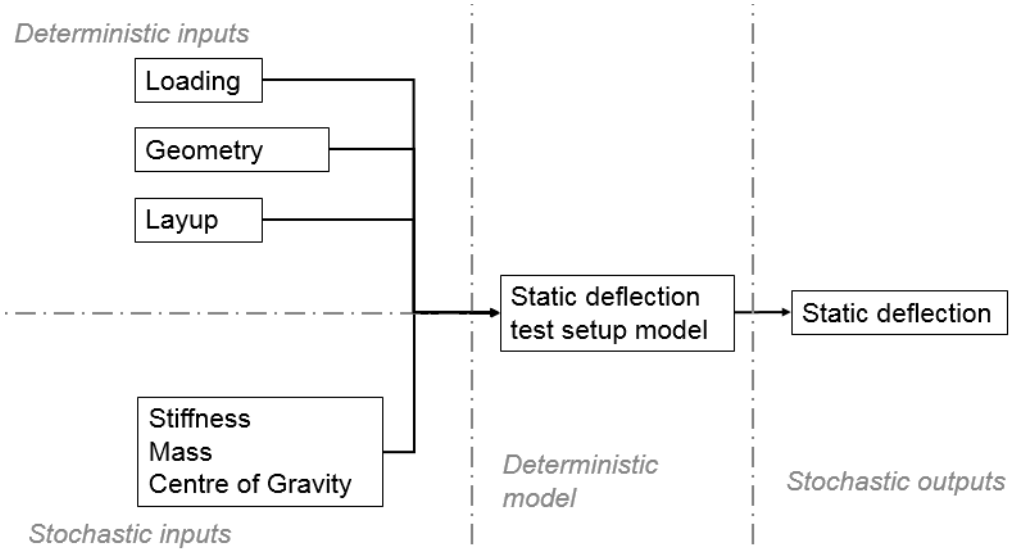


FIGURE 4.15: UQ for static deflection test simulation.

Quantile-quantile plots (qq-plots) for experimental vs MC-LHS results can be seen in Figure 4.16; hence, this can be used to justify the assumption that both experimental and simulation results from the MC-LHS come from the same normal distribution, even though the qq-plot indicates a limited "heavy tail" behaviour. Fitted normal distributions can be seen in Figure 4.17 (again the normal distribution was used to avoid any other assumption over the data); the statistical moments for the fitted pdf are presented in Table 4.4.

TABLE 4.4: Uncertainty levels comparison between simulation and experiment.

	CoV (%)		**Mean value**	
Parameter	**Experimental**	**MC-LHS**	**Experimental**	**MC-LHS**
Mass	0.92	1.03	1.00	0.99
CG	0.55	0.48	1.00	0.99
Static deflection	2.16	3.45	1.00	1.00

A few observations can be made:

- The MC-LHS has virtually the same expected value as the experimental data, this can be interpret as a well-calibrated, accurate deterministic model for both the blade structural properties and the test simulation.

- The CoV for both mass and CG differ less than 10% from the experimental CoV, which can be interpreted as an accurate representation for the density and laminate thickness uncertainties (which are the only ones affecting CG and mass).

- The simulated CoV for the static deflection is higher than the variations seen in the experimental data; this suggests that the variations in laminate stiffness that actually happen on the blades are smaller than the variations seen on coupon testing data. Another possibility is that the independent characterisation of laminate properties is too pessimistic. In reality, it could be expected that there are correlations between different stiffness terms and mass. However, the lack of experimental evidence to define this correlation justifies the independence as a conservative assumption to not add extra bias to the model, prioritising data consistency instead of speculative realism. Important to highlight that the lack of correlation is a conservative assumption but it is not necessarily conservative in results as for example, random lower bound correlated samples would result in worse results, higher deflections and less stiffness.

- The CoV of the E_{11} of the UD fibre (3%), which is the main fibre property in the direction of the blade span, can be seen almost directly propagating to the mean flapwise stiffness (CoV = 2.8%), and to the static deflection (CoV = 3.45%). This effect is in accordance with the idea that there are no nonlinear effects happening in the blade static deflection, and uncertainties in material properties should be seen directly in the deflection.

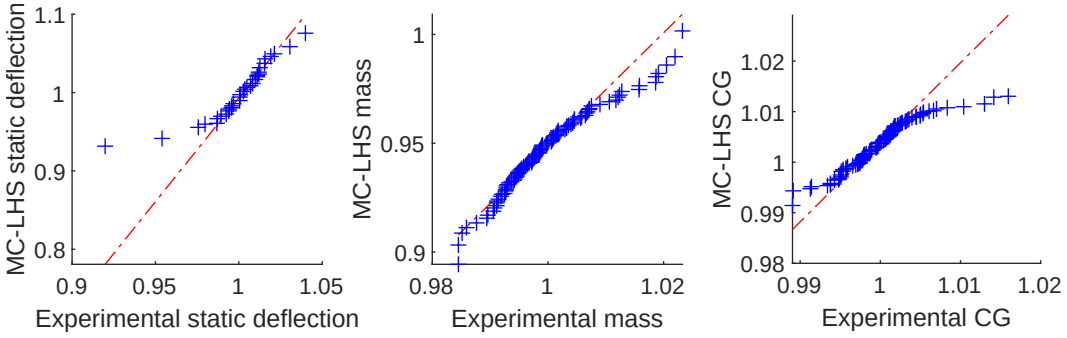


FIGURE 4.16: Simulation (MC-LHS) VS Experimental information.

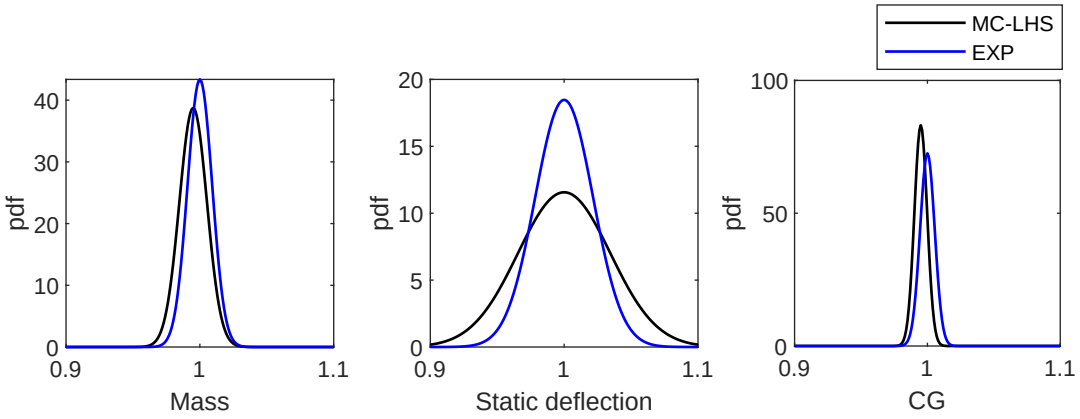


FIGURE 4.17: Simulation (MC-LHS) VS Experimental information.

4.5.2 Statistical Difference and Hypothesis Test

To evaluate whether the data from the experiment and MC-LHS are from the same continuous distribution, the two-sample Kolmogorov-Smirnov (KS) test [76] is performed.

This is a non-parametric hypothesis test that evaluates the difference between the cdfs (cumulative distribution function) of the distributions of the two sample data vectors over a range of x in each data set. KS-test is chosen because no assumption of a distribution type is made - therefore it can be used to evaluate if independent dataset behave similarly, and it is specially indicated for continuous data (as mass or deflection measurements). The KS test checks whether the results from the MC-LHS and experimental data are statistically consistent — not only in mean but in spread, skewness, and overall shape of their distribution.

The test statistics is defined as the maximum absolute difference between the cdfs:

$$D^* = \max_x(|F_1(x) - F_2(x)|) \tag{4.3}$$

where $F_1(x)$ is the proportion of x_1 values less than or equal to x and $F_1(x)$ is the proportion of x_2 values less than or equal to x.

The hypotheses for this test can be written:

Hypothesis H_0: Experiment and MC-LHS are samples from the same distribution with a significance level of $\alpha = 0.05$.

Hypothesis H_1: Experiment and MC-LHS are not samples from the same distribution with a significance level of $\alpha = 0.05$.

Result (static deflection): $p = 0.3293$ $D^* = 0.2061$

Result (mass): $p = 0.3370$ $D^* = 0.1074$

Result (CG): $p = 0.3144$ $D^* = 0.1095$

$p > \alpha$ indicates a failure to reject the null hypothesis (H_0) at the Alpha ($\alpha = 0.05$) significance level, in other words, the hypothesis that experimental data and MC-LHS realisations come from the same distribution cannot be rejected.

4.6 Comparison to IEC61400-5 standard

IEC61400-5 [68] outlines minimum design requirements for wind-turbine blades. Its purpose is to provide an appropriate level of protection against damage from all hazards during the planned lifetime. The scope includes:

- aerodynamic and structural design;
- material selection, evaluation and testing;
- manufacture;
- transportation, installation, operation and maintenance of blades.

One relevant topic from the standard is Section 6.2.2 on functional design tolerances for wind-turbine blades. Table 4.5 shows the comparison among the results from the MC-LHS simulation defined in Section 4.4, experimental values and IEC standard. The natural frequencies are also an output from the modal blade model defined in Section 4.3, by solving the eigenvalue problem with the mass and stiffness matrix. Figures 4.19 and 4.18 show the pdfs for this comparison, where the tolerances are interpreted as uniform distributions. One can note that Fn1 is in the lower side of the distribution from the MC-LHS results, this can indicate that the boundary conditions for the model is too rigid in comparison with the real boundary conditions for the experiment, which is an

TABLE 4.5: Coefficient of variance (%) vs IEC tolerances (%).

Parameter	**IEC**	**MC-LHS**	**Experimental**
Mass	3.00	1.03	0.92
Mass moment	4.50	1.20	0.90
1st Natural frequency	5.00	1.48	
2dn Natural frequency	5.00	1.44	
3rd Natural frequency	5.00	1.36	
4th Natural frequency	5.00	1.62	
5th Natural frequency	5.00	1.13	

usual effect due to higher impact of the forces rotations and translations at the support for the first mode of vibration. Changes in support stiffness have a smaller impact in the higher modes as they have mode nodes and interior bending, but nevertheless the experimental and the majority of the MC-LHS results are within the IEC limits.

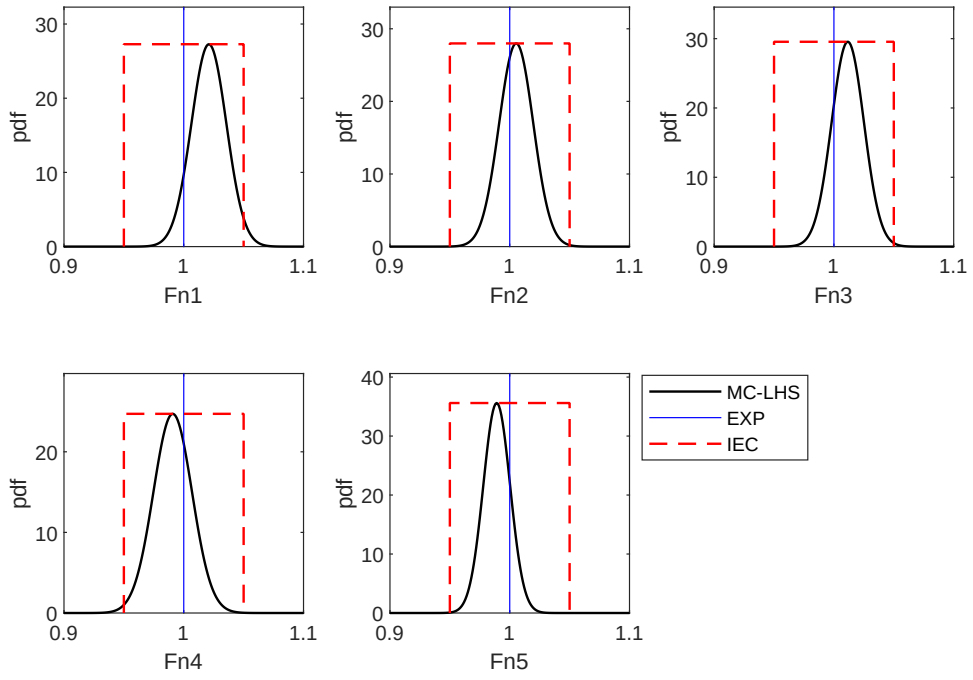


FIGURE 4.18: Normalised natural frequencies, IEC tolerances and experimental data.

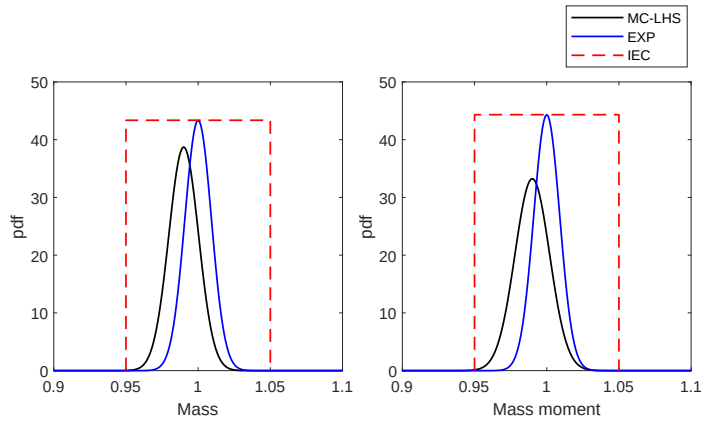


FIGURE 4.19: Mass and mass moment, IEC tolerances and experimental data.

4.7 Chapter summary

In this chapter the structural uncertainties of the blade were investigated, a model was built based on experimental data, validated and compared to the IEC standards.

First, the uncertainties in the blade laminate material properties were defined by means of coupon test data, with the help of a finite-element model (FEM) of the blade cross section: The effect of those uncertainties were defined on the blade characteristics. A CoV of approximate 3% was defined in relation to the material properties uncertainties on the blades mean stiffness parameters (see Tab. 4.2).

The validation of these uncertainties was made by propagating them to the blade deflection (with the use of another FEM to simulate the setup of the blade static test). Similar levels of uncertainties were shown by the simulation and experimental data, and these were shown not to be statistically different by a two-sample Kolmogorov-Smirnov test. For every parameter, the uncertainty level is found to be smaller than the tolerance defined by the IEC61400-5[68], which can be interpreted as an indication that the standard is too conservative and could be used as supportive information to justify the lowering of safety factors in the future.

As discussed in Section 4.5.1, the uncertainty model developed is conservative as no other correlations were assumed (e.g. between material properties and spatial location), although this could be a fair assumption (also in regards to the blade manufacturing process), its validation is not possible with the current available experimental data. Nevertheless, the developed stochastic description of the blade can be assumed to be adequate and its effect on the loads will be investigated in Chapter 6.

Chapter 5

Aerodynamic uncertainties

5.1 Introduction

Aerodynamic uncertainties refer to variations in the airflow dynamics around an aerofoil that can affect its performance and stability. These uncertainties originates from a variety of factors, including variations in geometry, surface finish, changes in wind speed and direction, turbulence, variations in atmospheric conditions, among many others.

Aerodynamic uncertainties can lead to variations in the power output of wind turbines and lower-than-expected power output which in turn can result in reduced revenue, grid destabilisation and breach of contractual obligations. They also have the potential to affect the dynamic behaviour of the entire turbine structure, altering the loads distribution. With relation to product development they can also impact financial projections, already under pressure in times of expensive raw materials and a volatile energy market.

Another possible and major consequence (of aerodynamic uncertainties) is regarding operation and maintenance costs, because unpredictable aerodynamic behaviour may lead to increase wear and tear on components which in turn end up requiring more frequent maintenance or early replacements.

This chapter presents an attempt to model the combined effect of different uncertainty sources on the blade aerodynamic characteristics, using both experimental data and reasonable assumptions to achieve an accurate and representative characterisation of such uncertainties.

Following traditional blade element theory [77],which is used in relation to wind turbine aeroelastic model development, the blade aerodynamic is defined by modelling several phenomena, which requires a variety of input parameters to characterise the flow through a blade, thrust and torque generated. Inputs such as lift and drag coefficients, blade twist angle and chord length are within the most important (and most affected by uncertainties) to a blade model. Such parameters can be defined with the help of Figures 5.1 and 5.2:

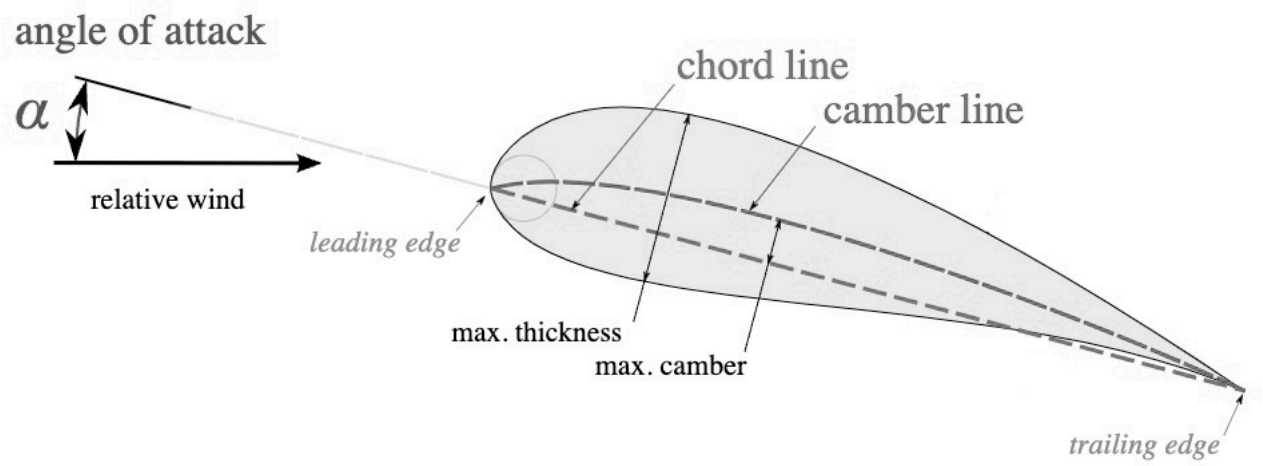


FIGURE 5.1: Blade aerofoil cross-section, adapted from [10]

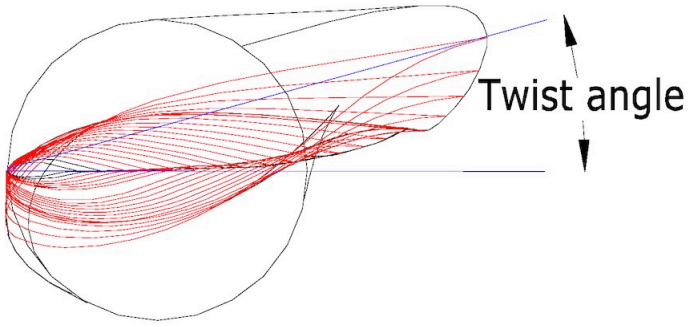


FIGURE 5.2: Blade twist angle, adapted from [11]

Aerofoil thickness: Ratio between the maximum thickness of an aerofoil (perpendicular to its chord line) and the length of its chord.

Blade twist angle: The angle between the aerofoil chord line and the rotor plane of the non deformed blade.

Angle of Attack: The angle between the line of the chord of an aerofoil and the relative airflow.

Lift (and lift coefficient): A fluid flowing around an object exerts a force on it. Lift is the component of this force that is perpendicular to the oncoming flow direction. Lift depends on the size of the blade, being approximately proportional to the area [78]. It is often convenient to quantify the lift of a given aerofoil by its lift coefficient, C_L, which defines its overall lift in terms of a unit area of the blade.
Drag (and drag coefficient): It is the component of the force parallel to the flow direction, an airfoil has a correspondent drag coefficient C_D.
Surface roughness: It is quantified by the deviations of a real surface from its ideal form. If these deviations are large, the surface is rough; if they are small, the surface is smooth. With relation to aerofoils, when roughness height and density increase, lift-curve slope, maximum lift, and lift-to-drag ratio decrease, meaning a worse aerodynamic performance than expected [79].

The assessment of aerodynamic properties in wind turbine blades and their uncertainty is obtained by a combination of experimental and numerical techniques, normally involving CDF (computational fluid dynamics) simulations, wind tunnel measurements and tuning the aerodynamic coefficients used in the aeroelastic simulations with relation to measurements from a wind turbine. However, this is usually only performed to characterise the "clean state" of a blade. The so called clean state of an aerofoil means its nominal aerodynamic behaviour, without any contamination or geometric deviation. This is the state considered in wind turbine simulations and in most wind tunnel experiments.

Contaminated or "rough" blade conditions are responsible for a reduced blade aerodynamic performance, is a recurring phenomena in most operating aerofoil surfaces; it may arise during manufacturing process, period of service, by insect contamination, and/or natural accumulation from weather related events [80]. Its consequences can be seen in real turbine output, however its modelling, simulation and validation is seldom possible.

Although wind turbine blade design aim for roughness-insensitive aerofoil shapes [79], it still is a relevant challenge because surface roughness can cause transition in the boundary layer, which can result in increased drag, lower lift and therefore less energy captured. The rough behaviour of an aerofoil is a random process, and can be extremely challenging to model but a similar transition can be reproduced in wind tunnel experiments by means of zigzag-tape[56] (or tripwire) application.

In this chapter, the focus is to define a stochastic model for the aerodynamic properties of a wind turbine blade based on geometric tolerances, wind tunnel measurements (presented in chapter 3) and surface roughness. These uncertainties are driven by physical uncertainty (aleatory) or by lack of evidence (measurement or model uncertainty) as shown in Table 5.1.

TABLE 5.1: Sources of uncertainty included in this chapter.

	Physical	Measurement
Geometric tolerance	x	
Surface roughness	x	
Variation in wind tunnel measurement: clean		x
Variation in wind tunnel measurement: rough		x
Degration level throughout the blade	x	

5.2 Geometric tolerances

A wind turbine blade is built with a complicated geometric evolution, it starts with a cylindrical aerofoil, with $RT = 100\%$ (relative thickness) that evolves to a thinner profile towards the tip (that can be as low as $RT = 15\%$), while following a twist angle evolution (see Figure 5.2).

Geometric uncertainties can come from any distortions in the blade aerofoils (it can be defined in terms of chord length, aerofoil thickness, twist angle, etc.) and can originate during manufacturing, handling, transportation, installation and even operation.

In order to characterise these uncertainties and estimate the deviation from nominal aerodynamic performance, 3D scanning or detailed measurement of several blades' geometry of the same type would be necessary. Despite the fact that a few 3D measurement tools are already commercially available, (e.g. laser based systems), such experimental campaign would have significant practical limitations, as it would be necessary to scan a large enough population of blades in an offshore environment. The complexity and cost of such, measurement campaigns limits the feasibility of an experimental characterisation of the geometric uncertainty in blade aerofoils.

A feasible approach is to estimate the effect of geometric conditions via simulations. The challenge is then to describe what would be a realistic geometric distortion, so that the simulations are able to predict useful results. Due to the lack of blade specific

data, the allowed tolerances defined on the standards can be used as inputs to setup such simulations. IEC 61400-5:2020[65] defines functional design tolerances that must be accounted for in the evaluation of loads, performance and structural integrity of a blade. The tolerance for aerofoil local chord length is set at ±1%.

The design tolerance from IEC 61400-5:2020[65] can be used to build a distribution for the geometry of the aerofoil, which can then be simulated on a Monte Carlo framework. The uncertainty effect captured under such evaluation would then be a conservative scenario, but still representative of the maximum effect allowed in a line produced blade.

The chord length of the aerofoil is considered to be a uniform random variable with bounds defined at ±1% of its nominal value (samples from this distribution can be seen in Fig.5.4A, where the green dashed line represents the nominal geometry). The uniform distribution is chosen to avoid any additional assumption with the available information, as the design tolerance represent a max and min allowance not a continuous variable distribution.

The aerodynamic coefficients of a distorted aerofoil (RT=18%) are simulated in XFOIL[81]. XFOIL is an open source model developed in the late 80s, which calculates the pressure distribution (thus lift and drag coefficients) over an isolated aerofoil given its Mach number and its 2D geometry. Although this model is somewhat simple, not considering any 3D flow, or heat transfer effects, the comparative change in lift and drag coefficients for a specific aerofoil can be used, together with the actual numbers obtained on wind tunnel testing.

For these calculations, the Mach number was set at Re=4e6, which is equivalent to the Reynolds number of a aerofoil with 18% RT experiences when the rotor is at rated wind speed. This is equivalent to the conditions used in the wind tunnel testing described in Chapter 3.

XFOIL[81] simulation setup requires normalisation of the chord length, so after a sample is generated the new chord length has to be normalised before simulated (which then gives the appearance of a thickness uncertainty seen in Fig.5.4). A total of 150 samples were randomly generated and had their normalised CL and CD calculated, see Fig. 5.3. While the observed geometric uncertainties' effect in our study may not be substantial, it is crucial to underscore the importance of quantifying and considering their impact. Despite their seemingly minor nature, these variations of CL and CD around the AoA could cumulatively influence the turbine dynamic behaviour.

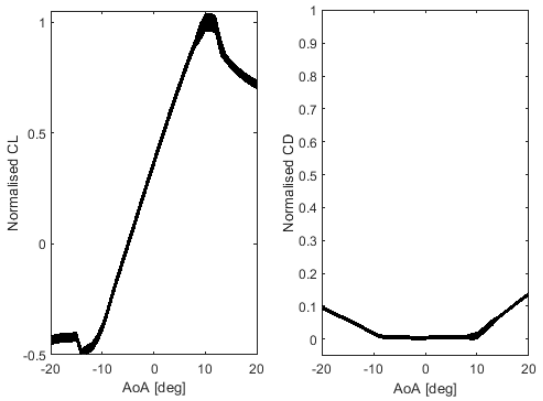


FIGURE 5.3: CL and CD for geometric tolerances Monte Carlo simulation.

To simplify the parametrisation the results of the Monte Carlo simulation can be divided in two different regions of the CL curve: an uncertainty high impact region identified by **H** around the maximum CL angle of attack (also refereed to as design AoA), and a uncertainty low impact region identified by **L**. The **H** is defined by a range of angles of attack around the design AoA.

The results for lift can be summarised by a range of approximately 2% of the CLMax (maximum lift coefficient) in the linear region of the CL curve (low impact) ,and of around 4% of the CLmax in the region close to stall ±2% deg of the design AoA (high impact). For the drag coefficients the **H** region is also defined by ±2% deg of the design AoA, but the effect (increased drag) is around 1% of the CLMax, whilst in the **L** region only 0.5% of the CLMax. Tab. 5.2 summarises the results.

TABLE 5.2: Parametrised results for geometric uncertainty.

	CL	DC
Region H (% of the CLMax)	±3%	±1%
H range (around the AoA_D)	±3 deg	±3 deg
Region L (% of the CLMax)	±2%	±0.5%

Fig.5.4B show the $\pm 3\sigma$ results for both lift and drag coefficients. Summarised in Table 5.2.

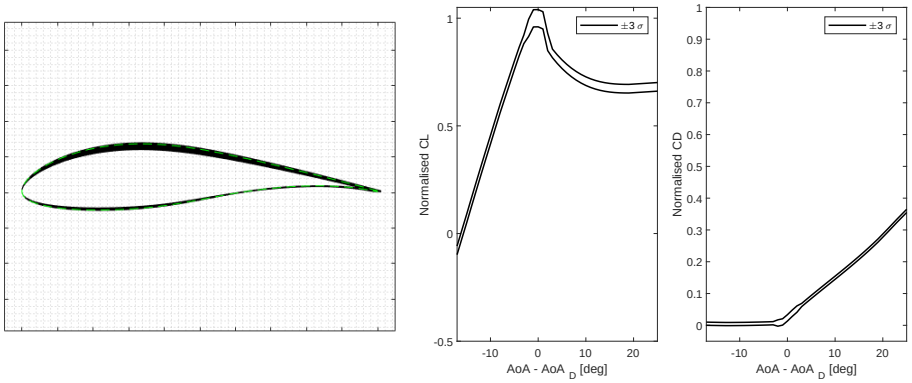


FIGURE 5.4: (A) Aerofoil geometric tolerance and (B) variation in lift coefficient.

5.3 Roughness aerofoil characteristics

In this section, we investigate the impact of aerofoil roughness on wind turbine blade performance, presenting an in depth look into the results of the wind tunnel measurements conducted under both clean and rough conditions, introduced on Chapter 3. Aerofoil roughness is a critical factor in understanding the real-world challenges faced by wind turbines, as it significantly influences aerodynamic characteristics and overall efficiency. Through a systematic exploration of wind tunnel data, we aim to quantify the effects of roughness on key aerodynamic coefficients. Additionally, we extend our investigation by constructing a stochastic model to capture the inherent variability associated with aerofoil roughness in wind turbine applications, which will be later used to quantify its effect in the turbine loads.

5.3.1 Wind tunnel measurements

There can be a range of factors contributing to the uncertainty in the measurement of aerofoil aerodynamic static coefficients in wind tunnels [82]. The focus herein will be on the results obtained when measuring the same aerofoil geometry (RT=18%) in two different surface conditions as shown in Chapter 3. Fig.5.5 shows 17 independent measurements in clean condition and 6 in rough conditions for the same aerofoil geometry. The black line is the nominal value, which is defined by a numerical simulation of the aerofoil and calibrated by the mean value of the wind tunnel tests results. The wind tunnel data can also be used to build a stochastic model for the clean and rough behaviour. In the same fashion as the geometric tolerances, the uncertainty model can be defined in two regions: one of *High* uncertainty, around the the AoA_D(or AoACLmax)

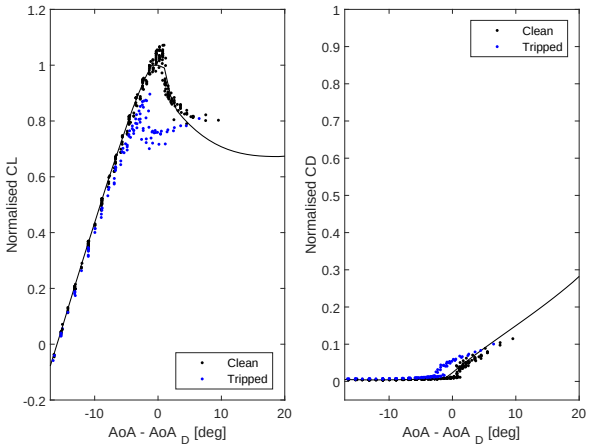


FIGURE 5.5: Wind tunnel measurements: Clean and tripped (rough) states

and another of *Low* uncertainty defined as the remainder of the domain, illustrated by Fig. 5.6. However, the regions cannot be defined in the same range for both clean and rough, as can be seen in Fig.5.5, the high uncertainty range in the rough behaviour is larger than on the clean. Table5.3 and Fig.5.6 show the ranges of high uncertainty and the CoV in terms of the CLmax.

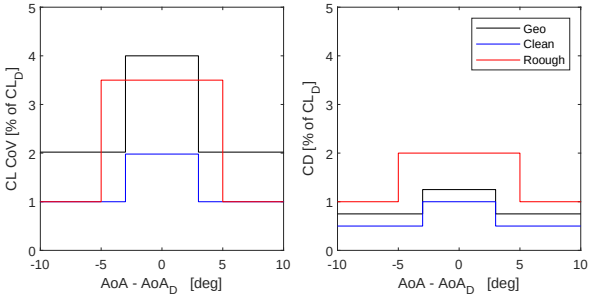


FIGURE 5.6: Uncertainty in wind tunnel measurements: clean and rough.

TABLE 5.3: Uncertainty in aerodynamic parameters

	CL			CD		
	Geometric	Wind tunnel		Geometric	Wind tunnel	
	Clean	Clean	Rough	Clean	Clean	Rough
Region H (% of the CLMax)	±4%	±3%	±3.5%	±1%	±1%	±2%
H range (around the AoA_D)	±3 deg	±3 deg	±5 deg	±3 deg	±3 deg	±5 deg
Region L (% of the CLMax)	±2%	±1%	±1%	±0.5%	±0.5%	±1%

One can parametrise the rough CL and CD curves by the clean CL maximum value (CLmax) and the angle of attack (AoA) at which it happens (AoACLmax or the AoA_D), just before the stall. Fig.5.7A shows the change in CD and CL in terms of the CLmax, as seen in the wind tunnel tested aerofoil.

One can validate this model by comparing the wind tunnel measurements to the parametrisation results. Fig.5.7B shows the results of this parametrisation model (the red line represents the mean value of the measurements for rough condition, the blue line the rough behaviour estimation parametrised in terms of the clean CLmax). Even though this is not a perfect physics-based model, this parametrisation allows the approximation of a rough behaviour for aerofoils only tested clean.

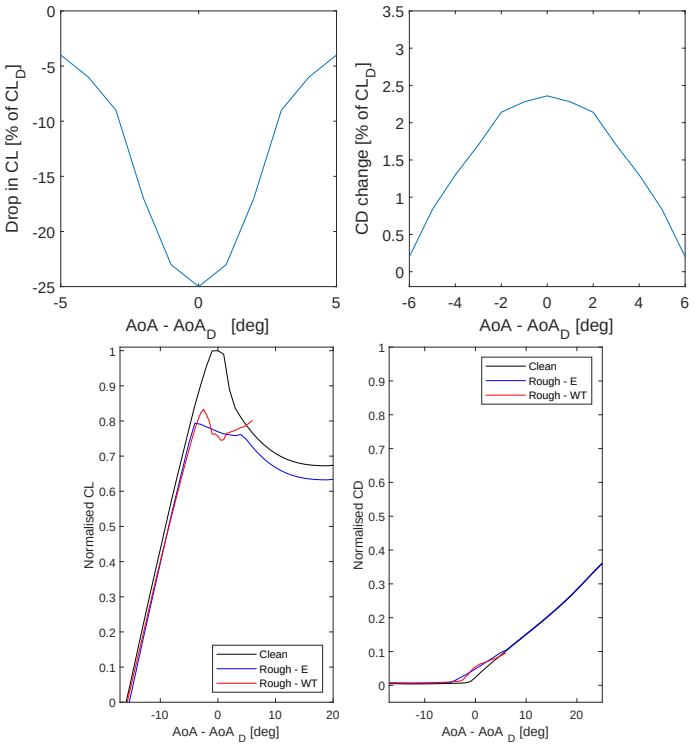


FIGURE 5.7: Wind tunnel measurements: parametrisation (A) and validation (B) of the model.

5.3.2 Extrapolation from wind tunnel measurements

Although the wind tunnel data presented in Fig.5.5 and the subsequent parametrisation shown in Fig.5.7 are specific to a single aerofoil utilized within a blade, these findings can nevertheless be employed to construct an extrapolation to approximate the rough behaviour for the whole blade. This approximation is deemed sufficient, given that the characterization of the intrinsic roughness behaviour across all aerofoil surfaces of the blades would require a prohibitively extensive series of experimental evaluations. Such an endeavour would not only be impractical but also financially infeasible. Nevertheless, as will be shown in Section 5.4, knowledge of the exact rough behaviour of the aerofoil is

not necessary because the stochastic model developed in this study interpolates between clean and rough conditions, with only a limited contribution from the rough.

Thick aerofoils (which are used close to the blade root section) respond differently to surface roughness than slender aerofoils like the one shown in Fig.5.4 (normally used towards the tip of the blade). Even though the discussion of the aerodynamic phenomena causing this difference in behaviour falls beyond the scope for the present study, it is important to find an appropriate description, so that the model built is as close as possible to reality.

Due to the lack of wind tunnel measurements on thick aerofoils, this study adopts an approximation based on Van Rooij's [56] results (DU 00-W-401 aerofoil) for the all the aerofoils $35-50\%$RT, a CL curve for this approximate rough behaviour can be seen in Fig.5.10A. For aerofoils with RT$>50\%$, an interpolation between Van Rooji[56] results and the aerodynamic coefficients of a cylinder are used to define the rough behaviour.

5.4 Stochastic model

To build a stochastic model of the aerodynamic coefficients of a wind turbine blade with the goal of building a pool of randomly-generated blades, there is need to account for each of the uncertainty sources previously:

1. Uncertainty due to geometric tolerances.
2. Uncertainty due to wind tunnel measurements (around the clean behaviour).
3. Uncertainty due to wind tunnel measurements (around the rough behaviour).
4. Uncertainty on the level of aerodynamic degradation throughout the blade.

The first three uncertainties have been previously defined in this Chapter. The last source is addressed first by the model for degradation uncertainty and level of profile unevenness introduced by Bortolotti[55], which defines a particular blade state as an interpolation between fully-clean and fully-rough states by means of a variable β, following a beta distribution (Eq.5.2), where 1 means a fully-rough and 0 fully-clean aerofoil as shown by,

$$C_L = C_{LR} \cdot \beta + C_{LC} \cdot (1 - \beta) \tag{5.1}$$

In addition, the expected level of aerodynamic degradation can also vary through the blade span; aerofoils towards the tip are subject to higher speeds, which can make them more susceptible to erosion/degradation. In contrast, the root section experiences much lower velocities and therefore the expected degradation level is limited. This motivates the introduction of a spatial variation in roughness levels throughout the blade. To include this progression in the stochastic model, the blade is divided into three sections as seen in Fig.5.8, and the parameters for each beta distributions a_1, a_2 parameter are defined in Table 5.4 and shown in Fig.5.9. Each beta variable is generated from a single CDF and are fully correlated so that a random blade will always have a coherent evolution of roughness behaviour throughout its length.

$$P(a_1, a_2) = \frac{x^{a_1 - 1}(1 - x)^{a_2 - 1}}{B(a_1, a_2)} \quad , B(a_1, a_2) = \frac{\Gamma(a_1)\Gamma(a_2)}{\Gamma(a_1, a_2)} \tag{5.2}$$

where Γ is the Gamma function.

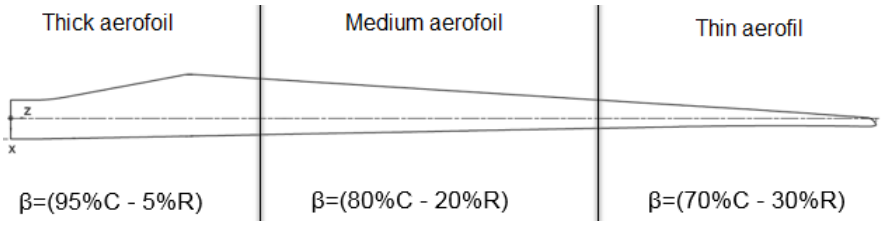


FIGURE 5.8: Blade regions: interpolation between (C) clean and (R) rough.

Location	Expected value [%]	Parameter	
		a_1	a_2
Root	5	4	75
Mid	20	2	8
Tip	30	5	11.66

TABLE 5.4: Blade regions: Beta pdf definition.

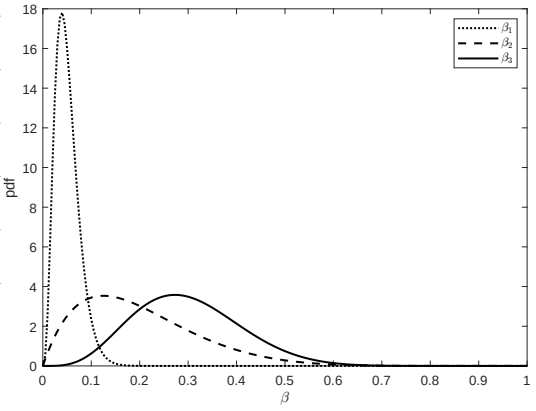


FIGURE 5.9: Betas pdfs.

Fig.5.10 shows samples for CL curves on each of the three blade regions (root (RT=50%), mid (RT=35%), and tip (RT=18%)) where the respective expected contribution from

the rough behaviour is 5%, 20% and 30% (Table 5.4). The procedure to generate a random mixed aerofoil characteristic can be defined as follows:

1. Sample N_1 from a distribution defined for each aerofoil (Tab.5.3), this variable is used as a perturbation for both clean and rough behaviours to account for the effect of the geometric tolerance,

2. Sample N_2 from the previously-defined distribution for the uncertainty of clean and rough aerofoils (only one random variable is defined because the behaviour for clean and rough are considered to be fully correlated),

3. Sample N_3, variable following a uniform pdf, to which the inverse beta function to sample β_is from the previously defined uncertainty for the degradation level model.

4. Use β_is to define the aerodynamic coefficients by interpolation (Eq. 5.1) for each aerofoil on the blade.

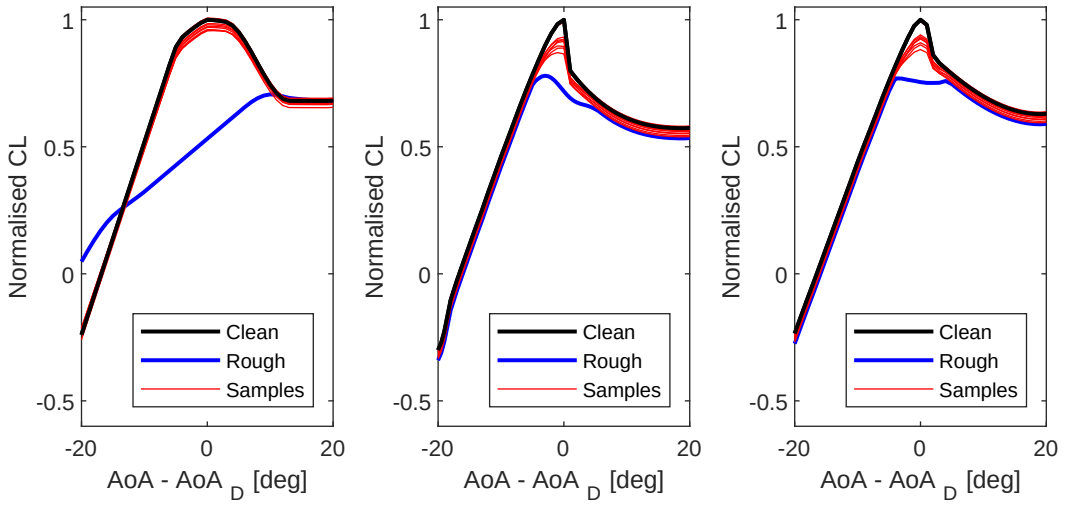


FIGURE 5.10: CL for blade mixed aerofoil, respectively root, mid and tip.

Fig.5.10 show that the variation of random generated samples from this stochastic model are closer to the clean state than to the rough, but the aerodynamic performance can drop significantly towards the tip of the blade. The parametrisation from wind tunnel measurements (used on mid and thin aerofoils) and the approximation to Van Rooji[56] results (used on thick aerofoils) can be considered a solution to problem of defining a complete model for blade rough behaviour. In the next chapters the effect of these uncertainties will be propagated to the turbine behaviour.

5.5 Chapter summary

In this chapter the aerodynamic uncertainties were investigated, a stochastic model for lift and drag coefficients was built based on experimental data, engineering judgment and reference data. This model combine uncertainties coming from geometric, roughness and spatial contributions.

The geometric uncertainties were defined based on the IEC 61400-5:2020[65] design tolerances, building a uniform distribution for the maximum allowed geometric distortion in a wind turbine blade. The roughness component is modelled with the help of the wind tunnel testing first introduced in Chapter 3. The wind tunnel data is the basis for a parametrisation of the so-called rough behaviour, which is then extrapolated to different aerofoils in the blade.

Previous contributions from Van Rooji[56] and Bortolotti[55] were key to introduce the rough behaviour of thick aerofoils and to define the Beta variable that interpolates between clean and rough states for a particular aerofoil in the blade. Engineering and expert judgment were used to define the different blade regions shown in Figure 5.8, and which level of rough behaviour each of them can expect.

In summary, this chapter presents a comprehensive stochastic model capable of generating random aerodynamic profiles for wind turbine blades, while thoroughly addressing the various sources of uncertainty previously discussed.

Chapter 6

Turbine Simulation

6.1 Introduction

Aeroelastic simulations is one of the (if not the main) tool during wind turbine development, design and evaluation. Such simulations allow the engineers to investigate concepts, evaluate new variants, and build their knowledge before prototypes are built. Once in the prototyping or production phase, aeroelastic simulations are benchmarked and validated against measurements, laboratory conditions and even different simulation tools. This allows for assumptions to be tested, and validated, increasing the trust in such an important analysis.

This chapter introduces the propagation of the uncertainties previously discussed to the turbine level, and how these affect the overall turbine behaviour. A brief discussion of the aeroelastic model design load cases (DLCs) is also included. This investigation will also focus on defining if there are differences in uncertainty effect when the turbine is in different load cases and on the uncertainty effect of some environment parameters

Some of the questions to be answered by this chapter are:

- How much effect do blade uncertainties have in loads and responses of an offshore wind turbine in normal power production under extreme(DLC 13) and normal turbulence (DLC 12)?
- Is there a difference of uncertainty levels on DLC 12 and DLC 13?
- What is the variance contribution on each case?

- Which turbine load is more affected by the uncertainties?
- Are the blade structural uncertainties significant when compared to environmental or aerodynamic uncertainties?

6.2 Uncertainties in Aeroelastic Turbine Simulation

The analyses of this study were performed using the aeroelastic code BHawC[40], to simulate a multi-Mega Watts (5 to 10MW) pitch-controlled offshore turbine with a rotor diameter between 150 to 200m (equipped with the blade described in the previous chapters) in design load cases specified by IEC[83]. BHawC[40] includes effects related to:

- Non-linear flexible multi-body Dynamics;
- Large rotation and displacement capability via co-rotating beam element formulation;
- Advanced models for external conditions and aerodynamics;
- Take into account gravity, inertia, centrifugal and Coriolis effects;
- Full modelling of coupling between blade bending and twist.

The structural module in BHawC is built around the co-rotational formulation providing geometric nonlinearity [40]. The substructures for the tower, shaft and blades are modelled using Timoshenko beam elements which are defined by continuous cross-section properties tabulated in a reduced cross-section format [41].

The aerodynamic module is included via blade element moment theory with aerodynamic coefficients related to each aerofoil of the blade span. The external conditions module follows the IEC[83] standard, using the approach defined by Mann[84] for turbulence model.

The model can be divided in 5 main substructures, illustrated in Fig.6.1 : aerodynamic, strucutral, foundation, controller and external conditions. The analysis presented on this chapter is result of the uncertain characterisation of blade (aerodynamic and structural), tower (structural), external conditions (wind seed for turbulence model, turbulence

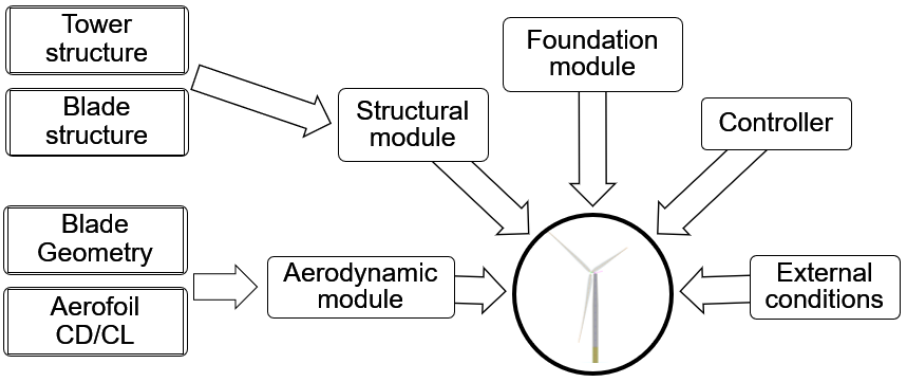


FIGURE 6.1: Turbine aeroelastic model - modules.

uncertainty, and shear coefficient). No alterations, tuning or adaptation was performed in the controller and in the foundation structure.

More aspects of the aeroelastic model cannot be disclosed due to proprietary reasons but the nominal turbine model/configuration through which the uncertainties are propagated is considered as high quality and high accuracy, extensively used commercially.

Even though the model outputs forces and moments for each node in the structure, the analysis will focus on loads described on Tab.6.1 and illustrated in Fig.6.2. The reasoning for choosing these locations is due to the fact that these are the highest loading points for the blade (root section) and for the tower (base), and they are normally on the designing envelope for turbines. The blade tip is included due to its deflection being critical for the design - not for the loads. The energy production (EP) variance under uncertainties.

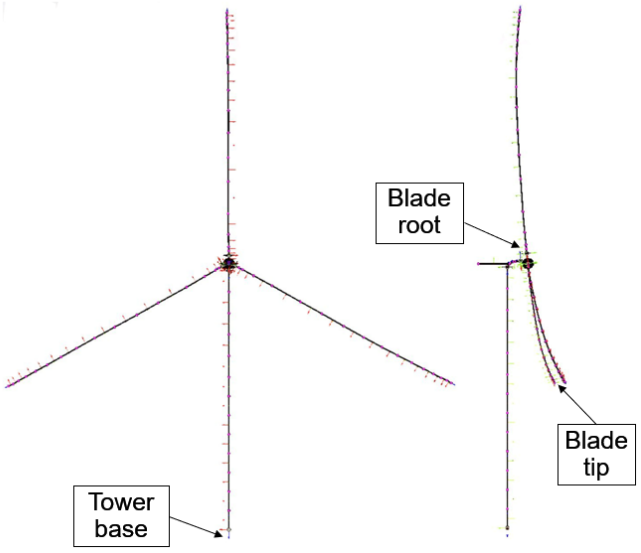


FIGURE 6.2: BHawC structure - Turbine aeroelastic model.

TABLE 6.1: Analysed load outputs.

Component	Load	Location
Blade	Flapwise moment	Root
	Edgewise moment	Root
	Out of plane deflection	Tip
Tower	Side-side moment	Base
	Fore-aft	Base

The uncertainties modelled through chapters 4, and 5 were used to generated Latin hypercube samples describing the distribution of properties in the blade's structure and aerodynamic characterisation.

For the tower structure, the uncertainty in Young's module is considered. As the tower geometry and manufacturing are not subject to considerable uncertainties, its material property is the only source modelled.

Both ultimate (ULS) and equivalent fatigue (FLS) loads will be analysed throughout this chapter depending on the design load case considered.

FLS are of extreme importance for wind turbine design, being the critical factor in many components. Equivalent fatigue loads [85] are calculated by the use of Eq.6.1:

$$S_o = \left(\frac{\sum_i n_i S_i^m}{N_{eq}} \right)^{1/m} \tag{6.1}$$

where N_{eq} is the equivalent number of cycles to which one is calculating the equivalent load S_o, m is the Wöhler slope; $m = 10$ and $m = 5$ are used for blade and tower loads respectively, these are defined by following the IEC61400 [86] together with SGRE internal practices. S_i is the load range which is determined based on Rainflow counting.

The set of design load cases described by the IEC61400 [86] has the purpose of representing a range of situations covering the most significant conditions that a wind turbine experiences and may affect their loading, durability and operation. To ensure the appropriate level of safety and reliability, environmental, electrical and soil parameters shall be taken into account in the design and shall be explicitly stated in the design documentation.

The load cases are determined from a combination of operational modes, design situations and external conditions. The necessary load case to verify the structural integrity of a wind turbine are calculated by combining:

- normal design situations and appropriate normal or extreme external conditions;
- fault design situations;
- transportation, installation and maintenance situations.

The comprehensive list and description of design load cases are presented in the Chapter 7 of the IEC61400[86].

The environmental conditions can be further divided into wind, wave and soil, if offshore simulation is considered. There also the electrical conditions referring to the power network. The following section sdo not consider wave, soil or electrical conditions, as it is customary to evaluate the turbine performance and dynamics isolated before including site specific inputs to the simulations.

Wind conditions are the most important external condition impacting the turbine structure. There has been a long scientific effort to find realistic models of wind conditions for wind turbine simulations. One of the most widely accepted models is the Mann turbulence model, described by the standard [83], which is widely used in the industry.

The IEC61400 [83] also defines classes and categories for wind turbines. Wind turbine classes are defined in terms of wind speed, wind turbine class I, II and III, and turbulence parameters, turbulence category A+ (very high), A, B, and C (low). These relate to the turbulence intensity, which in turns is the normalised standard deviation of the wind speed for a 10min interval. The intention of the classes is to cover most applications, see Table 1 on section 6.2 of the standard.

Wind category B (medium turbulence characteristics) will be used throughout this study, as it can be considered a generic site, where the turbulence is neither too low nor too high, ideal for turbine design. However site specific studies are required in case the generic design does not apply due to specific circumstances including wake or near coast conditions.

In the next sections the uncertainties effect will be investigated on DLC 12 (normal power production), DLC 13 (power production under extreme wind conditions), DLC 61 (parked on extreme wind conditions) and DLC 11 (extrapolation of extreme events). The uncertainty sources considered on each simulation case are shown in Tab. 6.2.

TABLE 6.2: Uncertainties sources considered for each DLC.

DLC	12	13	61
Blade aerodynamic uncertainties	x	x	x
Blade structural uncertainties	x	x	x
Tower structural uncertainties			x
Wind seed	x	x	x
Turbulence intensity			x
Wind shear			x
Yaw error			x

6.3 DLC 12: Normal Power Production

In this design situation, a wind turbine is running and connected to the electric grid. The simulation of power production occurs without faults, and it is performed for wind speeds in the entire operational range with normal turbulence according to the IEC class. The standard [86] also requires at least six seeds (independent random realisations of the stochastic wind field) per wind speed to be simulated before analysing the results. This environment is defined as the atmospheric turbulence that mostly occurs during the lifetime of the turbine, and this load case as the condition the turbine spends most of its lifetime (standard assumption is that the turbine will spend 70-85% in DLC 12, depending on wind resource available at site and the specific design and maintenance practices of the turbine designer/operator).

In order to streamline computational resources and minimize data volume, the turbine simulation in the DLC 12 is performed at three distinct wind speeds, that represents the main dynamics throughout a pitch-controlled wind turbine (see Fig. 6.3):

- Cut in (lowest 10 min average wind speed at hub height at which the wind turbine starts to produce power in the case of steady wind).
- Rated (minimum wind speed at hub height at which a wind turbine's rated power is achieved in the case of steady wind): Above this wind speed, the blades start to pitch out.
- Cut out (highest 10 min average wind speed at hub height at which the wind turbine is designed to produce power in the case of steady wind).

From chapters 4 and 5, 150 samples are generated from the structural characterisation, 150 samples are generated from the aerodynamic characterisation and 150 seeds are

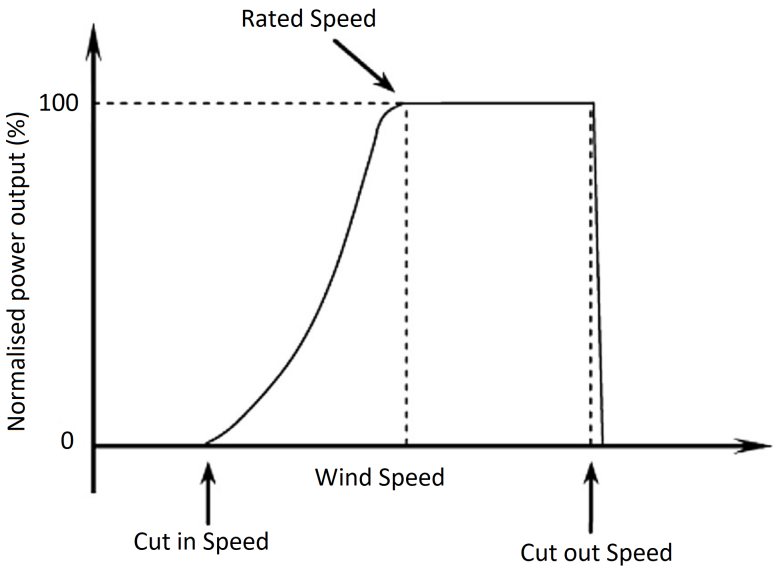


FIGURE 6.3: Power curve - Pitch controlled wind turbine. Adapted from [12]

generated for the turbulence model to defined the wind profiles (also referred to as turbulence box).

A Latin hypercube sampling is used to define 5000 representative samples (illustrated in Fig.6.5) out of the 150x150x150 (above 3 million) possible combinations. A simulation output is defined by 600-seconds time series, for each of the load channels.

Due to the stochastic nature of the wind turbulence model, there will be some variation of the mean wind speed for each of the turbulence boxes. A turbulence box is the representation of the generated 3D wind field during the 600-seconds time series, and a seed will generate an independent box, with the same turbulence characteristics defined (category B - in this study).

Fig. 6.4 shows the variation of mean, max and min wind speeds for the 5000 simulations, for the (normalised) rated wind speed with same turbulence characteristics for each time series.

For each simulation, the minimum, maximum and mean values outputs are extracted and analysed, the most relevant presented: For energy production the interest is in the variation (and uncertainty) of the mean values, for loads in the maximum absolute value as for blade deflection.

These 5000 simulations are grouped with respect to the 150 wind seeds to find the most likely CoVs, as illustrated by Figs.6.6, 6.7, 6.8, the goal is to estimate the uncertainty

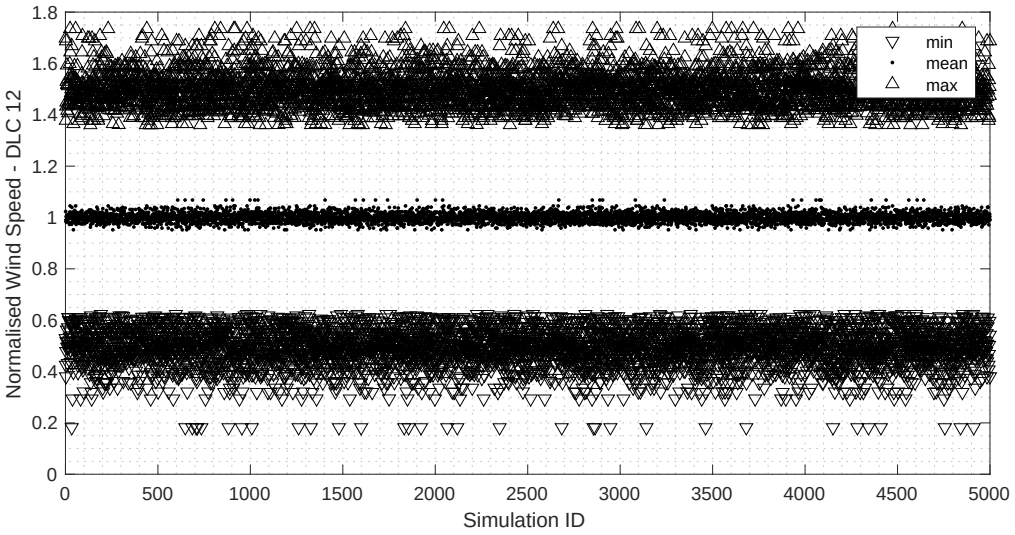


FIGURE 6.4: Normalised wind speed: DLC 12

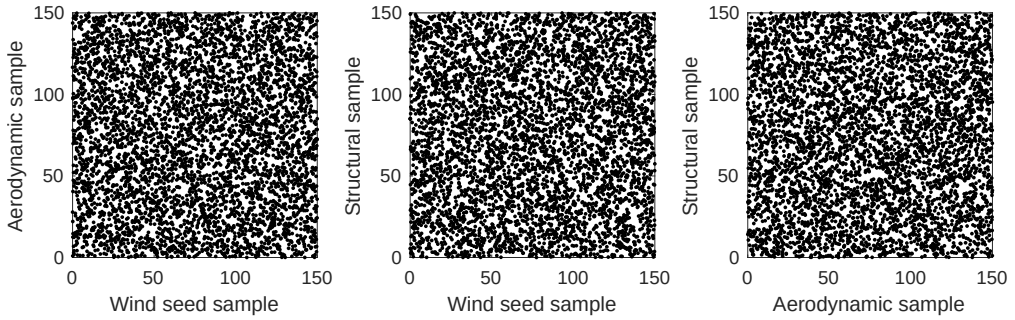


FIGURE 6.5: Samples for DLC12 - LHS

caused on loads by structural and aerodynamic uncertainties without the effect of the seed variation, in both ultimate (ULS) and equivalent fatigue (FLS) loads.

The normalised loads CoVs, for both ultimate and fatigue equivalent loads are presented in Table 6.3. The CoVs related to the highest mean values are highlighted (i.e. this allows us to define at which wind speed the uncertainty effect is more important - as a higher CoV in a low load level is not critical). General observations:

- The highest CoV is around 10% for the tower side-side moment at cut out wind speed, which is also where the highest mean values of this load happen, meaning that is the load on which the structural and aerodynamic has the most significant impact.
- There is an overall trend of smaller covs at rated wind speed, at this speed there is a smaller influence of the turbine operation/controller, the blades are at a low pitch, so the wind flow is most likely fully developed and a clean (without interaction) effect of the uncertainties is expected. For cut in is likely that the flow is not yet

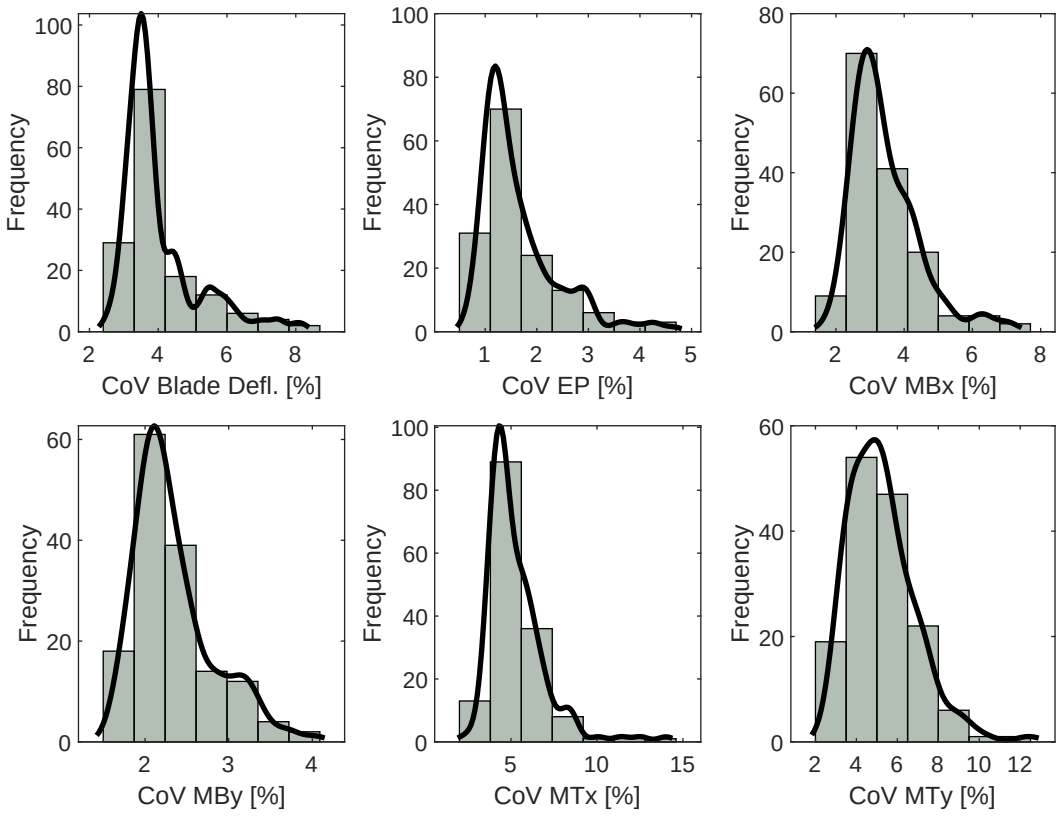


FIGURE 6.6: Most likely CoV for cut in wind speed: DLC 12.

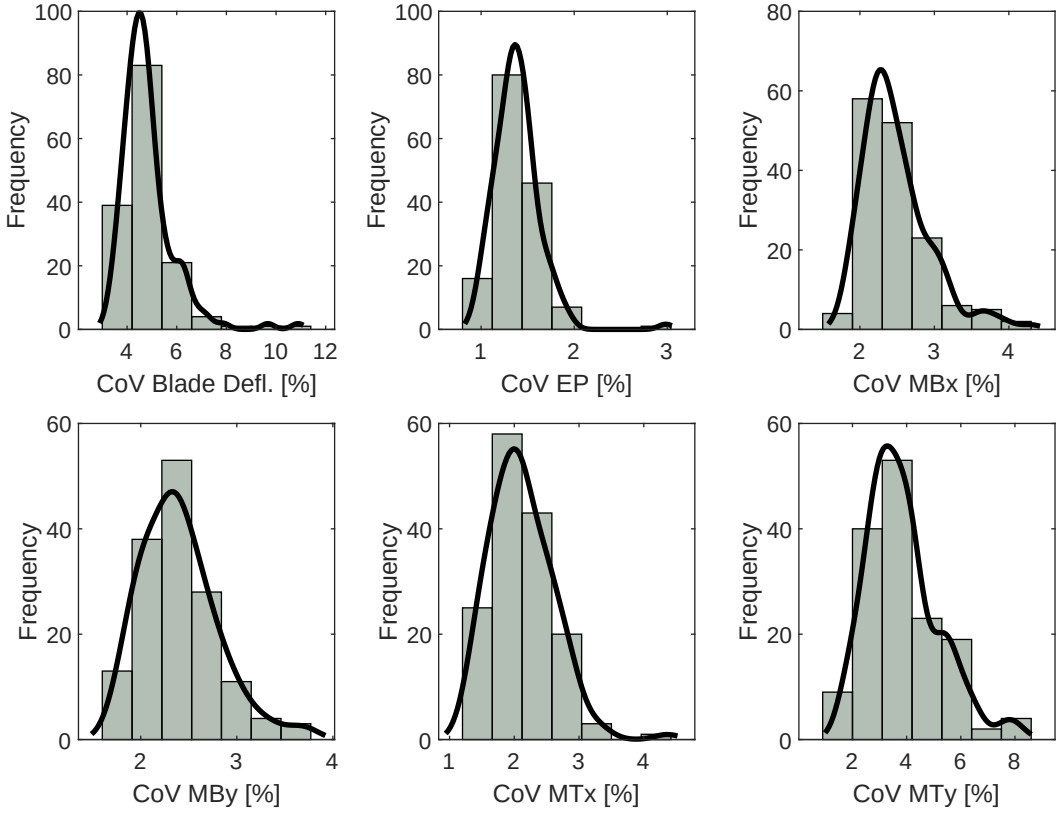


FIGURE 6.7: Most likely CoV for rated wind speed: DLC 12.

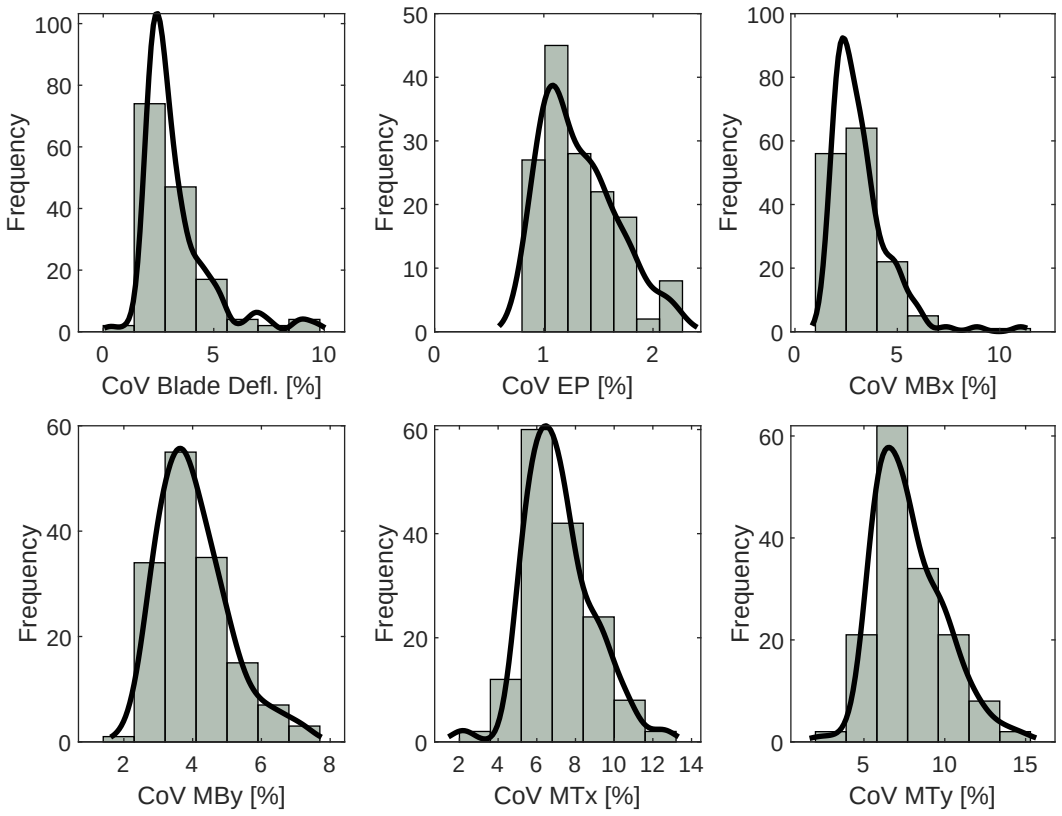


FIGURE 6.8: Most likely CoV for cut out wind speed: DLC 12.

fully developed in the blade and the variations (and uncertainty effects) can be higher but their overall loads mean values are smaller. For cut out, which is the highest wind speed the turbine can operate, there is some blade load reduction due to the characteristic high pitch, and together with the higher turbulence there will be some interaction between uncertainties, controller and turbulence that can cause big load variations.

- For tower loads the fatigue equivalent follows the same trend (of having the smaller CoV at rated) but for blade equivalent fatigue loads the behaviour is different: at flapwise the smallest CoV is at cut out, which is coherent with the blade load reduction caused by a higher pitch angle.

- Overall fatigue equivalent loads CoVs are higher than ultimate loads CoV, but these might be overestimated as they are averaged on 5000 simulations of 10min instead of the turbine lifetime.

- The blade deflection CoV is the highest at rated wind speed, this is also where the highest deflection occurs, meaning that is also the wind speed where there could be a higher risk of blade tower collision due to excessive deflection.

- Tower loads have in general higher CoVs than blade loads.

TABLE 6.3: DLC 12 Loads CoV: ULS and FLS

Wind speed	**Location**	**Cut in (%)**		**Rated (%)**		**Cut out (%)**	
		ULS	FLS	ULS	FLS	ULS	FLS
Energy Production		3.5		1.8		1.3	
Blade Tip deflection	Tip	6.0		**6.1**		5.9	
Blade Flapwise moment	Root	6.0	8.9	**3.0**	7.4	5.7	4.8
Blade Edgewise moment	Root	3.4	2.5	**3.0**	2.3	5.6	3.0
Tower Fore-aft moment	Base	8.7	10.8	**2.5**	6.4	9.0	8.1
Tower Side-side moment	Base	9.0	7.1	6.7	6.6	**10.4**	11.7

6.3.1 Sensitivity Analysis: DLC 12

The primary objective of performing a sensitivity analysis in a stochastic model is to assess the relative importance of the random inputs (aerodynamic or structural uncertainties) with relation to the output (turbine loads). There are several methodologies applied to study sensitivity, including meta-models, one-factor-at-a-time and variance based methods[87].

A particular useful approach is the based on linear regression of Monte Carlo simulations (also known as Standardised Regression Coefficients (SRC) [88],[89]). First a linear model for each output needs to be obtained in terms of the inputs:

$$Y_i = m_0 + sX_1 + aX_2 + ... + \varepsilon \tag{6.2}$$

where Y is the output, X_i inputs, s the regression coefficients related to the structure, a to the aerodynamic and ε the residual that can be caused by interaction (I) between inputs, inadequacy of the linear model and turbulence uncertainty. These can be normalised by the ratio of the standard deviation of each input (σ_A = standard deviation of the CLmax, σ_S = standard deviation of the mean flapwise stiffness) to the standard deviation of each load (σ_Y):

$$S = s\frac{\sigma_{Xi}}{\sigma_Y} \ , \ A = a\frac{\sigma_{Xi}}{\sigma_Y} \tag{6.3}$$

S and A are defined as the sensitivity measure or the standardised regression coefficients. In chapter 4 the mean flapwise stiffness was defined as a parameter to represent the stochastic behaviour of the blade structure with relation to the uncertainties in the

laminates parameters. This measure will be used in the sensitivity analysis as there is a bigger interest in differentiating the contribution coming from structural and aerodynamic instead of trying to define the relation between specific uncertainties in material properties to wind turbine loads.

In chapter 5 the stochastic model of aerodynamic coefficients was defined parametrised in terms of a CLmax, here this parameter (which is specific to one aerofoil, but correlated to the whole blade due to model) is used as the aerodynamic input to the sensitivity study.

The results of the variance decomposition is shown in Fig.6.9, it indicates how much each of the uncertainties sources contribute to the total variance of the chosen output that can be explained by the linear model. S represents the structural contribution, A the aerodynamic and I the interaction between them. An interesting evolution of contribution can be seen in the results that are coherent with aspects of the turbine operation (e.g. pitch control). The following conclusions can be made based on Fig.6.9, which shows the variance contribution for ULS:

- Overall, the linear model is best suited to distinguish between aerodynamic and structural uncertainties at rated wind speed. This can be explained by the operation point of the turbine, at rated wind speed there is no pitching of the blades, meaning that they are operating fully facing the wind, allowing them to capture as much energy as possible and that there are no other phenomena (for example turbine control actions) interacting.
- The aerodynamic is the main driver of energy production uncertainty, at all wind speeds it is the main contributor to the variance, with the highest contribution at rated. This is consistent with the importance given to have a good characterisation of these coefficients in wind turbine simulation.
- Blade deflection is highly influenced by the structural uncertainties, with over 60% of variance contribution at rated wind speeds. It is also interesting to note that, at cut out, because the blades are pitched out of the wind the contribution from the structure is diminished.
- For both blade edgewise and tower side-side moment most of the variance cannot be explained by a linear model, which means there is higher level of interaction

between the uncertainties and another methodology (non-linear) should be used to study its sensitivity.

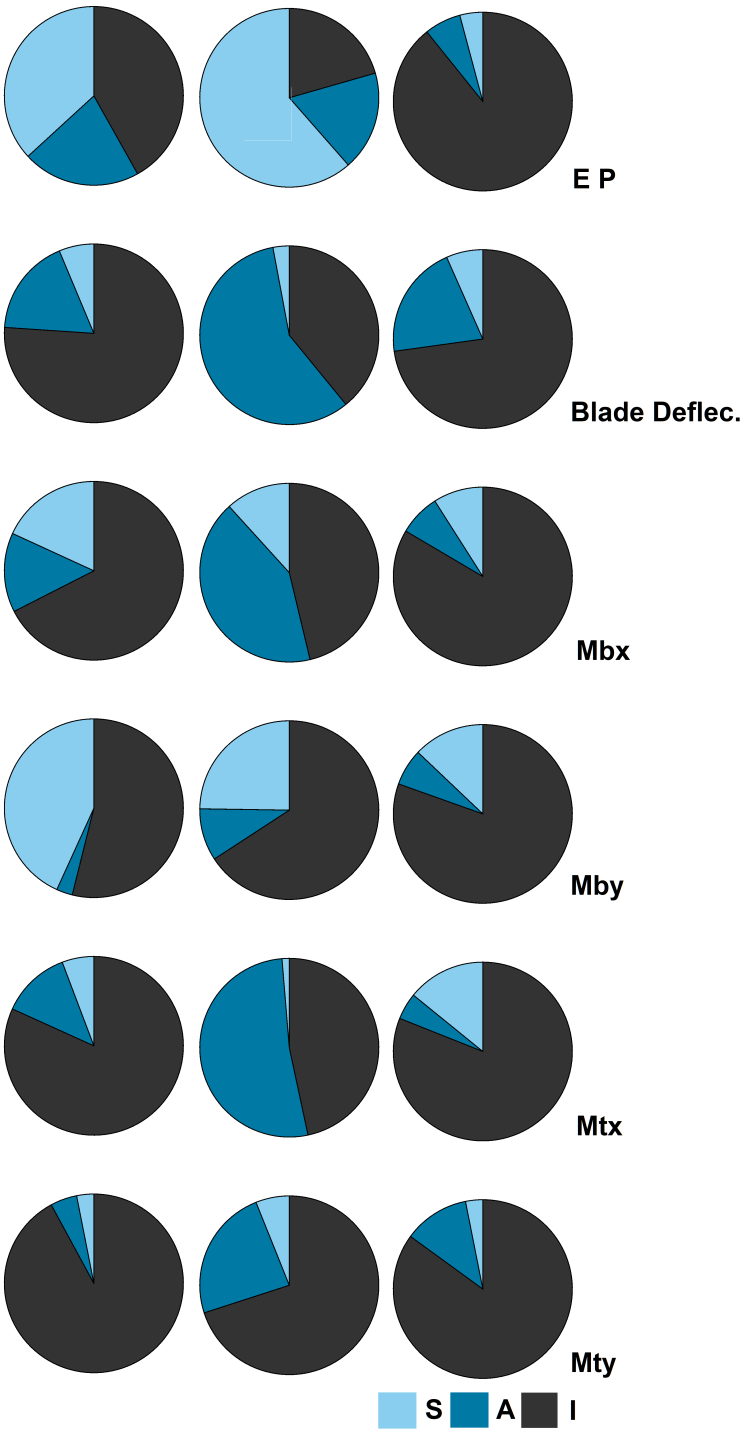


FIGURE 6.9: Variance decomposition at (A) cut in (B) rated and (C) cut out wind speed.

6.3.2 Results and discussion: DLC12

This section investigated the propagation of structural and aerodynamic uncertainties based on the variation of laminate properties and on wind tunnel measurements of aerodynamic coefficients in the aeroelastic model of a wind turbine (under DLC 12) by means of a Monte Carlo simulation with a Latin hypercube sampling.

The CoVs for ultimate loads and fatigue equivalent loads were defined and the variance contribution investigated via standardised regression coefficients. The findings indicate that these uncertainties of blades have an effect on turbine loads up to 10 % (in ultimate tower side-side moment), and that at different loads, and wind speeds have different variance contribution coming from structural or aerodynamic.

Tower loads in both directions were more affected than blade loads, as expected due to the bigger lever arm with the rotor mass. Such a rotor can weight upwards of 70 metric tons, and considering the blades having an uncertainty of COV of 1.2% in their mass-moment, the bigger impact in tower loads is justified.

The variance contribution at cut out wind speed is where there are the smallest linear effect captured by the SRC, this means the interaction (and the turbulence) is responsible for most of the uncertainty levels in the loads. Rated wind speed results showed the best fitting of the SRC, with the linear phenomena explaining most of the variance.

These results also show the importance of a correct characterisation of the blade structure to have a well defined blade to tower clearance, as the IEC[83] specifies that blade-to-tower clearance (i.e. blade deflection) should be designed with a safety factor of 15%. Whilst the effect of the aerodynamic and structural uncertainties have to evaluated in other design load cases, at normal power production the uncertainty is only 6%, which brings the possibility of using uncertainty quantification to support the reduction of this safety factor. Even though not necessarily this DLC represents a high chance of tower collision.

The IEC[83] standard also requires a value of 10% for the coefficient of variation on the uncertainty related to the assessment of the aerodynamic lift and drag coefficients. The current findings indicate that this value might be too conservative.

Stochastic modelling can become an important tool in the design of wind turbines. With the current trend of increased rotor sizes (and power ratings), optimisation has

never been more important, thus developing a full understanding of the effect that uncertainties can have on design critic parameters can be a part of the solution to decrease levelised cost of energy. Future research should integrate other uncertainties sources in the aeroelastic simulation as wind characterisation, damping estimation and expand the analysis to other design load cases.

6.4 DLC 13: Normal power production in extreme turbulence

The DLC 13 simulation scenario is designed to evaluate the turbine's ability to withstand turbulent conditions without compromising its power generation capabilities or risking damage to its components. It provides insights into the turbine's stability, control systems, and overall performance in challenging operating environments. This simulation of power production occurs without faults or yaw error and is performed for wind speeds in the operational range with extreme turbulence according to the B IEC class. In contrast to DLC 12, only the ultimate loads are analysed for DLC 13. As this load case is designed to find the extreme loads under extreme turbulence.

The same 150 samples from the structural characterisation and the 150 samples aerodynamic characterisation generated in the last section for DLC 12, are used here, together with 150 new seeds are generated for the extreme turbulence model (ETN) (Chapter 7 on IEC61400 [86]) to defined the wind profiles (also referred to as turbulence box).

Again a Latin hypercube sampling is used to define 5000 representative samples out of the 150x150x150 (above 3 million) possible combinations.

Due to the stochastic nature of the wind turbulence model, there will be some variation of the mean wind speed for each of the turbulence boxes. With the extreme turbulence model, one can notice a higher variation (higher max values when compared to Fig. 6.4) in the generated turbulence boxes for DLC 13. Fig. 6.10 shows the variation of mean, max and min wind speeds for the 5000 simulations, for the (normalised) rated wind speed with the same turbulence characteristics.

For each simulation, the minimum, maximum and mean values outputs are extracted and analysed, the most relevant presented: For energy production the interest is in the variation (and uncertainty) of the mean values, for loads in the maximum absolute value as for blade deflection.

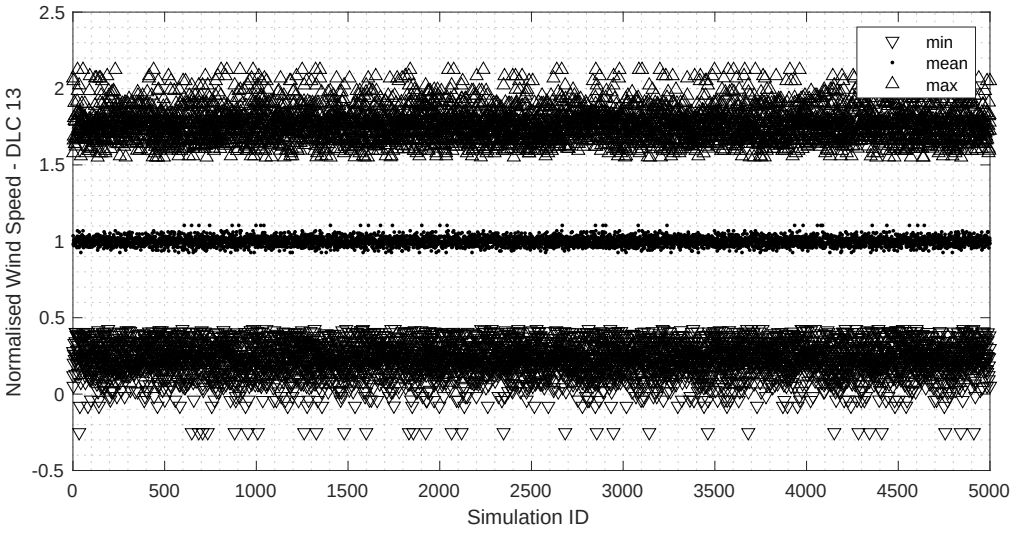


FIGURE 6.10: Normalised wind speed: DLC 13

These 5000 simulations are also grouped with respect to the new 150 wind seeds to find the most likely CoVs caused by the aerodynamic and structural uncertainties, as illustrated by Figs.6.11, 6.12, 6.13, the goal is to estimate the uncertainty caused on loads by structural and aerodynamic uncertainties without the effect of the seed variation.

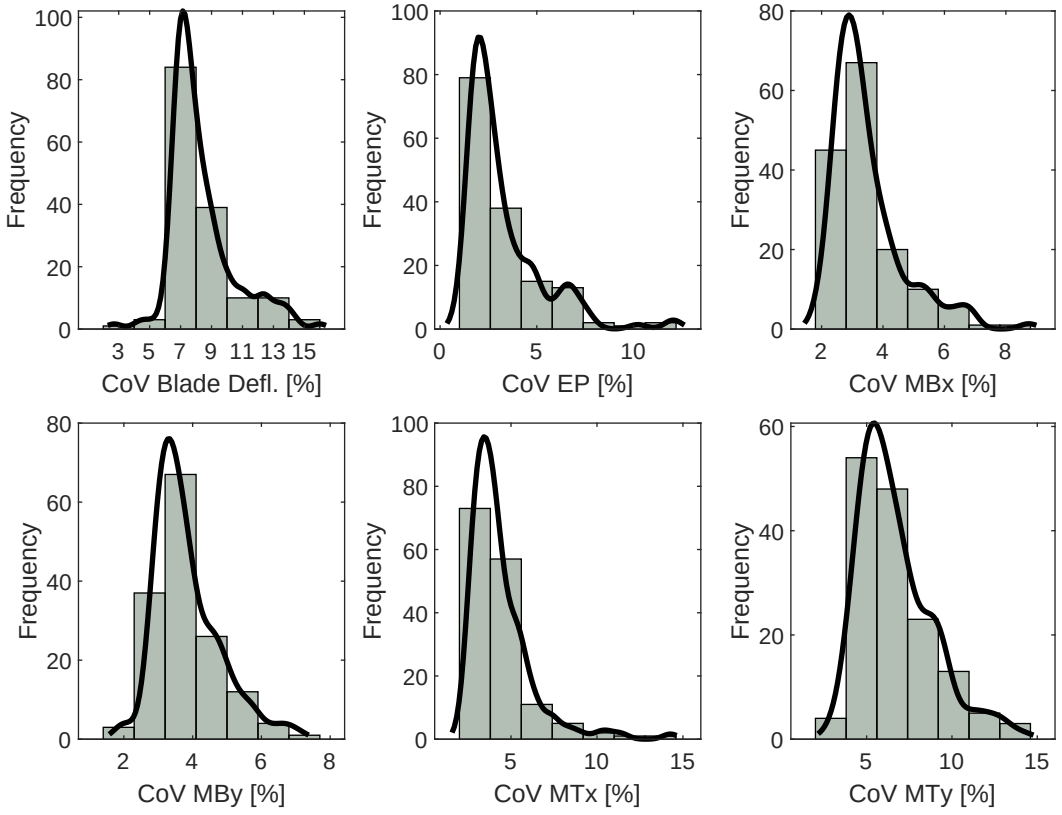


FIGURE 6.11: Most likely CoV for cut in wind speed: DLC 13.

Comparing the results for DLC 12 (Table 6.4) and DLC 13 (Table 6.4), one can see the turbulence model does not have a big influence in the uncertainty of the loads. The

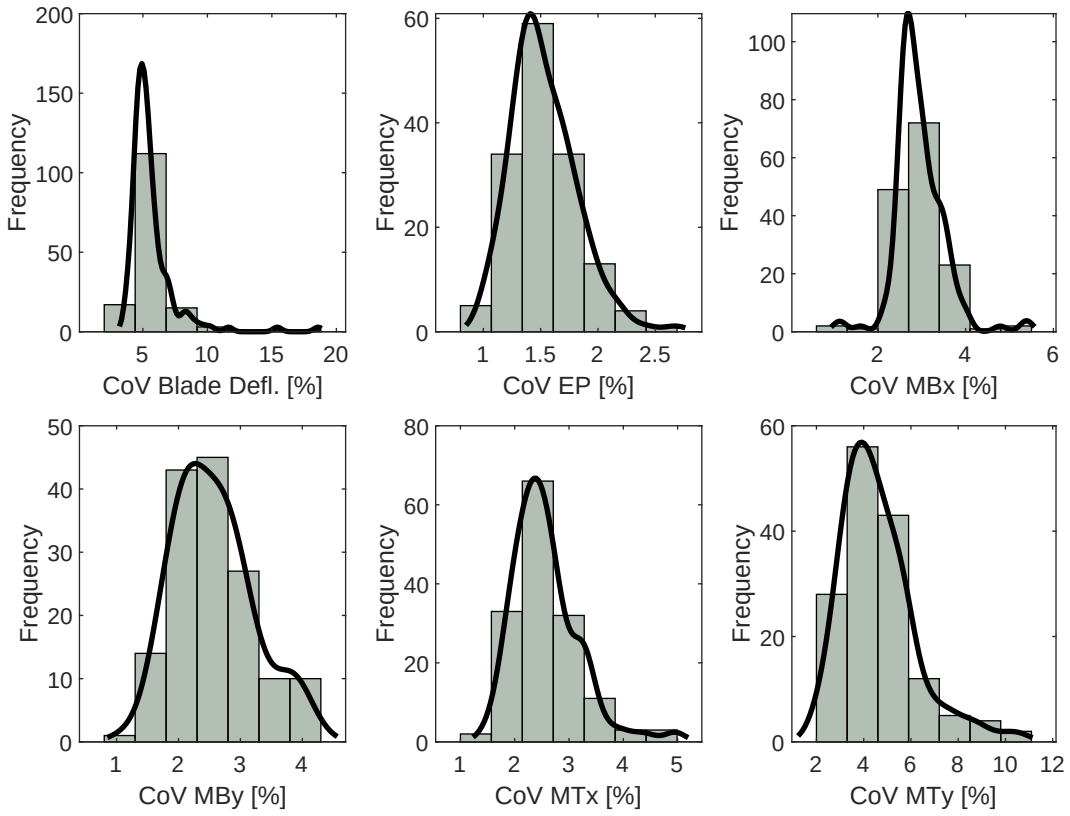


FIGURE 6.12: Most likely CoV for rated wind speed: DLC 13.

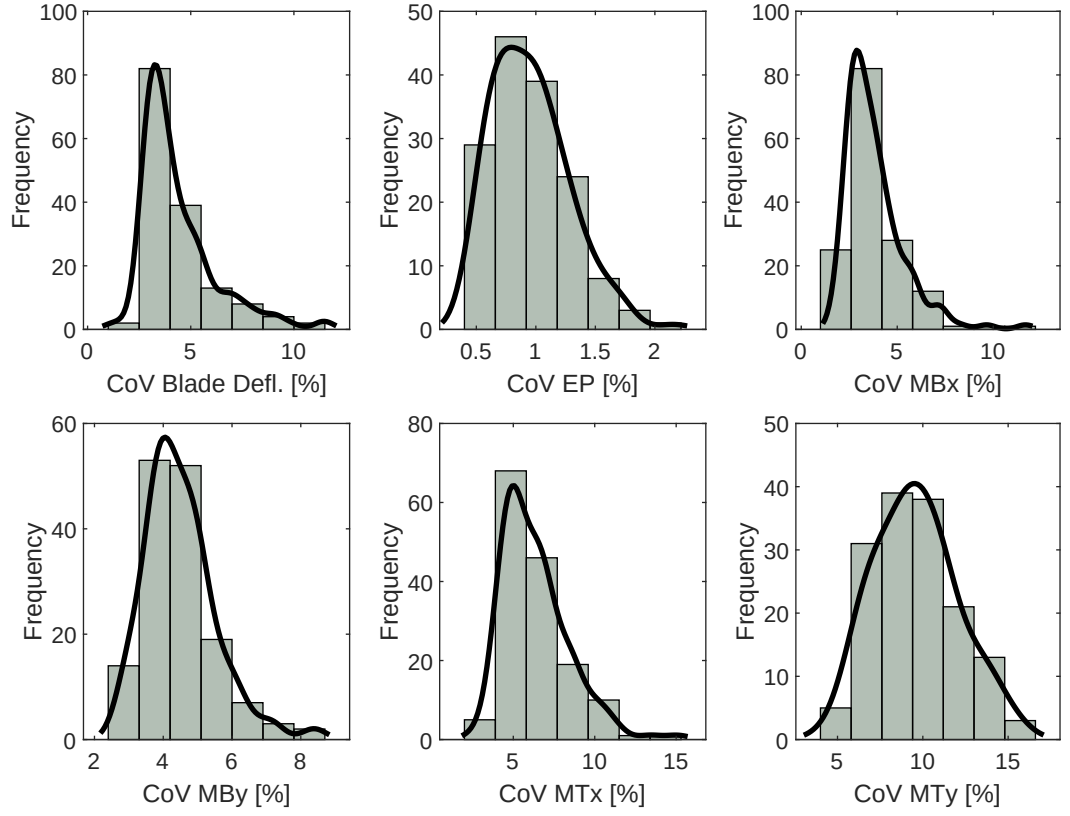


FIGURE 6.13: Most likely CoV for cut out wind speed: DLC 13.

overall trends (and uncertainty level) observed for the DLC 12 can also be seen in DLC 13.

TABLE 6.4: DLC 13 Loads CoV: ULS

Wind speed	**Location**	**Cut in (%)**	**Rated (%)**	**Cut out (%)**
		ULS	ULS	ULS
Energy Production		3.2	1.5	1.0
Blade Tip deflection	Tip	8.3	5.6	4.4
Blade Flapwise moment	Root	3.5	3.0	3.8
Blade Edgewise moment	Root	3.8	2.6	4.5
Tower Fore-aft moment	Base	4.4	2.6	6.3
Tower Side-side moment	Base	6.7	4.6	9.6

A fundamental consideration regarding DLC 13 is the loads mean values. As shown, the structural and aerodynamics uncertainties will not impact differently the loads coefficient of variation when the turbine is facing extreme turbulence, meaning that similar uncertainty levels can be expected in every scenario. However, the mean values for ULS loads are much higher in DLC 13, Table 6.5 shows the ULS mean values for DLC 13 normalised by DLC 12 mean values.

TABLE 6.5: ULS Loads mean values: DLC 13 vs DLC 12

Wind speed	**Location**	**Cut in (%)**	**Rated (%)**	**Cut out (%)**
		ULS	ULS	ULS
Energy Production		114.4	96.4	99.0
Blade Tip deflection	Tip	115.4	104.8	117.3
Blade Flapwise moment	Root	124.3	107.1	108.1
Blade Edgewise moment	Root	111.9	105.4	109.2
Tower Fore-aft moment	Base	126.3	103.5	112.0
Tower Side-side moment	Base	162.9	126.5	120.0

Such consideration becomes relevant once the probability of failure for specific components is considered. For example, the blade tip to tower clearance (BTC) is an important design metric in modern wind turbines. Assuming the (physical) limit to avoid blade tower collision of 120% of the mean value for blade deflection in normal turbine operation, with the uncertainty propagation it is possible to define the risk, or the probability of collision (assuming a normal distribution with parameters defined by Tables 6.3, 6.4 and 6.5). Fig. 6.14 shows the pdfs for the blade deflection together with the blade tower clearance limit: For DLC 12, the collision probability (or the probability that the blade deflection is bigger than the clearance) is around 0.05%, whilst for DLC 13, it is of around 1%. 20x higher than on DLC 12.

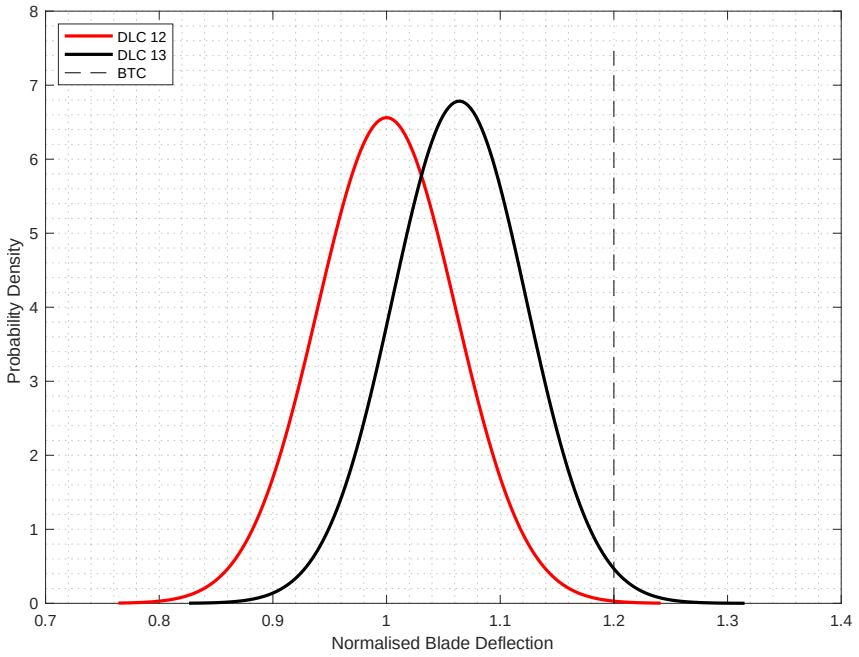


FIGURE 6.14: Blade tower collision probability: DLC 12 vs DLC 13.

6.4.1 Sensitivity analysis: DLC 13

The same procedure described on section 6.3.1 is applied to the DLC 13 results, to define the standardised regression coefficients, at the 3 different wind speeds. The results can be seen in 6.15, where the same macro trends observed in the DLC 12 can be seen in DLC 13, supporting the hypothesis that the DLC does not alter the quantified uncertainty effects in the turbine level. Nevertheless, some differences are worth highlighting:

- For energy production and blade deflection the standardised regression coefficients remain practically the same between DLC 12 and DLC 13.
- For blade and tower loads the impact of structural loads remain constant between the DLC 12 and DLC 13, however the pure aerodynamic effect is reduced in DLC 13, given place to a higher percentage of uncertainty that cannot captured by linear terms.

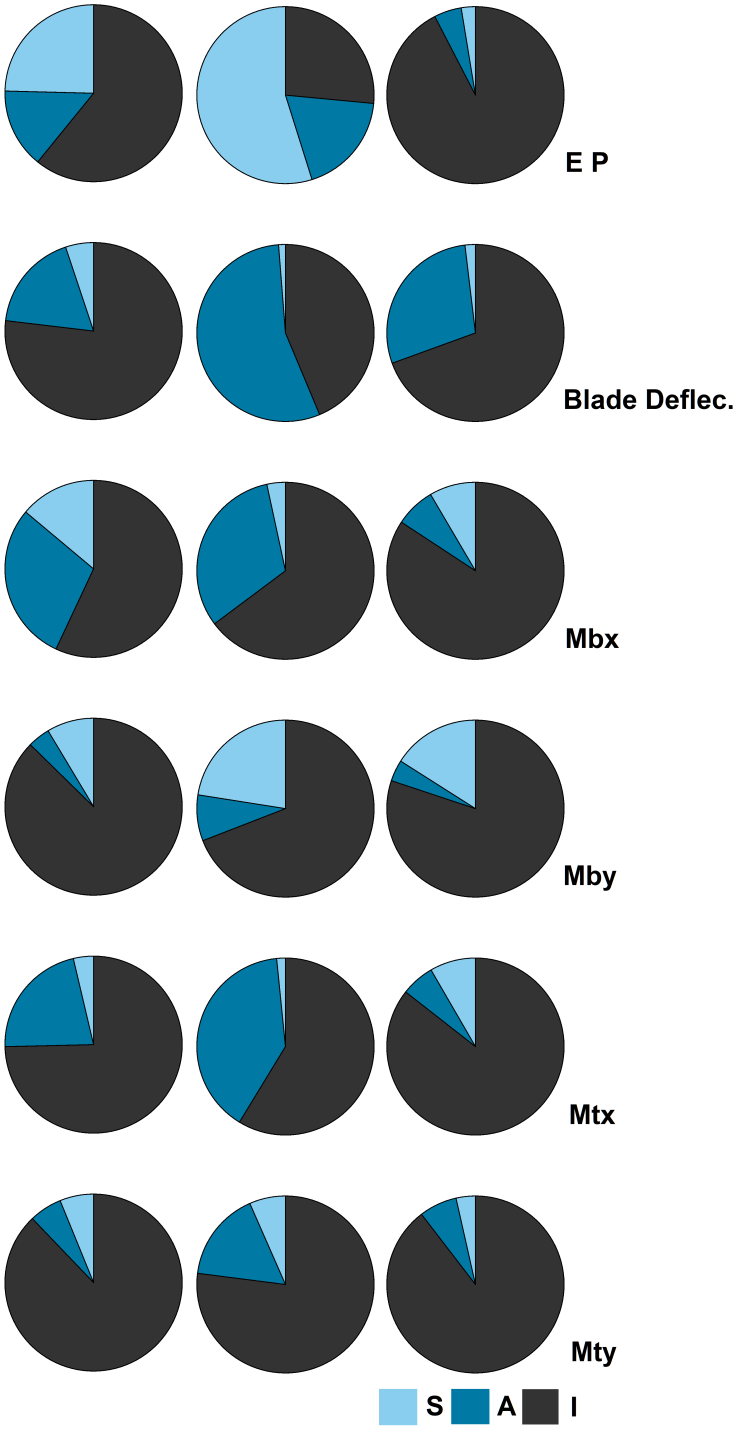


FIGURE 6.15: Variance decomposition at (A) cut in (B) rated and (C) cut out wind speed.

6.4.2 Results and discussion: DLC 13

This section evaluated the propagation of structural and aerodynamic uncertainties based on the variation of laminate properties and on wind tunnel measurements of aerodynamic coefficients in the aeroelastic model of a wind turbine under DLC 13 by means of a Monte Carlo simulation with a Latin hypercube sampling.

It was observed that the effect of uncertainties on the turbine loads are similar to the effect on DLC 13 (loads COVs are nearly the same for the 3 different wind speeds analysed). Nevertheless, such effects can be considered more critical under DLC 13, due to the loads level being generally higher than on DLC 12. By calculating the probability of blade tower collision on both DLCs, such importance was demonstrated, showing a possible increase of 20x higher chances of blade tower collision.

Another interesting result is that the standardised regression coefficients also remained very similar between the different DLCs, with the exception of blade and towers load, where the aerodynamic effect was substituted by the nonlinear interaction effect, driven by turbulence.

6.5 DLC 61: Parked in 50-year extreme wind

The DLC 61 is a different case then the previous DLCs, here the turbine is not producing energy and is subject to the 50 years maximum wind speed (which on this simulation setup is 400% of the rated wind). With the rotor parked, the main discussion on this section is regarding the maximum tower loads, and how they compare against the nominal maximum load defined by the standard simulation for DLC 61, according to the IEC 61400, [86] using the approach defined by Mann[84].

To characterise the setup for this simulation, the following environmental parameters shall be defined:

- Shear exponent (α): Following the power law profile for the wind speed variation with height above ground:

$$V(z) = V(z_r)\left(\frac{z}{z_r}\right)^{\alpha} \tag{6.4}$$

where V(z) is the wind speed at a heigh z, above the ground. z_r is a reference height above ground used for fitting the profile.

- Turbulence intensity (I): is the ratio of the wind speed standard deviation to the mean wind speed.
- Yaw error: is the wind misalignment with relation to the turbine in degrees.

These parameters are characterised according to the standard, and their deterministic definition will be later used in the nominal case. Table 6.6 presents their uncertainty characteristics. Together with the previously defined aerodynamic and structural uncertainties blade variation and with the tower Young's modulus (COV = 3%), those are the 6 uncertain parameters whose impact in the tower loads shall be investigated.

Generating 150 samples for each variable, there would be $1.14E13$ possible combinations, but by defining 20000 different aeroelastic simulations with the help of Latin hypercube sampling, one can assume this ensemble of results can represent the whole domain.

Table 6.6: DLC 61: Wind parameters uncertainty characterisation.

Parameter	**Distribution**	**COV (%)**
Shear exp.	Normal	18
Turb intensity	LogNormal	10
Yaw error	Uniform	[-8, +8]

The outputs loads for these simulation are the moments in both axis along the tower in six different points: 0, 12.6 %, 38.1%, 68.5%, 91.7% and 100% tower height(Th). The combined $Mtxy$ can be calculated according to:

$$Mtxy = \sqrt{(Mtx^2 + Mty^2)} \tag{6.5}$$

The histogram for the maximum combined moment along the tower height can be seen in Figure 6.16, together with the maximum moment of the nominal case (without considering the uncertainties), the COV for each load can be seen in Table 6.7. Figure 6.17 shows the distribution of the tower loads normalised by the tower base moment (at $Th = 0$). The exceedance probability for loads higher than the nominal maximum are presented on Table 6.8.

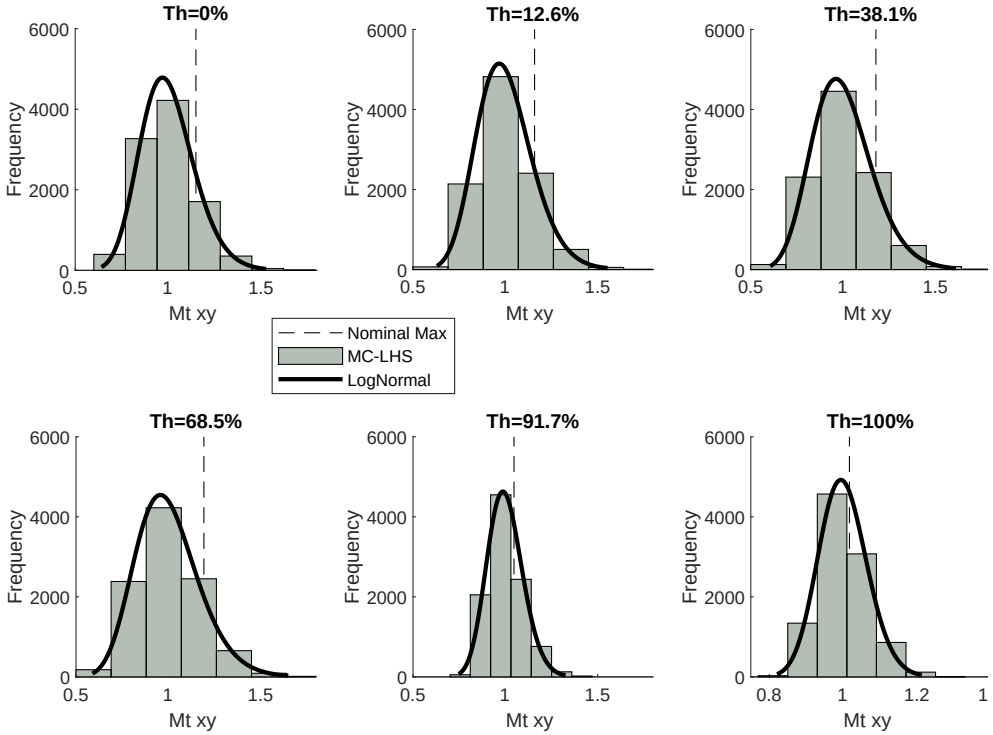


FIGURE 6.16: Tower moment: UQ simulations vs nominal.

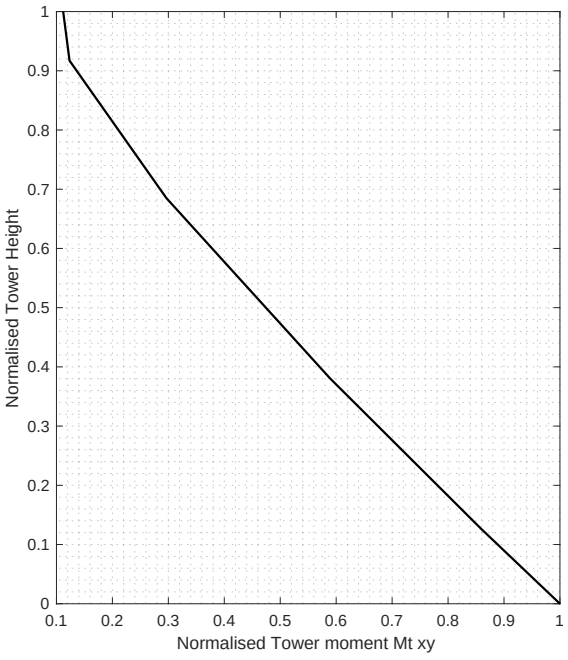


FIGURE 6.17: Normalised Tower moment distribution.

TABLE 6.7: Tower loads COV: DLC 61.

Th	COV Mtxy
0	14.6%
12.6	15.2%
38.1	16.4%
68.5	17.2%
91.7	9.8%
100	6.6%

TABLE 6.8: Probability of tower load higher than nominal: DLC 61.

Th	P(M>Mn)
0	15.1%
12.6	14.7%
38.1	14.0%
68.5	13.4%
91.7	30.0%
100	38.6%

6.5.1 Sensitivity analysis: DLC 61

The same Standardised Regression Coefficients procedure described on section 6.3.1 is applied for the base tower loads, as this is the highest load level in the tower and therefore the most important for design. A linear model can be used obtained in terms of the inputs,

$$Y_i = s \cdot X_1 + a \cdot X_2 + t \cdot X_3 + tb \cdot X_4 + y \cdot X_5 + sh \cdot X_6 + \varepsilon \tag{6.6}$$

where Y is the output and X_i the inputs. The regression coefficients can be normalised by the ratio of the standard deviation of each input to the standard deviation of each load (σ_Y),

$$S = s\frac{\sigma_{Xi}}{\sigma_Y} \ , \ A = a\frac{\sigma_{Xi}}{\sigma_Y} \ , \ T = t\frac{\sigma_{Xi}}{\sigma_Y} \ , \ TB = tb\frac{\sigma_{Xi}}{\sigma_Y} \ , \ Y = y\frac{\sigma_{Xi}}{\sigma_Y} \ , \ SH = sh\frac{\sigma_{Xi}}{\sigma_Y} \tag{6.7}$$

S, A, T, TB, Y, SH are defined as the sensitivity measure or the standardised regression coefficients, related to, respectively blade structure, blade aerodynamic, tower structure, turbulence intensity, yaw error, shear coefficient. Figure 6.18 and Table 6.9 show the results for the variance decomposition. Note that the majority of the uncertainty comes from the interaction among all the random inputs, important to remember that with the high wind speeds of the DLC 61 the turbulence would be expected to make it difficult to identify linear contributions.

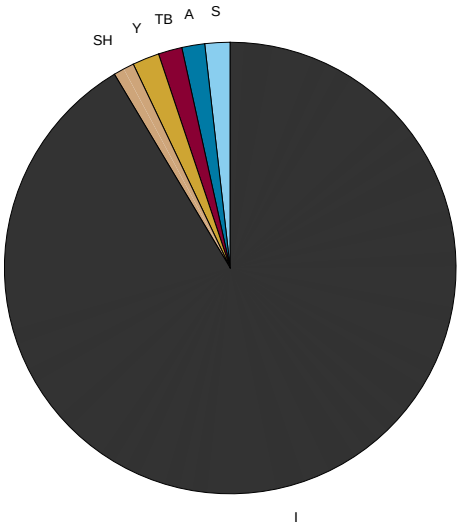


FIGURE 6.18: Variance contribution - sensitivity analysis: DLC 61.

TABLE 6.9: Variance contribution - sensitivity analysis: DLC 61.

Source	**Variance (%)**
B. struc (S)	1.8
B. aero (A)	1.6
T. struc (T)	0.5
Yaw (Y)	2.2
Shear exp (SH)	1.5
Turb. Intensity (TB)	1.7
Interaction (I)	90.7

6.5.2 Results and discussion: DLC 61

This section described the propagation of structural and aerodynamic uncertainties of blades, together with 2 wind model parameters (Turbulence intensity and Shear exponent) and one turbine position parameter (yaw error), on the DLC 61 by means of a Monte Carlo simulation with a Latin hypercube sampling.

Such setup is distinct from the results described previously in this chapter. Here, the turbine is not producing energy, the blades are at a high pitch angle (producing minimal lift), and only one single (extreme) wind speed is considered. Another main difference, is that we only consider the tower loads in such load case, because they will be critical in such situation.

With the help of 20000 realisation to capture the uncertainty effect of the 6 inputs, the COVs for the tower loads were defined. These results were compared to the maximum

nominal load, and the load exceedance probability calculated at each tower height. The sensitivity analysis for this load case showed that there is a high level of interaction among the inputs, which is expected due to the non-linear effect in high speed, high turbulence situations.

It is worth highlighting that tower loads are most critical at the base ($Th = 0$), which will be subject to the highest load levels of the whole tower. From Figure 6.17, one can see the maximum load at tower base can be as high as 10x the load at the tower top, meaning the COV for tower base is the most significant for tower design. Its exceedance probability is of $P(M > Mn) = 15.1\%$, as seen in Table 6.8. The IEC 61400 [86] recommends a partial safety factor of 1.35 for the loads in DLC 61, which can be expected to be on the conservative side when compared to the presented results.

6.6 Chapter summary

In this Chapter, an aeroelastic model was introduced for a multi-Mega Watts pitch-controlled turbine, equipped with the blades characterised in Chapters 4 and 5. With the aeroelastic code BHawC[40], inside a uncertainty quantification framework based on Monte Carlo simulations and Latin Hypercube Sampling, the turbine behaviour has been investigated.

Three design load cases were chosen to provide insight into the effect of the uncertainties in the turbine dynamics. For DLC 12 and 13, where the turbine is producing power in normal operation under normal and extreme turbulence, the influence of the blade aerodynamic and structural uncertainties seem to be independent of the turbulence model, even though the loads' level are directly influence by it. Because the turbine is expected to spend most of its lifetime in such conditions the COVs defined in Tables 6.3 and 6.4 can have a big cumulative effect both on wind turbine and on wind park design. The tower blade collision probability was calculated for both DLCs, showing a 20x increase in risk of collision when the uncertainties are considered. In practice, this risk is avoided with the use of a partial safety factor of 1.35 defined by the IEC 61400[68]. The current results show such a high safety factor might not be necessary.

In the last section of the chapter, DLC 61, is evaluated. Here, the turbine is in parked position, with blades in high pitch (producing low lift), under the 50-years extreme wind speed. Such wind speed is, of course, site specific, but the simulation setup here

was defined in a generic manner so to describe the turbine behaviour under a wind 4x faster than the rated. Due to the parked rotor, such load case focus in the tower loads, some environmental parameters are also characterised as uncertain together with the tower steel material property (E11). The results of the uncertainty propagation were compared to the nominal simulation, defining an exceedance probability in the tower base of approximately 15%., which can be again used to argue that the safety factor associated with such load is too high.

Chapter 7

Conclusion

This thesis develops a method for propagating uncertainties from blade aerodynamics and structural characteristics to the turbine level. The methodology developed in this thesis is simple and robust based on Monte Carlo simulations with Latin Hypercube sampling. The characterisation of the inputs was done by a combination of experiments, engineering judgement, and previous literature contribution. The model for the uncertain characteristics of the blade structure was validated with full scale blade testing, while the model for the uncertain behaviour of the aerodynamic characteristics was validated with the help of aerofoil wind tunnel testing. Although there was no experimental data available to validate the uncertainty in turbine loads, the results presented in Chapter 6 are highly reliable due the experimental validation of the uncertain inputs and the long-standing commercial application, validation and certification of the aeroelastic model employed.

The main findings from the literature review was that, there are several methodologies to propagate uncertainties in different types and complexity of models, raging from intrusive to non-intrusive methodologies, the last one preferred when handling already-validated models. The main benefit of Monte Carlo based approaches is the ability to *plug and play*, without extensive modification of the deterministic model. In terms of wind turbine simulations, the complex iteration between various physical phenomena mainly aerodynamics and structural (elastic and inertia) has motivated the use of so-called "aeroelastic simulations". Many aeroelastic models exist in the market, ranging from in-house developed by each market player, and others commercially available. The turbine model used in the analysis presented in this thesis is property of Siemens

Gamesa Renewable Energy, which has been used to design turbines in the last 20 years. The challenge in characterising the inputs can be regarded as probably the most important in uncertainty quantification, as inaccurate characterisations will lead to distorted conclusions on the problem, missing the improvement and optimisation opportunities brought by this type of study.

The reasons behind the lack of generally accepted uncertainty models in wind turbine simulation were the absence of trustworthy propagation done with accurate inputs characterisation using validated deterministic models. Many researchers have focused on defining new propagation methodologies to minimise the computational costs of evaluating complex models, which can become a challenge on its own, or in developing measurement techniques necessary to characterise uncertain inputs.

The approaches employed in this thesis to overcome these problems can be largely categorised as: (a) Usage of measurement techniques available in the market to define uncertainty in parameters that would have to be measured independently of a uncertainty quantification study, (b) validation of the inputs characterisation with different scales of tests, raging from coupon testing to full blade testing and when characterisation/validation was not possible by experimental data, the assumptions were built on top of the IEC 61400 [90], which is the main standard used across the industry (c) usage of a non intrusive uncertainty methodology, flexible to the inclusion of new inputs, based on a commercially validated deterministic model.

As mentioned, the key novel contribution of this thesis is the definition of loads uncertainties on multi-Mega Watts (5 to 10MW) pitch-controlled offshore turbine based on experimental validation of the uncertainties in both blade aerodynamic and structural characteristics. This type of analysis currently does not exist in the literature, and has the potential to aid the turbine design optimisation away from a still very popular usage of safety factors. This thesis also demonstrate the use of different experimental data to build stochastic models that can be applied to simulate the wind turbines and their dynamic response under uncertainties.

The key conclusions and a summary of the work related to the main themes of the thesis will be provided in this chapter. Section 7.1 summarises the definition of the blade structural model based on laminate coupon testing and its validation with full scale blade testing and finite element modelling. Section 7.2 summarises the challenges in defining a reliable characterisation for the blade aerodynamics uncertainties. Section

7.3 summarises the turbine simulation findings and its most relevant results. Section 7.4 suggests further topics to complement the study of uncertainty quantification of wind turbine simulation, and comments on its potential to the industry.

7.1 From coupon testing to full scale testing

In structural dynamics literature, coupon testing is one of the main methodologies to define material properties which are normally used in constitutive equations. Laminate coupon testing is necessary for wind turbine blade design as theoretical models cannot predict the complex micro-macro structure properties accurately. In Chapter 4, repeated coupon testing from the blade laminate panels were used to characterise their moduli and their probability distributions. The mean or nominal value from these experiments are normally the only information taken into the models describing the blade's geometry, mass and structure properties distribution.

With the material's properties probability distribution and the blade cross sectional model, the spatial stiffness distribution (Figure 4.10) variance was defined. Because the coupons are 600x smaller than the blades, this scale different could be proven too big for a representative and reliable blade characterisation.

The validation of these uncertainties was then needed and made possible by propagating them to the blade level, in specific to the static deflection, and validating the results by comparing them to full scale blade test. With the use of a FEM to simulate the setup of the blade static test, similar levels of uncertainties were shown by the simulation and experimental data, and these were shown not to be statistically different by a two-sample Kolmogorov-Smirnov test. All uncertainty levels were found to be smaller than the tolerance defined by the IEC61400-5[68], this was the first indication that the standard assumption might be too conservative.

The uncertainty model built may be deemed conservative in its assumptions for failing to model any type of correlations between properties and/or were assumed (e.g. between material properties and spatial location) however no experimental data supported this assumption. Nevertheless, the developed stochastic description of the blade is assumed to be adequate and accurate, and presenting the following novelty:

- Experimental characterisation of mass and stiffness distribution uncertainties for wind turbine blades.
- Experimental validation of uncertainty using multi-scale testing of wind turbine blades.
- Definition of a stochastic blade structural model.

7.2 Characterising blade aerodynamics uncertainties

Wind tunnel testing is one of the most challenging experimental procedures regarding aerodynamics. The complexity and cost of the experiments, the required measurement equipment and the delicate geometry of aerofoils, are a difficult research objective on their own. The limited availability of such data, with the necessary accuracy and repeatability for an uncertainty characterisation, makes the model developed in Chapter 5 one of the most novel elements presented on this thesis. Even though the model was not developed solely based in the wind tunnel testing, also making use of (geometric) tolerances defined by the IEC 61400-5:2020[65], engineering assumptions and in the literature (to define rough behaviour of thick aerofoils), the stochastic model developed to characterise the uncertainty behaviour of blade aerodynamics is expected to have a high degree of reliability and accuracy.

The wind tunnel test data was used to define a parametrisation of the rough behaviour, describing the lift decrease and drag increase, making it possible to fully describe the rough behaviour of the complete blade. An interpolation model was also developed in order to establish a spatial dependent degree of contamination of the blade, this allows the simulation to reflect the real conditions observed in field: the blade aerodynamic performance will be more impacted closer to tip and it would be too pessimistic to assume blades' aerofoils behaving 100% rough in reality. Engineering and expert judgment were used to define the different blade regions shown in Figure 5.8, and which level of rough behaviour each of them can expect.

In summary, Chapter 5 describe a comprehensive stochastic model capable of generating random aerodynamic profiles for wind turbine blades, validated against wind tunnel measurements, while thoroughly addressing the various sources of uncertainty discussed. Nevertheless, the developed stochastic description of the blade aerodynamics is assumed to be adequate and accurate, and presenting with the following novelty:

- Experimental uncertainty characterisation of clean and rough behaviour in a wind turbine blade based on repeated wind tunnel testing.
- Experimental validation of parametric model to describe aerofoils rough behaviour.
- Definition of a stochastic blade aerodynamic model, taking into account: clean-rough behaviour, geometric tolerances and spatial correlation of contamination levels.

7.3 Wind turbine loads uncertainties

On Chapter 6, the aerodynamic and structural uncertainties were propagated to the turbine level and their resultant uncertainty effect analysed in the main load channels, in 3 different design load cases; both in normal turbine operation (DLC 12 and DLC 13) and parked under extreme wind speed(DLC 61). A Monte Carlo based simulation with Latin Hypercube sampling was implemented to describe the effect of the uncertainties in the turbine main loads. Such methodology, showed to be ideal as a non-intrusive approach with an already established simulation infrastructure.

The results showed the COV effect on the loads are similar for DLC 12 and DLC 13, but without the normalisation, the effect in DLC 13 is higher, due to its higher mean values. Figure 6.14, that defined the risk of blade tower collision illustrates that well: The probability for the collision is 20x higher on the DLC 13 (due to its higher load levels, and higher turbulence) than on DLC 12. Nevertheless, the turbine is expected to spent most of its life in DLC 12 (up to 97% of a turbine estimated lifetime is expected to be under normal operation), but this risk is still significantly lower than the indicated safety factor for such load case.

The turbine dynamics are different in DLC 61, as the rotor is parked. This means the tower is put under a high stress, due to the high wind speeds considered in such load case. The uncertainties in wind parameters (shear exponent and turbulence intensity) together with the yaw error (turbine misalignment from the main wind direction) were also considered in the uncertainty propagation. The characterisation for such parameters followed their definition on the IEC 61400[68]. The most important result of a DLC 61 simulation, is the tower base combined moment, which showed a COV of 14.6%, with an exceedance probability of approximately 15% (to the maximum nominal load).

Such results are the culmination of the main novelty presented in this thesis: the definition of realistic and validated uncertainties characterisation and their effect in wind turbine loads, which can be used towards design optimisation and argument to reduce the conservative safety factors from the IEC 61400[68] standard.

7.4 Further work

This work has focused primarily on developing a practical method for assessing the effect of blades uncertainties in wind turbine simulation. Because of the amount of inputs, different models, physical phenomena and conditions the turbines need to be tested and simulated on, there were a number of questions which remain unanswered and could form the basis for future investigations.

With the same blade uncertainty inputs together with site specific environments, it could be interesting to verify the impact in other design load cases, such as start up or shut down. Such load cases rarely are design critical due to their limited time and occurrence, but they can induce high loads in the turbine, as the dynamics would be dominated by substantial inertial forces. Therefore it could worthy to investigate the uncertainties effects there as well.

The uncertainty due to environmental parameters uncertainties was only lightly touched on in this thesis, the overall assumption was to use the nominal turbulence model defined by the standard IEC 61400[83]. Because such parameters can vary significantly between sites, it is possible to estimate a site specific uncertainty quantification which would benefit from the so-called site assessment campaigns and could give answers to whether site specific designs adaptions would be needed.

The investigation in Chapter 5 only considered the maximum tolerance as geometric uncertainty, however it is known in the industry that blades can be deformed in different phases of the turbine lifetime (transport, installation and even under normal operation), although challenging, a 3D measurement campaign would be ideal to understand the actual of state of operational blades in terms of their geometry and effect in the turbine.

Using the framework described in this thesis, it would be easy to adapt the uncertainty model to account for more inputs. Offshore wind turbine simulation can also include foundation, soil and wave characterisation. As a COV of 14.6% was defined in DLC 61

for the tower bottom moment, it can be expected that the foundation design (and loads) will be significantly impacted as well. Because the foundation can represent more than half of the financial commitment in an offshore wind park project, the study of their loads uncertainty can potentially bring a big improvement in the business cases, drifting away from conservative and expensive standard designs.

Bibliography

[1] United kingdom: Dept for business energy and industrial strategy. 2019. polices paper offshore wind sector deal. *available at https://www.gov.uk/government/publications/offshore-wind-sector-deal/offshore-wind-sector-deal*, 2019.

[2] Marla Keene. Comparing offshore wind turbine foundations. *available at https://www.windpowerengineering.com/comparing-offshore-wind-turbine-foundations/*, 2022.

[3] L. Van den Bos and B. Sanderse. Uncertainty quantification for wind energy applications - literature review. 08 2017.

[4] R. Zhao Y. Zheng and H. Liu. Optimization method for girder of wind turbine blades. *Mathematical Problems in Engineering*, 2014, 2014.

[5] P. Hibbard and M. Hancock. Sesctional wind turbine blades. *United States patent application Nr US 2012/0269643*, 2012.

[6] N K Dimitrov. Structural reliability of wind turbine blades: Design methods and evaluation. *Kgs.Lyngby: Technical University of Denmark (DTU)*, 2013.

[7] Laboratory for Plastic Testing. Static testing of glass-reinforced laminates for swt blades. *Internal Report No.: B437/15.1*, 2015.

[8] Department of noise and vibration. *Operational modal analysis of BXX - Internal report*. Siemens Gamesa Renewable Energy, 2016.

[9] S.L. Ogin and P. Potluri. *Textile-reinforced composite materials*. Woodhead Publishing, 2016.

[10] W. Peng. *Fundamentals of Turbomachinery*. Wiley, 2008.

[11] P. Schubel and R. Crossley. Wind turbine blade design. *Energies*, 5:3425–3449, 2012.

[12] Y. Katsigiannis and G. Stavrakakis. Estimation of wind energy production in various sites in australia for different wind turbine classes: A comparative technical and economic assessment. *Renewable Energy*, 67:230–236, 2014.

[13] Plato. *Plato's The Republic: Book VII.* New York :Books Inc., 1948.

[14] D. Bigoni. Uncertainty quantification with applications to engineering problems. *PhD Thesis: Technical University of Denmark*, 2015.

[15] NASA. The effects of climate change. *available at https://climate.nasa.gov/effects/*, 2019.

[16] Third Planet Windpower. Early wind power. *available at http://www.thirdplanetwind.com/energy/history.aspx*, 2019.

[17] Z. Ivanovski. Direct drive wind turbines. *International Journal of Scientific and Engineering Research V*, 2, 2011.

[18] 4coffshore. Vindeby: First offshore wind park. *available at https://www.4coffshore.com/news/dong-to-dismantle-vindeby-nid3279.html*, 2017.

[19] H. Ziady. The worlds largest wind farm. *available at http://www.thirdplanetwind.com/energy/history.aspx*, 2019.

[20] V. Ramirez. The biggest offshore wind project in the us is underway. *available at https://singularityhub.com/2019/06/28/the-biggest-offshore-wind-project-in-the-us-is-officially-underway/*, 2019.

[21] B. Radowitz. Orsted targets 1.9gw of taiwan offshore wind running by 2025. *available at https://www.rechargenews.com/wind/1876113/orsted-targets-19gw-of-taiwan-offshore-wind-running-by-2025*, 2019.

[22] Orsted SA. Decarbonising society with power-to-x. *available at https://orsted.com/en/about-us/whitepapers/decarbonising-society-with-power-to-x/power-to-x*, 2020.

[23] Adrijana Buljan. Scotland's new floating wind projects – what we know so far. *available at https://www.offshorewind.biz/2022/01/18/scotlands-new-floating-wind-projects-what-we-know-so-far/*, 2022.

[24] D. Veldkamp. Chances in wind energy, a probabilistic approach to wind turbine fatigue design. *PhD thesis, Delft University of Technology*, 2006.

[25] L. Hook. Orsted warns on wind farms' power generation - financial times. *available at https://www.ft.com/content/62029f9e-fa63-11e9-98fd-4d6c20050229*, 2019.

[26] A. Ahlstrom. Aeroelastic simulation of wind turbine dynamics. *PhD thesis, Swedish Royal Institute of Technology - Department of Mechanics*, 2005.

[27] T. O'Hagan. Dicing with the unknown. *Significance*, 1:132 – 133, 09 2004.

[28] A. Der Kiureghian and O. Ditlevsen. Aleatory or epistemic? does it matter? *Structural Safety*, 31:105–112, 03 2009.

[29] Oliver Le Maitre. Spectral methods for uncertainty quantification: with applications to computational fluid dynamics. *Scientific Computation - Springer*, 2010.

[30] Lorenze Ciani, Diego Galar, and Gabriele Patrizi. Risk assessment of a wind turbine: A new fmeca-based tool with rpn threshold estimation. *IEEE Access*, PP:1–1, 01 2020.

[31] D. P. Kroese. Why the monte carlo method is so important today. *Wires Computational Statistics*, 6:386–392, 2014.

[32] L. Salles, E. Peradotto, A. Panunzio, and C. Schwingshackl. Stochastic methods for nonlinear rotordynamics with uncertainties. In *Proceedings of ASME Turbo Expo 2015*, Montreal, Canada, June 2015.

[33] R. Bhattacharya. A polynomial chaos framework for designing linear parameter varying control systems. *CoRR*, abs/1503.07943, 2015.

[34] N. Wiener. *The homogeneous chaos.* Amer. J. Math, 1938.

[35] R. Ghanem and P. Spanos. *Stochastic Finite Elements: A Spectral Approach.* Springer-Verlag, New York, 1991.

[36] J. Didier and B. Faverjon. Analyzing the dynamic response of a rotor system under uncertain parameters by polynomial chaos expansion. *Journal of Vibration and Control*, 5:587–607, 2012.

[37] D. Xiu and G. Karniadakis. Active health monitoring in a rotating cracked shaft using active magnetic bearings as force actuators. *SIAM Journal on Scientific Computing*, 24:619–644, 2002.

[38] T. Catanach and J. Beck. Bayesian updating and uncertainty quantification using sequential tempered mcmc with the rank-one modified metropolis algorithm. 2018.

[39] M. Ageze, Y. Hu, and H. Wu. Wind turbine aeroelastic modeling: basics and cutting edge trends. *International Journal of Aerospace Engineering*, 2017:132 – 133, 09 2004.

[40] R. Rubak and J. Petersen. Monopile as part of aeroelastic wind turbine simulation code. 2005.

[41] P. Couturier and P. Skjoldan. Implementation of an advanced beam model in bhawc. *Journal of Physics: Conference Series*, 1037, 2018.

[42] M. McGugan, G. Pereira, B. F. Sørensen, H. Toftegaard, and K. Branner. Damage tolerance and structural monitoring for wind turbine blades. *Philosophical Transactions: Mathematical, Physical and Engineering*, 372:v, 2015.

[43] P. J. Schubel and R. J. Crossley. Wind turbine blade design. *Energies*, 5, 2012.

[44] R. D. Adams and P. Cawley. A review of defect types and nondestructive testing techniques for composites and bonded joints. *NDTInternational*, 21:208–222, 1988.

[45] D. Tal. Uncertainty quantification in composite materials. *Columbia University*, 2018.

[46] Hu N. *Composites and Their Properties*. InTech, 2012.

[47] M. Li. Temperature and moisture effects on composite materials for wind turbine blades.

[48] A. Griffin and T. Ashwill. Alternative composite materials for megawatt-scale wind turbine blades. Technical Report 0696, s.l., American Institute of Aeronautic, RG Reston, Hunter Mill, VA, USA, 2003.

[49] J. F. Mandell. Analysis of snl/msu/doe fatigue database trends for wind turbine blade materials. Technical Report SAND2009-XXXX, Bozeman, MT : Montana State University, 02 2009.

[50] B. Ernst, H. Schmitt, and J. R. Seume. Effect of geometric uncertainties on the aerodynamic characteristic of offshore wind turbine blades. *Journal of Physics*, 555, 2014.

[51] DNV-GL. Rotor blades for wind turbines. Technical report, Oslo, Norway, 12 2015.

[52] D. R. V. Van Delft and J.L. Van Leeuwen. Full scale fatigue testing of wind turbine rotors. *IEA Experts Meeting on Wind Turbine Fatigue*, 1994.

[53] P. H. Nielsen, P. Berring, C. Pavese, and K. Branner. Rotor blade full-scale fatigue testing technology and research. *DTU Wind Energy. DTU Wind Energy E*, 41, 2013.

[54] K. Sepahvand and S. Marburg. On uncertainty quantification in sandwich structures with spatial random damping behaviour. *Proceedings of the 9th International Conference on Structural Dynamics, EURODYN 2014*, 2014.

[55] P. Bortolotti, H. Canet, C. Bottasso, and J. Loganathan. Performance of non-intrusive uncertainty quantification in the aeroservoelastic simulation of wind turbines. *Wind Energy Science*, 4:397–406, 07 2019.

[56] V. Rooij and W. Timmer. Roughness sensitivity considerations for thick rotor blade airfoils. *Journal of Solar Energy Engineering*, 125, 01 2003.

[57] I. Abdallah and J. Sorensen. Impact of uncertainty in airfoil characteristics on wind turbine extreme loads. *Renewable Energy*, 75:283–300, 2015.

[58] T. Ashuri, T. Zhang, D. Qian, and M. Rotea. Uncertainty quantification of the levelized cost of energy for a 20 mw research wind turbine model. *34th Wind Energy Symposium: American Institute of Aeronautics and Astronautics*, 555:1–11, 2016.

[59] D. Bastine, L. Vollmer, M. Wächter, and J. Peinke. Stochastic wake modeling based on pod analysis. *Wind Energy Science Discussions*, page 1–36, 2016.

[60] J. Carta, P. Ramírez, and S. Velázquez. A review of wind speed probability distributions used in wind energy analysis: Case studies in the canary islands. *Renewable and Sustainable Energy Reviews*, 13(5):933–955, 2009.

[61] P. Doubrawa, R. J. Barthelmie, H. Wang, and M. J. Churchfield. A stochastic wind turbine wake model based on new metrics for wake characterization. *Wind Energy*, 20(3):449–463, 2017.

[62] C. M. Engelen. The nonlinear effect of combining uncertainties on the energy yield of an offshore wind farm. *Master's thesis: Delft University of Technology*, 2015.

[63] M. Fluck and C. Crawford. A stochastic aerodynamic model for stationary blades in unsteady 3d wind fields. *Journal of Physics*, 753, 2016.

[64] M. Gaumond, P.E. Rethore, S. Ott, A. Peña, A. Bechmann, and K. S. Hansen. Evaluation of the wind direction uncertainty and its impact on wake modeling at the horns rev offshore wind farm. *Wind Energy*, 17(8):1169–1178, 2013.

[65] *IEC 61400-5 Wind turbines - Part 5: Wind turbine blades.* 2020.

[66] Rune Brincker and Carlos Ventura. *Introduction to Operational Modal Analysis.* John Wiley and Sons, Incorporated, 2015.

[67] B. H. Thacker, D. S. Riha, D. P. Nicolella, S. J. Hudak, L. J. Huyse, and L. Francis. Uncertainty quantification for structural dynamics and model validation problems: Reliability and optimization of structural systems, working conference. 2003.

[68] *IEC 61400-5:2020 Wind energy systems - Part 5: Wind turbine blades.* International Electrotechnical Commission, Geneva, Switzerland, 2020.

[69] *ISO 527-4 Tensile Properties of Isotropic and Orthotropic Fiber-Reinforced Plastic Composites - Part 4: Test conditions for isotropic and orthotropic fibre-reinforced plastic composites.* International Organization for Standardization, Geneva, Switzerland, 1997.

[70] T. M. Cover. *Elements of Information Theory.* New York: Wiley, 1991.

[71] S. Krenk and B. Jeppesen. Finite elements for beam cross-sections of moderate wall thickness. *Computers and structures*, 32:5, 1989.

[72] A. Olsson. On latin hypercube sampling for structural reliability analysis. *Structural Safety*, 25:47–68, 20103.

[73] M. Kennedy. The gaussian emulation machine for sensitivity analysis - software. *available in <http://www.tonyohagan.co.uk/academic/GEM/>*, 1, 2004.

[74] M. Kennedy. Description of the gaussian process model used in GEM-SA. GEM-SA help documentation. 2020.

[75] Det Norske Veritas Germanischer Lloy. *DNVGL-ST-0376: Rotor blades for wind turbines.* 2015.

[76] Laha Chakravarti and Roy. *Handbook of Methods of Applied Statistics - Volume I.* John Wiley and Sons, 1967.

[77] J. Ledoux, S. Riffo, and J. Salomon. Analysis of the blade element momentum theory. *IAM Journal on Applied Mathematics, Society for Industrial and Applied Mathematics*, 81 (6):2596–2621, 2021.

[78] J. Anderson. *Fundamentals of Aerodynamics*. McGraw-Hill Education, NY, 2017.

[79] E. White R. Ehrmann. Effect of blade roughness on transition and wind turbine performance. *Wind Energy*, 00:01–25, 2010.

[80] A A Abdel-Rahman and W Chakroun. Surface roughness effects on flow over aerofoils. *Wind Engineering*, 21:125–137, 1997.

[81] Mark Drela. Xfoil: An analysis and design system for low reynolds number airfoils. pages 01–12, 1989.

[82] Christian Bak, Helge Aagaard Madsen, Mac Gaunaa, Uwe Schmidt Paulsen, Peter Fuglsang, Jonas Romblad, Niels A Olesen, Peder Enevoldsen, Jesper Laursen, and Leo Jensen. Comparisons of airfoil characteristics for two airfoils tested in three different wind tunnels. *The science of making torque from wind*, 2010.

[83] *IEC 61400-1 Wind turbines - Part 1: Design requirements*. 2019.

[84] Jakob Mann. Wind field simulation. *Probabilistic Engineering Mechanics*, 13:269 –282, 1998.

[85] K. Thomsen. The statistical variation of wind turbine fatigue loads. *Riso natioonal laboratory technical report Riso-R-1063(EN)*, 1997.

[86] *IEC 61400-22 Wind turbines - Part 22: Conformity Testing and Certification*. 2010.

[87] J.C. Helton and F.J. Davis. Latin hypercube sampling and the propagation of uncertainty in analyses of complex systems. *Reliability Engineering and System Safety*, 81:23–69, 2003.

[88] Gurkan Sin, Krist V. Gernaey, and Anna Eliasson Lantz. Good modeling practice for pat applications: propagation of input uncertainty and sensitivity analysis. *Biotechnol. Progress*, 4:1043–1053, 2009.

[89] Joey Velarde, Claus Kramhofty, and John Dalsgaard Sorensen. Global sensitivity analysis of offshore wind turbine foundation fatigue loads. *Renewable Energy*, 140:177–189, 2019.

[90] *IEC 61400-12-1 Wind turbines - Part 12: Power performance*. 2017.